ALLOMETRIC GROWTH PATTERNS OF LABORATORY-REARED FLORIDA BLENNY (*CHASMODES SABURRAE)* AND PHYLOGENETIC REVIEW OF *HYPLEUROCHILUS* BLENNIIDS IN THE NORTHWEST ATLANTIC AND GULF OF MEXICO

A Thesis

by

JOSH EDWARD CARTER

Submitted to the Office of Graduate and Professional Studies of
Texas A&M University
in partial fulfillment of the requirements for the degree of

MASTER OF SCIENCE

Chair of Committee,	Ron I. Eytan
Committee Members,	Thomas J. DeWitt
	David R. Wells
Intercollegiate Faculty Chair,	Anja Schulze

May 2021

Major Subject: Marine Biology

ABSTRACT

Cryptobenthic reefs fishes (CRFs) occupy a critical functional group in the trophodynamics of their respective ecological system. The percomorph suborder Blennioidei encompasses ~900 species in size families of mostly tropical and warm temperature marine fishes. The most well-studied of these families are the combtooth blennies (f: Blenniidae) comprising 58 genera and 401 species. Recent decades have seen a resurgence of interest in blenny phylogenetic relationships and the evolutionary mechanisms driving their high diversity, diverse ecology and ability to invade new habitats, and changing biogeographic landscapes. To address inquiries into these topics, some organisms may serve as models which require robust captive-breeding protocols. Blennies exhibit many traits (i.e. ease of culture, adaptability to captive conditions, fecund demersal spawning, and immediate exogenous feeding) that qualify them as a potential model group for studying marine fish ecology, biogeography, and mechanisms of diversification including speciation. In this study, the Florida blenny (*Chasmodes saburrae*) was cultured to establish reliable larviculture protocols for combtooth blennies and document early development to improve culture productivity. We sampled a complete larval growth series (n = 115; 1 – 21 dph) to determine allometric growth patterns of 11 morphometric characters and described ontogeny based on assigned intervals of development including changes to gape morphology to improve feeding regimes. All but one morphometric character followed a positive allometric increase after hatching and featured at least one inflection point of allometric growth rate change corresponding to phenotypic changes during notochord flexion or preparation for the completion of metamorphosis and settlement. Maximum gape size (S_G) was calculated and used to estimate an optimal feeding based on size (SL) and age (dph) at first feeding of food item size class. During larviculture efforts of other combtooth species,

specimens of an unidentified *Hypleurochilus* blenny (n = 11) previously unreported in the Gulf of Mexico (GoM), was collected on Galveston Island, TX. These specimens, along with others of the same species collected from offshore platforms in Louisiana, were included in a phylogenetic review of with seven *Hypleurochilus* species native to the northwest Atlantic and GoM. A molecular-taxonomic approach was applied involving phylogenetic tree reconstructions, species delimitation methods (GMYC & BPP) using four nuclear genes and mtDNA cytochrome oxidase subunit I (COI) along with morphological comparison and principal component analysis (PCA) of 13 morphometric characters. Sequenced COI revealed a ~5.4% divergence from congeners and high delimitation support (posterior probability = 1.0 for BPP) for the undetermined species. The species is distinguished from congeners by coloration, snout length, laterosensory pore structure, and density of cephalic sensory pores. We recognize this unreported species as a unique lineage but cannot confirm taxonomic identity at the species level due to a lack of comparative material from congeners not included in this study, specifically those of the oyster blenny (*H. aequipinnis*). This species shares diagnostic traits and superficial similarities to *H. aequipinnis*; thus, we designate this species to *H. cf. aequipinnis* until comparative study confirms identity. These findings highlight the importance of continued research into larviculture methodologies and development of model organisms and the need for ongoing genetic and biodiversity inventories on coral reefs and artificial structures, particularly as natural reef habitat is increasingly under threat and artificial habitats grow in number and ecological value.

DEDICATION

This work is dedicated to my grandfather, Bayne Alfred Jackson. I would not be the person I am today without his teachings and guidance as a father figure, as a mentor, and as a friend. His encouragement and support in everything I have aimed to do in life has given me the confidence to complete this work and this step in my life. My wish is that he could be here to see this accomplishment through. I miss him dearly now that he is gone.

ACKNOWLEDGEMENTS

I would like to thank my committee chair, Dr. Ron Eytan, and my committee members, Dr. Thomas DeWitt and Dr. David Wells for their guidance and support throughout the course of this research.

Thanks also goes to my lab mate and lab volunteers, M. Weber, N. Reynolds, J. Albach, and M. Sitter, for their assistance with field collections and long hours driving in a truck along the southeastern coast trekking to new sites to collect fish. For assistance in caring for broodstock and larviculture I would like to give a big thanks to J. LeMoine for the countless hours spent caring for baby fish. Special thanks to R. Willeford for hours spent tediously measuring and photographing fish in the lab.

For SCUBA diving logistic support I thank L. White from TAMUG Dive Locker. A huge thank you to K. St. Clair, manager of the Sea Life Facility at Texas A&M University at Galveston, and her staff for assistance with live food cultures and care of broodstock and larvae during times of absence, power outages, and COVID restrictions.

Lastly, I would like to thank Carol D. Cox of Mexico Beach Artificial Reef Association for supplying photos taken on surveys of artificial reef habitat off Mexico Beach, Florida, John Roach for supplying photos taken on reefs in Bonaire, and Dr. Peter Wirtz for supplying photos taken in the eastern tropical Atlantic.

CONTRIBUTORS AND FUNDING SOURCES

Contributors

This work was supervised by my thesis committee consisting of Professor Ron Eytan and Professor David Wells of the Department of Marine Biology and Associate Professor Thomas DeWitt of the Department of Wildlife and Fisheries Science.

All other work conducted for this thesis was completed by Joshua E. Carter independently.

Funding Sources

Funding for this research was provided by the Marine Biology Department at Texas A&M University at Galveston and the Ron Eytan Lab.

NOMENCLATURE

CRF	Cryptobenthic Reef Fish
GoM	Gulf of Mexico
SL	Standard Length
NL	Notochord Length
HPF	Hours Post Fertilization
DPH	Days Post Hatch
cf.	Notation for Possible Species Identity
S_G	Gape Size
GMYC	Generalize Mixed Yule Coalescence
BPP	Bayesian Phylogenetics and Phylogeography
MCMC	Markov Chain Monte Carlo
COI	Cytochrome Oxidase Subunit I

TABLE OF CONTENTS

LIST OF TABLES

LIST OF FIGURES

CHAPTER I

INTRODUCTION

Cryptobenthic reef fishes (CRFs) occupy a critical functional group in the trophodynamics of their respective ecological system (Ackerman & Bellwood, 2000; Ahmadia et al., 2012; Brandl et al., 2019). The percomorph suborder Blennioidei is among the most diverse clades of CFs, comprising almost 900 species of mostly tropical and warm temperature marine fishes with a global distribution in shallow coastal waters (Hastings and Springer, 2009). Recent decades have seen a resurgence in interest surrounding blennies most notably their phylogenetic relationships and the evolutionary mechanisms driving diversity, invasion of new habitats, and demographic changes amidst fluctuating shallow coastal environments and the phylogeographic landscape at large (Eytan and Hellberg, 2010; Hundt et al., 2014, Brandl et al., 2018). Moreover, we are now beginning to understand the ecological contribution to marine food webs of shallow marine habitats occupied by these and other CRFs (Brandl et al., 2020). This diverse group currently supports six morphological and ecologically diverse families; the most well-studied of these are the combtooth blennies (f: Blenniidae) (Hastings and Springer, 2009). Small, demersal fishes (most <100mm total length), combtooth blennies commonly inhabit a diverse range of shallow, mostly marine, communities such as coral reefs, tidepools, mangroves, oyster reefs, and some supralittoral environments (Hastings & Springer, 2009). Taxonomically and ecologically diverse, blenniidae includes approximately 58 genera and 388 species worldwide and new species continue to be described with regularity (Hastings & Springer, 2009).

The western central North Atlantic and Gulf of Mexico (GoM) feature nine genera and 21 recognized species of combtooth blenny (Van Tassell, 2019). Combtooth blennies are frequent

residents of artificial structures and the hard substrate they provide as a source of food and predation refuge for CFs like blennies (Topolski & Szedlmayer, 2004). The introduction of offshore oil and gas exploration platforms in the 1950s has resulted in a. network of ~3600 structures (Atchison et al., 2008). These artificial structures are the dominant complex marine habitat along the northwestern GOM and serve as oases for aggregate fish populations in an otherwise unsuitable eco-space (Ajemian et al., 2015; Pajuelo et al., 2016; Sheehy & Vik, 2010). Five species of combtooth blennies have been reported on offshore petroleum platforms in the northern GoM – *Scartella cristata* (Linnaeus, 1758), *Hypleurochilus multifilis* (Girard, 1858), *Parablennius marmoreus* (Poey, 1876), *Ophioblennius atlanticus* (Valenciennes, 1836) and *Hypsoblennius invemar* (Smith & Vaniz, 1980) – and in many cases are the most abundant fishes associated with biofouling communities on offshore platforms (Ditty et al., 2005; Rauch, 2004).

Combtooth blennies are popular in the marine aquarium trade throughout the world and continue to command a sizeable portion of this market as one of the ten most traded marine ornamental families (Von Linden et al., 2020). The freshwater and marine aquarium trade is a multi-billion dollar market with a value of US$15-30 billion with a vast majority of species harvested from wild stocks to supply the growing demand of public aquaria, households, research institutions, and private businesses (Penning et al., 2009). For the research institution, the option of purchasing wild-caught organisms to facilitate experimentation can carry a high price tag and present difficulties in appropriate husbandry once acquired. An alternative approach to this is the captive production of the study organism. The high market demand of ornamental fish and the advancement of aquarium and culture technology has seen a sharp increase in aquaculture protocols to raise even the most difficult species (Moorhead and Zeng, 2010; Groover et al., 2020). Despite their popularity, few studies have been published regarding the breeding and rearing of

blennies and that of other blenny families. Information on protocol and feeding strategies for combtooths is scarce, and almost nonexistent for other blenny families; however, many species are currently cultured and additional research is underway to bring new species to the market (Rhyne et al., 2012). Several characteristics make combtooth blennies an appropriate choice for aquaculture and application as model organisms for marine research. Their marked abundance, high site fidelity in shallow, easily accessible habitats make locating and capturing blennies a relatively easy task compared to many other fish species (Harding et al., 2019). Combtooth blennies a highly adaptable to captive conditions and are equipped to handle changes in water chemistry and water flow as many species reside in intertidal zones that experience frequent disturbance (Tellock and Alig, 1998). The majority of aquacultured ornamental marine species are demersal spawners, making the ease of egg handling and relocating larvae to growout tanks is much easier than pelagic spawners. The larval period is marked by the immediate onset of exogenous feeding and is generally short between 17 to 35 days post hatch (dph). Once larval settlement is reached, newly settled individuals can be transferred to a suitable growout environment in relatively high densities. Lastly, some blennies may reach sexual maturity shortly after the juvenile stage is reached at around 18 – 20 mm SL or after the initial bifurcation of the primary caudal elements (Ditty et al., 2005), although observations in our lab noted spawning and sexual dimorphic characteristics at around 30 mm standard length in species from northern Gulf of Mexico. These aspects of blenny reproductive biology make them particularly equipped for aquaculture-based research activities and present the researcher with a potential model of marine teleost for numerous applications to ecological and evolutionary study.

The genus *Hypleurochilus* (Gill, 1861) comprises 11 recognized species of combtooth blennies broadly distributed across the Atlantic with seven species endemic to the Greater

Caribbean and three occurring in the eastern Atlantic, one of which (*H. bananensis*) also occurs in the Mediterranean Sea (Pinheiro et al., 2013). Members are small (<100 mm SL) and characterized by having prominent incurved canines at the rear of each jaw posterior to the comb of incisiform teeth, gill membranes broadly fused to the isthmus, typically 14 pectoral rays and a single branched supraorbital cirrus (Randall, 1966). Due to their cryptic coloration and phenotypic plasticity, there is taxonomic uncertainty within the genus and current distributions are not well understood for some species. In particular, taxonomic placement of the Atlantic oyster blenny (*H. pseudoaequipinnis*) and its eastern Atlantic counterpart the oyster blenny (*H. aequipinnis*) currently identified as its sister species (Bath, 1994) are of particular interest to this study. Defining distributions of these two species has varied over the past century with both having been reported in the eastern and western Atlantic at various times in the past 150+ years. Past studies have reported difficulties in distinguishing these two species based on morphological characters alone. Bath (1980) revisited the description of *H. aequipinnis* with newly acquired material from tropical west Africa and distributions were revised by Bath (1994) assigning *H. pseudoaequipinnis* as a new species segregated to the western Atlantic and *H. aequipinnis* to the eastern Atlantic. Studies employing an integrated molecular-taxonomic approach may resolve group systematics and elucidate evolutionary histories of this diverse group (Almada et al., 2005; Araujo et al., 2019; Levy et al., 2011). Recent collections of blennies (2013-2014 and 2018) from the northern GoM have revealed the presence of a previously unreported species of *Hypleurochilus* associated with nearshore artificial reef structures and mainland rocky shoreline.

Live specimens of this unknown *Hypleurochilus* at a size <20mm SL were collected in 2018 from Galveston, Texas and transported to the Texas A&M University Sea Life Facility for captive-raising and eventual larviculture. Establishing a captive-breeding and larviculture

protocols first relies on the application of prior research and demonstrated culture success coupled with an understanding of early larval development for the species of interest. Successful culture can then provide a complete growth series for detailed morphological study and may complement existing knowledge of larval development of the cultured or similar species. Studies involving wild-caught larvae may encounter gaps in a larval series or see a deficit in counts of larvae during various stages of development (Ditty et al. 2003). Captive-breeding can supplement existing knowledge and potentially replace the need to conduct collections of wild-caught larvae and juveniles (Stevens and Moser, 1982; Watson, 1987). Once a tested and reliable protocol is established to, the culture thereof can lead to scientific investigation of early life history, development, and improve existing culture methodologies. In the case of fishes, researchers exploring alternative model species must first refine culturing methods that allow for subsequent study (Lencer and McCune, 2018). Aquaculture infrastructure dedicated to captive-raising and larviculture of blenniid species from the northern GoM was established to study early larval development and evolutionary mechanisms of biodiversity using blenniids as model organisms.

In this study we used laboratory-reared Florida blennies (*Chasmodes saburrae*) to characterized allometric growth patterns from a complete larval growth series of an estuarine-dependent blenny based on assignment of natural intervals of development and a suite of morphometric characters related to gape morphology, body depth, and swimming ability. Additionally, we conduct a phylogenetic review of recognized *Hypleurochilus* species of the northwestern Atlantic and GoM and the unidentified species collected in Texas and Louisiana using a molecular-taxonomic approach involving phylogenetic tree reconstructions and species delimitation methods (GMYC & BPP) and pairwise morphological comparisons and principal component analysis (PCA) of 13 morphometric characters. These findings highlight the

importance of continued research into methodologies to establish larviculture protocols for blenniids as study organisms and the need for ongoing genetic and biodiversity inventories on coral reefs and artificial structures, particularly as natural reef habitat is increasingly under threat and artificial habitats grow in number and ecological value.

CHAPTER II

LARVICULTURE AND ALLOMETRIC GROWTH PATTERNS OF THE FLORIDA BLENNY (*CHASMODES SABURRAE*)

INTRODUCTION

For the research institution, the option of purchasing wild-caught organisms to facilitate experimentation can carry a high price tag and present difficulties in appropriate husbandry once acquired. Once a tested and reliable protocol is established to, the culture thereof can lead to scientific investigation of early life history, development, and improve existing culture methodologies. In the case of fishes, researchers exploring alternative model species must first refine culturing methods that allow for subsequent study (Lencer and McCune, 2018).

Several characteristics make combtooth blennies an appropriate choice for aquaculture and application as model organisms for marine research. Their marked abundance, high site fidelity in shallow, easily accessible habitats make locating and capturing blennies a relatively easy task compared to many other fish species (Harding et al., 2019). Combtooth blennies a highly adaptable to captive conditions and are equipped to handle changes in water chemistry and water flow as many species reside in intertidal zones that experience frequent disturbance (Tellock and Alig, 1998). Blennies are demersal spawners and often can spawn inside of removal spawning substrate for easy transfer between broodstock tank and larval growout container. The larval period is marked by the immediate onset of exogenous feeding and is generally short between 17 to 35 days post hatch (dph). Once larval settlement is reached, newly settled individuals can be transferred to a suitable growout environment in relatively high densities. Lastly, some blennies may reach sexual maturity shortly after the juvenile stage is reached at around 18 – 20 mm SL or after the initial bifurcation of the primary caudal elements (Ditty et al., 2005), although observations in our

lab noted spawning and sexual dimorphic characteristics at around 30 mm standard length in species from northern Gulf of Mexico. These aspects of blenny reproductive biology make them particularly equipped for aquaculture-based research activities and present the researcher with a potential model of marine teleost for numerous applications to ecological and evolutionary study.

Establishing a captive-breeding protocol first relies on the application of prior research and demonstrated culture success coupled with an understanding of early larval development for the species of interest. Successful culture can then provide a complete growth series for detailed morphological study and may complement existing knowledge of larval development of the cultured or similar species. Studies involving wild-caught larvae may encounter gaps in a larval series or see a deficit in counts of larvae during various stages of development (Ditty et al. 2003). Captive-breeding can supplement existing knowledge and potentially replace the need to conduct collections of wild-caught larvae and juveniles (Stevens and Moser 1982; Watson 1987).

One area of study that may be complemented by cultured species is ontogenetic development and allometric growth changes in morphological traits important to the functional development of fish larvae (Ditty et al., 2003; Osse and van den Boogaart, 2004; Rowlands et al., 2006; Solomon et al., 2017). One such trait is gape size and gape morphology. At the onset of exogenous feeding, the major limiting factor for the size of prey consumed is gape size (Shirota 1970). Understanding the development of gape morphology during early development is key to developing culture protocols and the dietary needs of a cultured species. Studies have shown that fish larvae prefer prey smaller than predicted by gape size-prey size relationships (Krebs and Turigan, 2003). There is a general consensus that fish larvae feed on prey items 25-50% that of the maximum gape size as was first reported by Shirota (1970) and supported by a number of studies (Yufera and Darias ,2007; Krebs and Turigan, 2003). Furthermore, as larval development

proceeds through ontogenetic growth changes, gape morphology in particular can exhibit allometric growth changes to accommodate larger prey sizes and adverse effects of competition for survival (Osse & van den Boogaart, 1995; van Snik et al., 1997; Fuiman and Higgs, 1997). In general, as gape size increases the range of ingestible prey increases linearly in a progression towards larger prey capacity (Schael et al., 1991). The relationship between gape size and body size (SL) varies between taxa and measurements are absent for a majority of culture ornamental species, making it difficult to determine potential larval diets aimed at maximizing growth and survival (Burgess and Callan, 2018). Much research has been conducted on measurements of maximum gape size (S_G) and gape width (GW) the estimation acceptable prey sizes during early development (Shirota, 1970; Guma'a, 1978; Rolands et al., 2006).

Patterns of ossification and skeletal development have been well-documented in blenny larvae; however, few studies have been conducted on the timing of ontogenetic changes in blenniid larvae. Characterizing development beyond skeletal development and identifying the state of ontogeny in blenny larval can permit researchers to investigate the role of blenniid larval in ecosystem where they exist and elucidate their ecological roles and contributions to food webs. In this study I describe ontogenetic development and characterized allometric growth patterns of morphometric traits related to gape morphology, body depth, and swimming ability from a complete larval growth series of laboratory-reared Florida blennies (*Chasmodes saburrae*). Allometric growth studies of developing larval fish have demonstrated a shared common feature to prioritize changes in relative growth rate of body proportions to reflect successive functional priorities near the boundaries of ontogenetic changes, such as flexion and metamorphosis. Larval specimens are assigned to a natural interval of development based on a character suite of

ontogenetic characters developed by Ditty et al. (2003) specifically scaleless blenniid fishes to provide an underlying context of development under which to characterize changes in allometry.

METHODS

Broodstock Collection, Acclimatization, and Water Quality

Broodstock pars of *Chasmodes saburrae* (55 – 70 mm SL) were collected from Pensacola Bay, Florida (Figure 1) in summer of 2016-2017 and transported to the Texas A&M University at Galveston Sea Life Facility. After drip acclimatization, fish were added to 75-liter aquaria connected to a recirculating seawater system with established life support and biological filtration. Broodstock tanks were painted black on all but one side for observation with décor consisting of a non-porous rock and faux vegetation tank ornament place next a spawning tube and no substrate. A photoperiod of 14L:10D was maintained with ambient overhead compact fluorescent lights. Broodstock, larval growout, and juvenile growout tanks were kept on a shared recirculating system to minimize handling, temperature, and salinity stress when transferring eggs or fish between tanks. 10% water changes were performed every week in addition to water replacement after siphoning. System water quality was maintained at a salinity of parameters were maintained at a salinity of 28 – 30ppt, a temperature of 26 – 28°C, a pH of 8.0 – 8.2, NH_3 levels of 0 – 0.25 ppm, and undetectable levels of NO_2 and NO_3.

Broodstock Care

Broodstock pairs were fed a varied diet of krill, clam, mysid shrimp, squid and omnivore gel-based diet 3 times a day (0800, 1100, 1500) in order to provide nutritional requirements needed to maintain consistent spawning and egg quality. Tanks were siphoned fifteen minutes following

each feed. A single open-ended white PVC pipe of 100-mm length and 25-mm diameter with removable clear transparency film placed inside the tube as a spawning surface was provided to each pair. Males began to occupy the tube and inspect spawning surface almost immediately and a new egg clutch would be laid 2-3 days after a new tube was introduced. Under these conditions, spawning was continuous with new eggs being laid down daily until the tube was removed for hatching. Tubes were checked for eggs each morning and observations of courtship behavior were made which was usually followed by spawning activity between morning and noon similar to that described by Tavolga (1958) and Peters (1981).

Live Food Culture

C. saburrae were cultured using small rotifers (*B. rotundiformis, S*-Type, Reed Mariculture, USA) and three size classes of *Artemia salina* nauplii (INVE technologies, Thailand LTD; GSL). Rotifers were batch cultured in 20-litre Compact Culture Systems (Reed Mariculture, USA) at 24-28°C to allow for easy cleaning and harvesting. Three species of live phytoplankton (*Nannochloropsis oculata*, T-*Isochrysis galbana,* and *Rhodomonas salina*) were cultured to feed rotifer cultures twice daily at (0800 -1000) and (1600 -1800) at a concentration of 50,000 cells mL^{-1} (salinity 30-35‰, pH 7.8-8.2, NO_2 and NO_3 <0.03 mg L^{-1}). A 5-liter (25%) volume was harvested daily from each culture bucket to maintain density and production. *Artemia* nauplii were decapsulated and hatched in 15:00 hours followed by harvesting into one container left at room temperature (25 °C) for further growth and another container refrigerated below 10°C to slow nauplii metabolism and retain hatching size (Leger et al., 1983). This was repeated for nauplii at 24hr and 48hr metanauplii stages for feedings of larger larval sizes. This method provided ever increasing size classes of nauplii with sustained nutritional value of newly hatched yolk-bound and

later metanauplii size enriched with phytoplankton and Vitachem (Boyd Enterprises) (Sorgeloos et al., 2001). A sample of 50 individuals was collected from each live food culture for size measurements.

Egg Incubation and Larval Rearing

Larval hatching and growout were carried out in 68-liter round, black plastic pond planter containers (*Lotus 23in X 10in*) with drain screens and submersible heaters with a total water volume of 54.5 liters. Once observed, eggs remained in the broodstock tank under continued male care for 144 hours, after which the spawning tube was carefully transferred to larval growout tanks. Tubes were secured to the standpipe drain screen with rubber bands and positioned vertically over the perforated bubble ring tubing to allow constant water flow over the eggs. Gentle laminar aeration with fine bubbles through the tube mimicked fanning by the male and creates water flow away from the standpipe screen in a vertical circular motion throughout the tank. A 4.0cm strip of transparency film was secured to the top of drain screen to cover the water line and prevent suction of larvae to the screen after hatching. Once transferred, a portion of the larvae began hatching immediately after introduction and were hatching continued through the following 24 hours after which time the tube was removed. Water flow was set to 2 drip/sec during the first 10 days for around a 16 % daily water exchange rate and increased to a slow constant flow for the remainder of the rearing period. Harvested rotifers and nauplii were transferred to 4-liter polycarbonate cambro containers with concentrations of 15 ind. mL^{-1} and 5 ind. mL^{-1}, respectively. This concentration dilutes to a final concentration of 3 ind. mL^{-1} and 1/mL in the larval tank. *N. oculata* and *I. galbana,* were used in a 1:1 ratio for the preparation of green water at a volume of 2-liters and added to the feed bucket. Larval feeds were performed twice daily at (0900-1000) and (1600-

1800) at a drip rate of 2-3 drips per second. Prior to feeding, larval tanks were flushed of remaining food by lowering the water level with the Hartford loop line and switching to a larger-size drain screen (Figure 2). Larvae were fed algae-enriched *S*-type rotifers (*B. rotundiformis*) (10 ind. mL^{-1})from day 1 at hatch to 11 days post hatch (dph), newly hatched *A. salina* nauplii (3 ind. mL^{-1}) from 6 to 11dph during the transition from rotifers to nauplii and (6 ind. mL^{-1}) from 12 to 14dph, algae-enriched 24hr *A. salina* nauplii (3 ind. mL^{-1}) from 15 to 21 dph, and algae-enriched 48hr *A. salina* nauplii (3 ind. mL^{-1}) starting at 20 dph until settlers were weaned onto an artificial pellet diet. Two groups of larvae (Group A and Group B) were cultured during this study.

Sampling and Specimen Preservation

During the course of development (1 – 21dph), larvae were sampled daily from group A and B to facilitate a complete larvae growth series for morphological analyses (n = 5 per day). Ten pre-juvenile settlers were also collected after the 21day period to extend the size range of the growth series beyond settlement. Larvae were anesthetized with MS-222 and placed into individual tubes and fixed in 4% buffered formalin (sodium acetate trihydrate) solution to reduce larval shrinkage (Hay, 1981; Rowlands et al., 2006). After 24hrs larvae were transferred to a final storage solution of 70% ethanol for long-term preservation (Ditty et al., 2005).

Morphometric Characters

Photographs of developing eggs and larval specimens using a *Leica* S6D Stereo Microscope with a *Moticam* 10.0+ MP camera (MOTIC). To provide the best view of all morphometric characters used in the analyses, images of three perspectives were taken for each specimen at either 1X, 2X, or 4X magnification (lateral head view, ventral head view, and lateral

body view). Prior to imaging, larvae were placed in a small petri dish with taxidermy pins placed in the mouth until a jaw angle of 90˚ was achieved. 10 morphometric characters associated with feeding and locomotion were measured (±0.00 mm) for each the 115 specimens included in this study. In addition to notochord length (NL) and standard length (SL), these measurements in include head length (HL), eye diameter (ED), preanal length (AL), pectoral length (PL), snout length (SNL), depth at pelvic (DAP), depth at anus (DAN), upper jaw length (UJL), lower jaw length (LJL), and gape width (GW). Pectoral length was not measured for a portion of specimens due to damage or position of the fin when photographed. Measurements were taken using *TPSDig* software and each image was scaled with a 1.0 mm scale bar applied to each image when captured (*TPSDig*) (Figure 3).

Gape Size Calculation

Maximum gape size (S_G) was calculated using the traditional gape size equation (A) given by Shirota (1970) and the later modified equation (B) by Guma'a (1978):

$$\text{A)}\quad S_{GS} = \sqrt{2}(L_{UJ})$$

$$\text{B)}\quad S_{GG} = \sqrt{(L_{UJ}^2 + L_{LJ}^2)}$$

Larvae were held under the microscope with forceps, while inserting a dissection pin into the mouth until a jaw angle of ~90° was achieved and an image was captured at the appropriate magnification with a set scalebar of 1.0 mm in the imaging software. A mouth angle of 90° was selected as this is assumed to be the maximum gape for larval fishes (Shirota 1970). To validate gape size calculated using the Guma'a equation, landmarks were placed on the 1) anterior tip of the premaxilla, 2) point of jaw articulation, and 3) anterior tip of the dentary in *TPSDig* (Guma'a, 1978; Kiorboe et al., 1985; Wittenrich and Turingan, 2011; Burgess and Callan, 2018). Landmark

placement was adjusted to a common angle of 90° by rotating the landmark at the tip of the dentary about the point of jaw articulation and the distance calculated between landmarks at the tip of upper and lower jaws (Figure 3b).

Ontogenetic Index and Intervals of Development

Assigning multiple discrete states to individual ontogenetic events can help define natural intervals of development (Ditty et al., 2003). Multivariate analyses of these character state variables reveal early development information useful to identifying the position along the progression of ontogeny, characterize timing and rate of ontogeny for a given species, and allow direct comparisons between species for defining interspecies characteristics.

Each specimen (n = 115) was scored for a suite of twelve characters following the methodology developed by Ditty et al., (2003) with each score representing a discrete ontogenetic event or character state. This procedure can be used to determine natural intervals of development and characterize the state of ontogeny in small scaleless combtooth blennies. 'State' designates an instantaneous position within an ontogenetic sequence and 'stage' represents an interval of development traditionally defined in early life history. To improve contrast of anatomical structures anatomical structures such as preopercular spines, cephalic cirri, and fin rays, specimens were dipped in Acid Blue 113 stain (or Cyanine Blue 5R stain) prior to character state assignment (Saruwatari et al., 1997) (Figure 4).

Agglomerative hierarchical cluster analysis was performed on character scores using complete linkage and Manhattan distance rules to organize and map 'interval' structure using the *pvclust* R-package (Maechler, 2019; Kassambara, 2020). The pvclust package also allows the user to test cluster validation and stability using a bootstrap resampling method (Suzuki et al., 2019).

A bootstrap resampling of 5000 iterations was used to determine the probability distribution and obtain nonparametric estimates of standard error (DePatta Pillar, 1999). A stability threshold with a confidence level of $\alpha = 0.10$ was used to reject the null hypothesis of stable group structure for the proposed number of clusters ($n = 3$) (Pillar, 1999). Resulting clusters were assigned descriptive labels (larval, metamorph, and settler) according to Ditty et al. (2003). After assigning individuals to an interval of development, a discriminant function analysis (DFA) was performed on character scores to summarize group differences and intraspecific criteria that discriminated intervals using the lda() function in *MASS* R-package and the *candisc* R-package (Venables and Ripley, 2002; Friendly, 2021). Multivariate normality and outliers were assessed using a chi-squared quantile-quantile plot with Mahalanobis squared distance (D^2) values. The larvae interval was further divided into traditionally defined stages of preflexion, flexion, and post-flexion based on direct observation of specimens assigned to the interval.

Allometric Growth

Patterns of growth for measured morphometric characters were modeled by a power function of NL or SL obtained from $\log_{10}$-transformation of each character. Patterns in allometry were described using the growth coefficient (i.e. power function exponent) with the equation $Y = aX^b$, where y is the dependent variable (measured character), and x, the independent variable (NL or SL), a is the intercept and b, the growth coefficient (Fuiman, 1983). The intercept and power exponent were obtained from linear or piecewise linear regressions on the log-transformed data (Nowosad et al., 2020). A growth coefficient of $b = 1$ indicates isometric growth while a growth coefficient of $b > 1$ or $b < 1$ indicates positive or negative allometric growth, respectively. Null hypothesis of isometric growth (H_0: $b = 1$) was tested for each linear model using the t-test for α

= 0.05. Assessment of regression model performance and output residuals plots for each character indicated that some data followed a nonlinear relationship, thus piecewise linear regressions were performed to determine inflection points. Piecewise regression models were performed using the *segmented* R-package (Muggeo, 2008) which uses an iterative procedure to estimate the breakpoint and summarize generalized linear models with segmented relationships. This package allows the user to estimate the initial guess for number and position of the breakpoint(s) in order to quickly assess possible differences with the computational efficiency of the algorithm (Muggeo, 2008). Slope comparison *t*-tests (α = 0.05, n – 4 degrees of freedom) were performed to check if the slopes (i.e. growth coefficients) of the two linear segments (3 in the case of SNL) were significantly different from each other using the following equations:

$$t = \frac{\text{b1 - b2}}{\text{S}_{\text{b1-b2}}}$$

$$\text{S}_{\text{b1-b2}} = \sqrt{\text{S}_{\text{b1}}^2 + \text{S}_{\text{b2}}^2}$$

b1 and b2 are the slopes of the line segments, and $\text{S}_{\text{b1-b2}}$ is the standard error of the difference between the two slopes. $S_1 + S_2$ is the standard error of the segment slopes. To compare model performance AIC (*Akaike's Information Criterion*) scores were compared with single regression model scores and F-tests were performed (n – 4 degrees of freedom) to determine whether piecewise linear functions were a better fit than a single linear regression. To avoid bias during back-transformation of data, once a regression model was chosen, back-transformed predictor values were multiplied by a correction factor computed by the *logbtcf*() function in R (Sprugel, 1983).

Estimating Feeding Protocol from Gape Size

Calculated gape size (S_G) was used to estimate the timing at which to introduce a new food item during the progression of development. A single linear regression analysis was performed between gape size and dph for both larval groups and a *t*-test was performed to compare the slopes of each model. Food size was recorded by measuring the width of each prey item size class from samples of each culture (n = 50) and calculating mean size. Width of each prey item was the smallest dimensional measurement and assumed to be the limiting size for consumption (Krebs and Turigan, 2003). Percent of maximum gape size during feeding was estimated using the mean gape size for 5dph larvae as a baseline for the transition from rotifers to *Artemia* nauplii as was observed during both group cultures. Based on this information, a more optimal feeding protocol was estimated which can then be tested with feeding trials.

RESULTS

Morphological Development

Pigmentation patterns followed that described by Peters (1981) and Ditty et al. (2003). During the larval interval the ventral midline of the tail featured a series of punctate melanophores associated with each anal pterygiophore, moderately pigmented pectoral fins gradually becoming heavily pigmented, pigment on the visceral mass, and a melanophore internally over the forebrain and nape. Pigmentation of the head increased late in the larval interval. Late metamorphs exhibited further increase in head pigmentation along with a reduction in pectoral fin pigment and the initiation of lateral pigment bands beginning with a band behind the nape shortly after settlement. Bands of pigment appear progressively along the trunk with the onset of the settler interval. Shortly

after settlement lateral pigmentation is complete and pectoral fins are free of pigment. Formation and pigmentation of the orbital cirrus precedes that of the nasal cirrus and nasal cirrus was not observed to appear during the growth series of this study. Orbital cirri begin to form during the metamorph interval and became pigmented just prior to settlement. Laterosensory pores were first present behind the head with bony ossicles development in tandem but did not appear until early settlement, much later than those reported for the five species studied by Ditty et al. (2003).

Caudal fin ray bifurcation used for the approximation of juvenile stage was not observed in the growth series of this study (Randall, 1966). Instead, wild-caught individuals from the same regional locality as the broodstock were examined. Specimens between 16.0 – 24.0 mm SL were examined, and a SL of 20.0 mm was determined to be the size at which caudal element bifurcation begins. Mean size and I_O values for observed settlement of *C. saburrae* was 8.93 mm SL (I_O = 73.1) and smallest size for individuals assigned to the settler interval was 9.27 mm SL (I_O = 74.3). Timing of settling to the bottom of the larval culture tank and assignment to a settler interval indicates that *C. saburrae* settle sooner than that of other GoM species as reported in Ditty et al., (2003) (Figure 5).

Intervals of Development

Cluster analysis of characters scores was carried out on 11 of the 12 characters examined, nasal cirrus which did not appear in samples for this study. Three clusters (I – III) were identified and tested for stability with multiscale bootstrap resampling (Figure 6). After 5000 replicate samples, the three clusters were partitioned with high approximately unbiased (AU) p-values (>90%) indicating stability in these clusters. AU p-values $\geq$ 90% were considered strong evidence for a cluster, thus the null hypothesis of stable group structure is consistent with the suggested

confidence level of $\alpha = 0.10$. Resulting clusters were assigned the same descriptive labels for interval of development (larvae, metamorph, and settler) following Ditty et al. (2003). Cluster I, termed 'larvae', contained individuals with total character state scores ≤ 9 and O_L values less than 62. Cluster II, termed 'metamorphs', contained specimens with total character state scores between 13 and 26 and O_L values > 61.3. Cluster III, termed 'settlers', included individuals with total character state scores > 28 and O_L values > 72.1 (Table 1). The period of development characterized by both 'larvae' and 'metamorph' intervals are commonly defined as the 'larval period' but require these artificial labels to more clearly illustrate changes in ontogeny along scaling metrics of time (dph), SL, and ontogenetic index.

To distinguish which characters contributed most to the grouping of individuals to an interval, a discriminant function analysis (DFA) was performed on the 11 characters used in the cluster analysis. Chi-squared qq-plot of the character score data confirmed the assumption of multivariate normality with only three outliers with high D^2-values. MANOVA results (wilks' $\lambda = 0.00665$; F-statistic = 116.02; $p < 0.0001$) indicated a large F-statistic and correspondingly small p-value providing support to reject the null hypothesis of equality of interval group means. Two canonical roots extracted all within-group variability. Canonical root 1 discriminated settlers from metamorphs and larvae (71.2% explained variability), and canonical root 2 separated between metamorphs and the other two intervals to a lesser extent (28.8% explained variability) (Tables 2 and 3, Figure 7). A comparison between standardized canonical root coefficients of the DFA for *C. saburrae* and those of five other species included in Ditty et al., (2003) are reported in Table 4.

Characters with the most contribution to discriminating ability of root 1 were orbital cirrus, number of teeth, and body pigmentation as explained by the initiation of lateral body pigment, orbital cirri size and pigmentation, number of teeth in settlers. Discriminating ability of root 2 was

largely driven by the state of the preopercular spine growth or resorption, caudal fin skeletal development and pigmentation, body pigmentation, and number of dorsal spine elements formed. Metamorphs of *C. saburra*e are defined by a higher tooth count, proliferation of pigment on the caudal fin and pectoral fin, initiation of dorsal spine formation, and resorption of preopercular spines. Settlers are defined by proliferation of trunk, orbital cirrus, and pelvic fin pigmentation, reduction in pectoral fin pigmentation, and complete incisiform dentition.

Timing of Development Intervals

Following assignment of development intervals, the 'larvae' interval was further divided into three periods of preflexion, flexion, and post-flexion based on direct observation. Preflexion stage began at hatch (0 – 3 dph) between (3.37 – 4.32 mm SL) and completed with the onset of flexion of the notochord. Flexion was observed in larvae at 4 dph (4 – 10 dph) at 5.05 mm SL (4.12 – 5.75 mm SL). Prior to the metamorph interval, larvae transitioning after flexion to metamorph but still assigned to the larvae interval featured proliferation of pigmentation on the head and pectoral fin, initiation of pigment along the dorsal rays, extension of the preopercular spines, and initial segmentation of primary and formation of secondary caudal elements. The period of postflexion occurred at 5.68 mm SL (5.17 – 6.40 mm SL) occurring simultaneously with many individuals still undergoing flexion. The metamorph interval began on 11 dph (11 – 20 dph) at 7.63 mm SL (6.28 – 9.27 mm SL) with a high degree of transformation taking place to prepare for settlement and taking on juvenile characteristics. Individuals were observed settling to the bottom of the culture tank and remaining there during feeding at 17 dph (8.5 mm SL). This was preceded by metamorphs often swimming or resting in a vertical orientation along the sides of the tank indicating the impending settlement. Physical settlement was complete by all remaining

individuals by 20 dph (9.00 mm SL). Individuals assigned to the settler interval that featured ontogenetic character states defining this interval acquired these traits after physical settlement to the tank bottom. The settler interval began on 21 dph at 11.24 mm SL (8.67 – 14.49 mm SL) with all remaining individuals completing metamorphosis. Note, ten individuals with ages beyond the 21-day culture period were included to extend the dataset and included description settler characteristics prior to entering the juvenile stage.

Allometric Growth Patterns

10 of 11 morphometric traits measured followed a positive allometric increase after hatching and featured at least one inflection point of change in allometric growth. Eye diameter maintained isometric growth throughout development (b = 1.0633). Gape size based on the equation given by Shirota (1970) followed the same allometric growth pattern as UJL as this was the measurement used to calculate the gape size. The Shirota equation did not represent the true growth pattern of gape size without the inclusion of the LJL as is the case with the Guma'a (1978) equation. Thus, gape size calculated based on UJL alone was not considered further. Snout length (SNL) was the only character with two inflection point changes in allometric growth rate with the third segment of growth experiencing negative allometry (b = 0.537). Residuals plots were assessed for nonlinear relationships and heterogeneity of variance and in all cases necessitated application of a nonlinear piecewise model (Figure 9). All t.test slope comparisons between piecewise segments were significantly different ($\alpha < 0.05$) and all piecewise regressions featured a high relative F-statistic and lower AIC score than that of single regressions, thus piecewise regression models were considered to be superior to a single linear regression for the 10 characters (Table 8).

Inflection points of allometry occurred at two points when scaled with standard length during progression of development. One growth condition featured a rapid positive allometric growth during the larvae interval during preflexion, flexion, and postflexion before slowing at the transition to the metamorph interval with either a lower positive rate, isometric, or negative rate. The second condition occurred at the transition between the metamorph to settler interval prior to settlement beginning with a lower positive allometric growth rate and shifting to a higher positive rate through the settler interval indicating preparation for the energetically expensive flexion period. SNL featured both of these conditions but with a negative allometric growth rate once becoming settlers. Size at inflection for HL (6.09 mm SL), PL (5.81 mm SL), DAN (6.01 mm SL), DAP (5.81 mm SL), UJL (5.86 mm SL), and S_{GG} (4.94 mm SL) all followed condition one with rapid growth until the start of the metamorph interval. Condition two characterized GW (8.33 mm SL), AL (8.57 mm SL), and LJL (8.28 mm SL) with higher positive allometric growth just prior to the settler interval and coinciding the metamorphosis (Figures 10 and 11). Changes in allometric growth of gape size was characterized by the shortest rapid period of positive growth (b = 1.515) before transitioning to isometric growth (b = 1.043) for much of the development period. This is likely due to the dichotomy between allometric growth patterns of the upper and lower jaws as these were used in the calculation of gape size and feature opposing conditions of growth change. This dichotomy appears to stabilize the gape size throughout early development likely allowing *C. saburrae* to consume new prey sizes at a relatively unchanging rate to the juvenile stage (Figure 12).

Gape-informed Feeding Protocol

Gape size at feeding was estimated from the maximum gape size calculate (S_G), mean width measurements of live food items, and the observation of age at first feeding of 0hr *Artemia* nauplii. Slope comparison *t*.tests indicated a significant difference in slopes between the two larval groups and difference in intercept indicated that group B hatched at a smaller size that group A (Figure 13). Accordingly, group A was used to estimate an optimal feeding protocol as this group included samples from 1dph, the age capable of transition from rotifers to *Artemia* nauplii (5 - 6 dph) and the end of the larval series at 21 dph. A mean size of 183 μm (± 17.33) was calculated for 0-hr *Artemia* nauplii indicating a feeding gape size at 26.6% that of the maximum gape size. The transition from rotifers to 0hr *Artemia* nauplii occurs at approximately the same point as the inflection point for allometric to isomeric growth in gape size. Thus, a consistent rate of growth was assumed with the introduction of larger sized prey items in a linear fashion with isometrically increasing gape size. Adjusted gape size plotted on scales of SL and dph allowed for an estimation of timing for introduction of progressively larger food through the course of development (Figures 13 – 15). At a feeding gape angle of 26.6% that of max gape size, newly hatched larvae are capable of feeding on *S*-type rotifers of mean size 113 μm (± 13.29) immediately after hatching as confirmed by observations during culture and a mean max gape size of 0.383 (± 14.56) mm or 383 μm (± 47.77) within the range needed to consume *S*-type rotifers. Diet transition to enriched 24-hr Artemia nauplii is possible prior to the metamorph interval at 9 dph and to enriched 48-hr nauplii soon after becoming a metamorph at 12 dph. A weaning diet of 300 μm artificial pellets can be introduced as earlier as 15 dph; however, the pellets used in this study immediately sink to the bottom and so should not be introduced until metamorphs begin to settle permanently to the bottom at 17 dph. Original feeding protocol was based on previous study of blenniid larviculture (Peters

1983; Olivotto et al., 2010; Moorhead and Zeng 2017). This included *S*-type rotifers from 0 – 11 dph, newly hatched 0-hr *Artemia* nauplii for 6 – 14 dph, enriched 24hr *Artemia* nauplii for 13 – 21 dph, and enriched 48-hr *Artemia* nauplii for 21 dph onward with introduction of artificial pellet diet later after settlement. According to gape size a more optimal diet is proposed here *S*-type rotifers from 0 – 8 dph, newly hatched 0hr *Artemia* nauplii for 5 - 10 dph, enriched 24-hr *Artemia* nauplii for 9-13 dph, enriched 48hr *Artemia* nauplii for 12 – 21 dph and a weaning diet of 300 µm artificial pellet at 17+ dph. This proposed diet includes a 3-day transitional overlap period with both rotifers and 0hr nauplii during which variable rates of flexion is occurring followed by 1-day transition period between subsequent nauplii size and period of overlap between enriched 48-hr nauplii and artificial pellet until all settlers are weaned from live food (Figures 14 and 15). Observation and protocol along with changes in morphology and allometric growth patterns are summarized in Figure 15.

DISCUSSION

Allometric growth has been observed during larval development in many fish species, including triplefin blennies (Solomon et al., 2017; Nowosad et al., 2020). A substantial amount of morphological variation expressed by larvae is due to allometric growth and quantification of shape change can help delimit intervals of development (Strauss and Fuiman, 1985). These changes in shape often occur at discontinuities in the course of development, such as postflexion or metamorphosis. Here we report allometric growth patterns for the development of *C. saburrae* larvae corresponding to thresholds between the three intervals (larvae, metamorph, settler). All but one of the morphometric characters examined followed changes in allometric rates ($b \neq 1$) corresponding with either the threshold between larval and metamorph intervals or prior to the

transition to settlement and metamorphosis, thus supporting the hypothesis of ontogenetic priorities and reflections of successive functional priorities during development (Osse and van den Boogart, 1995). The applied methodology developed by Ditty et al., (2003) designed for assigning small scaleless fishes like blennies to a developmental interval based on individual characters states provided a robust framework under which to characterize the state of ontogeny in *C. saburrae*. Using this method permitted direct comparison to other GoM blenniid species included in Ditty et al. (2003) and added to this body of work on early blenny development in the northern GoM. This study demonstrates the utility of this methodology to characterize development of blenniid larvae.

Together, the coupling of ontogenetic changes as characterized by character states with changes to allometric growth of morphometric characters indicates the time at flexion and just prior to settlement and completion of metamorphosis are critical periods of development for *C. saburrae* larvae. Similar patterns of development can be seen in larval fish of other species. A biphasic pattern of growth inflection exhibited in *C. saburrae* was seen in all but two morphometric traits examined; snout length followed development with two inflection points while eye diameter followed an isometric growth throughout development. Growth coefficients for all biphasic or triphasic characters followed pre-inflection positive allometry, indicating a rapid growth of those elements prior to transition to the metamorph interval or before settling. Positive allometric growth was followed by continued but reduced positive allometry in all but two biphasic characters (upper jaw and lower jaw lengths) during post-inflection development. Upper jaw length experienced a negative post-inflection allometric growth while lower jaw length showed an increase in post-inflection growth rate. The only character with two inflection points (snout length) experienced a

negative post-inflection growth rate during the third segment of development after settlement occurred.

Maximum gape size (S_G) is an important variable to measure for studies of feeding ecology and can be a useful metric to estimate timing to introduce successive food sizes in larviculture. Study of S_G and upper and lower jaw lengths used in the calculation thereof for *C. saburrae*, further reveal allometric growth patterns of growth corresponding to the onset of flexion agreement with other body proportions with a similar timing of rate change. This study compared both gape size equations as presented by Shirota (1970) and Guma'a (1978) and found that Shirota's used of only the upper jaw length results in an overestimated of actual maximum gape (as measured directly) and that using the Guma'a equation. Thus, the Guma'a equation was used for this study based on a consistently shorter lower jaw length relative to upper jaw length which matched that of direct measurement. Therefore, lengths of both upper and lower jaws were included in the calculation of gape size. Allometric change in S_G of *C. saburrae* exhibited a rapid positive allometry prior to flexion followed by a near isometric growth post flexion. An explanation for this could be that newly hatched larvae require rapid growth in order to reach a greater size spectrum of prey rapidly to avoid competition from more recently hatched larvae and avoid predation. This agrees with strategies of most fish larvae studied and may be particularly important for estuarine-dependent species, like *C. saburrae*, encountering a greater prey variety and elevated competition from other estuarine-dependent teleosts occupying estuaries during the early part of life (López-Herrera et al., 2021). Post-inflection isometric growth of S_G began at the point of transition from initial *S*-type rotifer feed to 0-h nauplii indicating a linear model of development proportional to increasing fish size (SL) for this trait. Thus, larger food items can be introduced according to a constant rate of growth until metamorphosis. Using this data, we estimated an optimized diet consisting of S-type

rotifers fed from 0 – 8 dph, 0-h Artemia nauplii from 5 – 10 dph, enriched 24-h nauplii from 9 – 13 dph, enriched 48-h nauplii from 12 – 21 dph followed by introduction of weaning artificial pellet diet (300 μm) at 20 dph.

CHAPTER III

PHYLOGENETIC REVIEW OF *HYPLEUROCHILUS* BLENNIIDS IN THE NORTHWEST ATLANTIC AND GULF OF MEXICO

INRODUCTION

Combtooth blennies (f. Blenniidae) are small (most <100mm total length) CFs commonly inhabiting a diverse range of shallow, mostly marine, communities such as coral reefs, tidepools, mangroves, oyster reefs, and some supralittoral environments (Hastings & Springer, 2009). Taxonomically and ecologically diverse, blenniidae includes approximately 58 genera and 388 species worldwide and new species continue to be described with regularity (Hastings & Springer 2009). Combtooth blennies are frequent residents of artificial structures and the hard substrate they provide as a source of food and predation refuge for CFs like blennies (Topolski & Szedlmayer, 2004). The introduction of offshore oil and gas exploration platforms in the 1950s has resulted in a network of ~3600 structures (Atchison et al., 2005). These artificial structures are the dominant complex marine habitat along the northwestern GOM and serve as oases for aggregate fish populations in an otherwise unsuitable eco-space (Ajemian et al., 2015; Atchison et al., 2008; Pajuelo et al., 2016; Sheehy & Vik, 2010). Five species of combtooth blennies have been reported on offshore petroleum platforms in the northern GoM – *Scartella cristata* (Linnaeus, 1758), *Hypleurochilus multifilis* (Girard, 1858), *Parablennius marmoreus* (Poey, 1876), *Ophioblennius atlanticus* (Valenciennes, 1836) and *Hypsoblennius invemar* (Smith & Vaniz, 1980) – and in many cases are the most abundant fishes associated with biofouling communities on offshore platforms (Ditty et al., 2005; Rauch, 2004).

Studies have revealed that artificial structures serve as transport vectors for non-indigenous species (NIS) to regions beyond their normal range (Pajuelo et al. 2016). The western Atlantic has

seen the expansion of blenniid species beyond their native ranges into the western Atlantic with established populations. The tessellated blenny (*Hypsoblennius invemar*) has become ubiquitous on artificial structures and nearshore reefs throughout the northern GoM and in parts of the northwestern Atlantic (Sheehy and Vik, 2010). The muzzled blenny (*Omobranchus punctatus*), native to the Indo-Pacific region, has become a common sight among mangrove habitats in coastal environments of the southwestern Atlantic (Gerhardinger et al., 2006). Both species are associated with biofouling community on hard substrates in their native ranges and both are generally considered to be introduced through shipping or transport of oilrigs occupying the similar fouling communities often associated with artificial structures.

One such genus of combtooth blenny associated with artificial structures in the norther GoM is *Hypleurochilus* (Gill, 1861) comprising 11 recognized species of broadly distributed across the Atlantic with seven species endemic to the Greater Caribbean and three occurring in the eastern Atlantic, one of which (*H. bananensis*: Poll, 1959) also occurs in the Mediterranean Sea (Pinheiro et al., 2013). In the northwestern Atlantic and GoM six species can be found and subdivide into two clades – 1) a northwestern "temperate" clade (hereafter referred to as clade 1) which includes *H. multifilis*, *H. caudovittatus* (Bath, 1994), and *H. geminatus* (Wood, 1825) distributed from Mexico to New Jersey, US and 2) a pan-Atlantic "tropical" clade (hereafter referred to as clade 2) which includes *H. bermudensis* (Beebe and Tee-Van, 1933), *H. springeri* (Randall, 1966), and *H. pseudoaequipinnis* (Bath, 1944) distributed across the Greater Caribbean and tropical Florida.

Recent collections (2013-2014 and 2018) in the northern GoM have revealed the presence of a previously unreported species of *Hypleurochilus* associated with nearshore artificial reef structures and mainland rocky shoreline. This unknown species features a morphotype unique to

that of other western Atlantic species. Published reports of fish assemblages associated with offshore artificial structures and coastlines in the northern GoM have not reported this additional species nor any morphologically similar species that resemble it suggesting this may be a recent transplant and/or a lack of taxonomic resolution by survey efforts (Ditty et al., 2005; Grabowski, 2002; Putt, 1982; Rauch, 2004; Rooker et al., 1997; Topolski & Szedlmayer, 2004). In this study, we conduct a phylogenetic review of recognized *Hypleurochilus* species of the northwestern Atlantic and GoM and aim to identify the previously unreported species collected from artificial structures using a molecular-taxonomic approach involving phylogenetic tree reconstructions and species delimitation methods (GMYC & BPP) with four nuclear and mtDNA cytochrome oxidase subunit I genetic markers accompanied with pairwise morphological comparison and principal component analysis (PCA) of 13 morphometric characters.

METHODS

Taxon Sampling

Specimens of the new species described herein were collected from two locations in the northern GoM (Figure 2) – Galveston Island, TX (29.269389 N, -94.819389 W) and the Ship Shoal platform cluster (28.14105 N, -91.32487 W) off the Southwestern Louisiana coast. Texas specimens were collected in April 2018 by the first author with dipnets from groins constructed from granite slabs on Galveston Island beach. These fish were acclimated to aquaria at Texas A&M University at Galveston Sea Life Facility for grow-out and captive breeding study. All Texas specimens did not exceed 20 mm when captured. Based on wild-caught larval and juvenile samples of GoM *Hypleurochilus* species (Ditty et al., 2005) and captive-breeding observations, fish under 20mm when collected belonged to a 2018 cohort only recently settled to the hard-structure on the

Galveston Island groins from which they were collected. Louisiana specimens were collected from the offshore platforms in the summer of 2013-2014 while on SCUBA using slurp guns and quinaldine sulfate anesthetic and immediately frozen for later examination. Specimens of western Atlantic *Hypleurochilus* congeners used as comparative material were collected from the northern Gulf of Mexico, Eastern United States, Bahamas, Belize, and Curacao. Tissue from the right lateral muscle block was sampled for DNA extraction and stored in 96% EtOH at -80°C. Specimens were photographed immediately after euthanasia to record fresh coloration followed by fixation in 10% formalin for 24 hours before being transferred to 70% ethanol for long-term storage. Frozen LA specimens were thawed, photographed, and sampled for lateral muscle tissue and stored in 96% EtOH at -80°C.

Morphometric Analysis

Morphological data were divided into two categories: meristic (discrete counts of segmented fin rays, supraorbital cirri count, cephalic pore count, and lateral line pore condition type) and morphometric data (continuous linear measurements). Measurements of external features generally follow Hubbs & Lagler (1958) and Bath (1994) with some additional measurements included. Methods for counts followed Springer and Gomon (1975). All measurements were acquired from preserved specimens to avoid effects on dimensions from potential shrinkage. A total of 74 individuals were measured for 13 morphometric characters (Table 1). Point-to-point measurements and pore counts were taken from the left side of each specimen using digital Vernier calipers to the nearest 0.1 mm. Standard length (SL) was measured from the tip of the snout to the center of the caudal peduncle at the posterior edge of the hyplural plate. The following characters were used: supraorbital cirri count (SC), cephalic sensory pore

count (CP), dorsal notch as ratio between length of last dorsal spine and 1st dorsal soft ray (DN), depth at pelvic (DAP), depth at anus (DAN), head length (HL), eye diameter (ED), anal length (AL), peduncle length (PL), maxillary length (ML), upper lip thickness (UL), snout length (SNL), interorbit distance (ID), and lateral line system type. Cephalic sensory pore count arrangement followed terminology of Murase (2007).

Continuous variable measurements were scaled proportional to SL and HL and to unit variance to reduce variation due to allometric difference using R 3.6.1 (R Core Team, 2017). Sex effects were not considered in this study; therefore, all statistical analyses were performed on a dataset containing both males and females since all measurements were scaled and collected samples were predominately male in all species. Using the *ggplot* R-package (Wickham, 2011), box plots and QQ plots were generated for each variable to visually assess variance and normality, respectively. Multiple characters, both standard and log-transformed, did not meet normality assumption, thus nonparametric methods were applied to test character significance between species. Levene's F-Test was used assess homogeneity of variance, Kruskal Wallis Chi-Square Test to evaluate character significance between species, and finally dunnTest post-hoc pairwise multiple comparison tests were performed to assess variance estimates of the Kruskal Wallis tests.

Morphometric and meristic data were combined and used to perform principal component analyses (PCA) using the PCA() function in the *FactoMineR* R-package. Two separate PCAs were performed, one on clade I species (*H. multifilis, H. caudovittatus, and H. geminatus*) and the other on clade II species (*H. pseudoaequipinnis, H. springeri, H. bermudensis*) with the unknown *Hypleurochilus* species included in both analyses. The most informative principal components (PC1 and PC2) and characters contributing most to PC variation were identified using their loading values and visualized in a biplot using the R-package *FactoMineR* (Lê et al., 2008).

Review of Museum Specimens

The following institutional codes are referenced to identify specimens in this study – Academy of Natural Sciences of Drexel University (ANSP), Smithsonian National Museum of Natural History (USNM) and Fish and Wildlife Research Institute (FWRI). Museum specimens of *H. pseudoaequipinnis*, *H. springeri*, *H. bermudensis*, and *H. aequipinnis* were reviewed to compare with collected material of new species with morphological features analogous to clade 2. Voucher specimens were acquired on loan from FWRI and ANSP. DNA tissue samples were acquired from FWRI, ANSP and USNM. All other material reviewed and included in this study were collected by the first author and housed at Texas A&M University at Galveston.

DNA Extraction and Sequencing

Genomic DNA was extracted and purified using the Qiagen DNeasy Blood and Tissue Kit according to recommend Spin-Column protocol (Valencia, CA). DNA was extracted from 83 individuals from the seven species examined (Table 7). PCR was performed to amplify protein-encoding gene mitochondrial cytochrome oxidase subunit I (*COI*) and four protein-encoding nuclear genes (*RAG1, PLAG12, MYH6* and *SH3PX3*). PCR products were purified using a polyethylene glycol incubation and centrifuge with an ethanol wash before resuspension. PCR conditions followed Li et al (2007). Consensus sequences were generated, edited and multiple-sequence alignments were performed with MAFFT alignment method in Geneious (version 9.1.8) (Biomatters, 2014). Heterozygous positions of nuclear genes were examined by hand and coded using IUPAC ambiguity codes. Alleles from sequences with multiple heterozygous single nucleotide polymorphisms (SNPs) were resolved using PHASE v.2.1 (Stephens et *al.*, 2001) with

input files generated by the online software package SeqPhase (Flot, 2010). A probability threshold of 0.7 was used for all runs. After alignment and phasing of heterozygous SNPs, the final dataset contained 480 nuclear and 60 mitochondrial alleles combined across all species. PartitionFinder2 was used to determine the best fit partitioning scheme and nucleotide substitution model(s) for each gene based on Bayesian information criterion (BIC) scores (Lanfear et al., 2017). The same partitioning scheme and nucleotide substitution models were used in all phylogenetic analyses.

Species Tree Estimation

Multilocus species-tree analyses were conducted using StarBEAST2 (Ogilvie et al., 2017) included in the BEAST2 software package (version 2.6.0) (Bouckaert et al., 2014). *H. bermudensis* was excluded from StarBEAST2 analyses as only one individual is present in the dataset. BEAUti was used to generate xml files. Substitution models were set according to PartitionFinder2 results. Clock models were linked among loci and tree models were unlinked across all loci. An uncorrelated lognormal clock model was applied to all loci under a birth-death tree prior and a linear with constant root population size model. Four independent Markov chain Monte Carlo (MCMC) analyses using resolved COI sequences and four nuclear genes for 200,000,000 steps (COI data only) and 200,000,000 steps (COI and nuclear markers) and sampled every 1000 generations for a total of 100,000 trees and discarding the first 10% as burn-in. As recommended by Rambaut and Drummond (2009), MCMC output trace files were analyzed using Tracer (version 1.7.1) to confirm convergence based on effective sample size >200 for each parameter and examination of trace files. Maximum clade credibility (MCC) trees with 95% highest posterior probability density and 10% burn-in were generated for separate COI and multilocus MCMC runs using TreeAnnotator (version 2.6.0) (Rambaut & Drummond, 2014). Tree outputs were visualized

in FigTree 1.4.3 (Rambaut, 2014) and final trees were created with the *ggtree* R-package (Yu et al., 2017).

Species Delimitation

Two approaches were used to delimit species – a discovery method (GMYC) and a validation method (BPP). Generalized mixed Yule coalescent (GMYC) is a single-locus method that uses a likelihood approach to identify the boundary between a Yule speciation process and intraspecific coalescence (Pons et al., 2006). The GMYC model was applied to ultrametric COI trees generated in BEAST. Two replicate GMYC runs were performed for two independent analyses using a Yule model (pure birth) using a constant clock model in the 'splits' R-package.

The Bayesian Phylogenetics and Phylogeography (BPP version 3.4a) program employs an MCMC for analyzing nuclear multilocus species delimitation under the MSC model (Yang, 2015). Given the sensitivity of BPP to selected parameters, we ran four runs of both 'A10' and 'A11' analyses each with different θ (ancestral population sizes) and τ_0 (divergence time among species) priors to determine how these parameters might influence species delimitation results in the BPP analyses (Leaché & Fujita, 2010). Each of these four independent analyses were ran twice and we used a phylogeny estimated by replicate StarBEAST2 v2.6 analyses as the guide tree in both 'A10' and 'A11' analyses. Each analysis was set to run 100,000 MCMC generations from different starting seeds with a burn-in period of 8,000 and a sampling interval of 2. In total, sixteen BPP runs were carried out using the four phased nuclear alignments. A species probability value of 0.95 was considered strong support of BPP estimated tree nodes representing lineage splitting or speciation event estimated by BPP analyses.

RESULTS

Morphology

The species under investigation is distinguished from congeners by coloration, snout length, laterosensory pore structure, and density of cephalic sensory pores. We recognize this unreported species as a unique lineage but cannot confirm new species level status due to a lack of comparative material from the eastern Atlantic, specifically that of *H. aequipinnis*. This species shares diagnostic traits and superficial similarities to the oyster blenny (*H. aequipinnis*) of the tropical eastern Atlantic. Thus, we designate this species as likely *H. cf. aequipinnis* until comparative study confirms identity.

Morphological analyses revealed character differentiation that distinguishes c.f. *H. aequipinnis* from congeners included in this study. Pair-wise multiple comparison test results indicate significant variation for multiple traits. *Hypleurochilus pseudoaequipinnis* and *H. cf. aequipinnis* appear to have a significantly greater number of supraorbital cirri (SC) relative to SL than both *H. bermudensis* and *H. springeri* within clade II and similar counts to clade I species. Dorsal notch height (DN) of *H. cf. aequipinnis* did not differ significantly from clade II species but is significantly longer than clade I species. c.f. *H. aequipinnis* and *H. bermudensis* feature deeper body depths at both the head (DAP) and anus (DAN) than *H. pseudoaequipinnis* and *H. springeri* and share similar depths with those of clade 1 species. Peduncle length (PL) is significantly shorter in c.f. *H. aequipinnis* than all other species. *H. cf. aequipinnis* and *H. springeri* feature significantly longer upper jaws (UJL) than either *H. bermudensis* or *H. pseudoaequipinnis* but share similar lengths with those of clade I species. Snout length (SNL) is significantly longer in c.f. *H. aequipinnis* than either species of clade II or *H. caudovittatus.* Interorbit distance (ID) was significantly shorter between *H. cf. aequipinnis* and *H. bermudensis*. Head length (HL), eye

diameter (ED), anal length (AL), and lip thickness (UL) did not vary significantly between *H. cf. aequipinnis* and species in either clade. Morphometric and meristic data for *H. cf. aequipinnis* specimens are reported in Table 9.

Cephalic sensory pore counts relative to size are significantly higher in c *H. cf. aequipinnis* than either species observed increasing in number with body size (Figure 20). A detailed arrangement of pore count and canal system can be seen in Figure 18. Patterns of the cephalic sensory pores can be seen in Figure 19 between the *H. cf. aequipinnis*, *H. multifilis* which shares a similar pore density count with *H. cf. aequipinnis*, and *H. pseudoaequipinnis* as the species most morphological similar to c *H. cf. aequipinnis*. Two lateral line system conditions designated Type A and Type B following Bath (1994) were observed in the examined species; however, the depiction of Type A with anterior portion of the primary canal featuring paired branches each with two sequential pores at the terminal end presented prior in Bath (1994) to an arrangement of the anterior portion of the primary canal and paired branches featuring clusters of 3 or more pores sporadically arranged at the terminal end of each branch. Type A lateral lines were observed in only *H. cf. aequipinnis* and *H. multifilis*. All other species feature the Type B condition with a single pore at the end of each terminal (Figure 19).

Principal component analyses (PCA) of clade I and *H. cf. aequipinnis* resulted in PC1 and PC2 explaining 21.8% and 15.8% of the total variance, respectively (Figure 6). PCA loadings indicate that PC1 was most influenced by DN, CP, DAP, PL, and SNL (>±0.30) and PC2 loadings were most influenced by DAP, DAN, and ED (>±0.30). PC1 and PC2 of clade II and *H. cf. aequipinnis* PCA explained 27.4% and 15.8% of the variance, respectively. According to the PCA loadings, clade II PC1 was most influenced by DAP, DAN, PL, and SNL (>±0.30) while SC, DAN, and AL (>±0.30) most influenced PC2. Clade 2 PCA biplot features a slightly greater partition

than clade I, indicating a greater morphological divergence between species of clade II and *H. cf. aequipinnis*. Both PCA analyses clearly partition *H. cf. aequipinnis* from species of either clade while clade species show clear overlap in the morphospace. Furthermore, in agreement with levels of genetic differentiation, it should be noted that PCA analysis indicates a clear morphological differentiation between *H. cf. aequipinnis* and *H. pseudoaequipinnis*. PC loadings for PCA analyses are presented in Table 8.

Molecular Data

New sequences generated for this study have been deposited in GenBank and Dryad databases. We obtained DNA sequence for the mitochondrial gene COI (597 bp) and nuclear genes MYH6 (615 bp), PLAG12 (564 bp), SH3PX3 (660 bp) and RAG1 (1122 bp). COI Sequence divergence ranged from 5.2 – 5.8% [5.4%]. 68 Hypleurochilus specimens representing seven species and one *Parablennius* specimen as an outgroup were used to generate mtDNA COI phylogenetic trees. 60 individuals for six species of *Hypleurochilus* were used to generate multilocus species trees. Optimal partitioning schemes were determined (in order of codon position) for 1) COI: TRNEF+G, F81, and HKY+G, 2) MYH6: HKY, HKY, and GTR+G, 3) PLAG12: F81, F81, and GTR+G, 4) SH3PX3; HKY, HKY, and HKY+G, and 5) RAG1: F81, F81, and HKY+G.

Phylogenetic Relationships and Species Tree

All multilocus and mtDNA COI phylogenetic reconstructions support *H. cf. aequipinnis* as a monophyletic lineage (PP > 0.95). Posterior effective sample sizes (ESSs) were high (ESS > 250) for all StarBEAST2 and BEAST runs. In addition, these runs recovered the species pair of *H. springeri* and *H. pseudoaequipinnis* as a strongly clade (*pp* = 0.99), and the group of *H. multifilis*,

H. caudovittatus, and *H. geminatus* as a moderately supported clade (*pp* = 0.74), and these two clades are recovered as sister clades with poor support (*pp* = 0.54). Multiple independent runs of mtDNA COI in BEAST recovered trees with similar topology to that of multilocus species trees; however, the placement of clade II shifted between a sister relationship with clade I or that of *H. cf. aequipinnis*. mtDNA-based trees included the addition of a single sequence for species *H. bermudensis* to be included in GMYC species delimitation. The two clades of *H. springeri* and *H. pseudoaequipinnis, H. bermudensis* and the group *of H. multifilis, H. caudovittatus*, and *H. geminatus* were recovered as clades with strong support of (*pp* = 1.00) and (*pp* = 0.99), respectively. There was disagreement on placement of clade II species in relation to other clades or as the outgroup to both clades across multiple tree runs as denoted by lower node posterior probabilities (33 – 41% without *Parablennius outgroup* and <75% with *Parablennius* outgroup) (Figure 22).

Species Delimitation

Discovery and validation species delimitation analyses both support *H. cf. aequipinnis*. as a putative lineage. GMYC analyses assigns all *H. cf. aequipinnis* specimens to a monophyletic lineage and collapses the *H. multifilis* and *H. caudovittatus* lineages into one and *H. springeri* and *H. pseudoaequipinnis* into another. Both GMYC models performed well and provided a significantly better fit to the data than the null models hypothesis of the entire sample being derived from a single species with uniform branching. The Yule prior model analyses are represented by 4 ML clusters (4-4) and 5 entities (5-5) and Constant Coalescent prior model by 4 ML clusters (4-9) and 5 entities (5-10). *H. bermudensis* is represented by only one sequences, thus the number of entities is greater than the number of clusters for both models. Delimited GMYC clusters (*H.*

multifilis/H. caudovittatus, H. geminatus, H. springeri, H. pseudoaequipinnis, and *H. cf. aequipinnis*) were largely congruent with clades defined by tree-based methods and disagreement on placement of *H. cf. aequipinnis* as sister to either clade as the outgroup to both clades across multiple tree runs similar to the tree discordance observed in multiple mtDNA-based COI tree analyses. Single-gene COI tree methods and GMYC analyses were unable accurately place the *H. cf. aequipinnis*. appropriately within the phylogeny with high degree of confidence but does strongly support its monophyletic species status unique to that of other species sampled. GMYC analyses also failed to support the split between H. *multifilis* and H. *caudovittatus* and instead collapsed into a single clade. BPP consistently found very high posterior probabilities (1.0) for species delimitations for all internal nodes across multiple analyses with different algorithms and prior distributions (Figure 22).

Material for *Hypleurochilus cf. aequipinnis* from Northern Gulf of Mexico

All paratypes were collected by JE Carter in April 2018. RIE2595, male, 44.3 mm SL, Galveston Island, Texas, United States, 29°16'09.8"N 94°49'09.8"W, depth 0.5 m; RIE2596, male, 49.0 mm SL, Galveston Island, Texas, United States, 29°16'09.8"N 94°49'09.8"W, depth 0.5 m; RIE2597, female, 48.39 mm SL, Galveston Island, Texas, United States, 29°16'09.8"N 94°49'09.8"W, depth 0.5 m; RIE4366, male, 58.7 mm SL, Galveston Island, Texas, United States, 29°16'09.8"N 94°49'09.8"W, depth 0.5 m; SIO 20-28, male, 54.3 mm SL, Galveston Island, Texas, United States, 29°16'09.8"N 94°49'09.8"W, depth 0.5 m; RIE4365, male, 57.5 mm SL, Galveston Island, Texas, United States, 29°16'09.8"N 94°49'09.8"W, depth 0.5 m; RIE4369, female, 39.80 mm SL, Galveston Island, Texas, United States, 29°16'09.8"N 94°49'09.8"W, depth 0.5 m; RIE 4370, female, 34.8 mm SL, Galveston Island, Texas, United States, 29°16'09.8"N 94°49'09.8"W, depth

0.5 m; RIE4371, female, 39.76 mm SL, Galveston Island, Texas, United States, 29°16'09.8"N 94°49'09.8"W, depth 0.5 m.

Diagnostic Traits and Description of *Hypleurochilus cf. aequipinnis* from Northern Gulf of Mexico

H. cf. aequipinnis can be distinguished from congeners by the following combination of characters: 1) cephalic sensory pore density of 106 to 241 [158 pores] relative to body length (Figure 4), 2) Anterior portion (dorsal spine I – XI) of lateral line canal system features a Type A condition with paired side branches from primary canal with two or more pores at the terminus of each branch; this condition is shared only with a portion of *H. multifilis* material examined (Figure 4), 3) Snout length of 2.9 – 6.5 mm [4.5 mm], 4) Peduncle length of 1.0 – 1.9 mm [1.6 mm], 5) head coloration in life commonly features an almost uniform reddish-orange color of the operculum, large irregularly-shaped reddish-orange spots along the nape extending along the body which fade posteriorly, base color ranging from yellowish to pale grey-flesh tone, upper lip with uniform reddish-orange color except for a thin lateral light grey to white band perpendicular to the maxillary bone extending from a light grey to white streak originating from the post-orbital margin down to the posterior edge of the upper lip, a pair of thin medial bands on the upper lip, snout with irregular reddish-orange streaks terminating at the upper lip margin; yellow pelvic fins (Figures 23 – 25).

Dorsal-fin rays XI-XII, 13 to14 (usually 13); anal-fin rays 15 to 16 (anal-fin spines of sexually mature males enveloped in fleshy rugosities that become larger and develop more folds with increasing size, females with first anal-fin spine embedded in tissue behind gonopore; pelvic-fin rays I, 4; pectoral-fin rays 13; all fin rays unbranched with exception of caudal rays; dorsal fin

deeply indented (mean length of last dorsal spine is 39% length of first segmented dorsal ray; snout length 2.9 – 6.5mm [4.5mm]; supraorbital cirri count 8 to 19 [12]; supraorbital cirri with primary branch of greater length and thickness surrounded by shorter, thinner secondary branches that increase in number with standard length; anterior nostril cirri 2 to 6 [2]; cephalic sensory pore system complex (4 or more pores in each cluster along preopercular margin, high pore density across nape, consecutive pairs of pores along post-orbital margin; number of pores increase with increasing SL) (Figure 20); lateral line canal system with sigmoidal shape nearly straight anteriorly, curving downward near end of pectoral fin and continuing a short distance mid-laterally terminating at sixth anal-fin ray, anterior portion (dorsal spine I – XI) of lateral line canal system features paired side branches from primary canal with two or more pores at the terminus of each branch, the rear portion consists of shore individual short tubes with pore opening on either side (Figure 19); dorsal-fin origin in line with dorsal-most point of gill opening; in males segmented anal-fin rays develop lateral spatulate projections on the distal position of each ray with a dorso-ventral infolding of tissue at the anterior base of the spatulate structure whereas females lack this form having only pointed ray tips; gill opening ending at or slightly above the lower edge of pectoral base with fleshy fold linking lower end of gill opening across isthmus to opening on other side; upper lip broad and deep, its greatest depth at 1.3 – 3.3 mm [2.2 mm]; maxillary incisiform teeth with rounded blunt tips, straight in the anterior view and slightly recurved in the lateral view; dentary incisiform teeth feature pointed tip, incurved in the anterior view and slightly less recurved in lateral view than maxillary teeth; enamel crown comprising half of exposed length; large recurved canines on each side of incisiform series in upper and lower jaw. During captive breeding study, males averaging a size of 30.5 mm SL were observed brooding eggs and exhibiting sexual dimorphism and anal fin rugosities evident of sexual maturity in combtooth blennies.

Morphological data for selected characters of *H. cf. aequipinnis* specimens are provided in Table 9.

Adult color in life of *H. cf. aequipinnis* specimens is pale grey-flesh tone to yellowish base color along the body. Sexual dimorphism in male and female life colors are quite evident; males exhibit orange irregularly shaped spots that fade in color posteriorly along the body but may extend the length of body; almost uniform reddish-orange color of the operculum, large irregularly-shaped reddish-orange spots along the nape extending along the body which fade posteriorly; base color ranging from yellowish to pale grey-flesh tone; lack of clearly defined spots and flush reddish-orange to yellow body cover observed in a portion of Louisiana specimens; upper lip with uniform reddish-orange color except for a thin lateral light grey to white band perpendicular to the maxillary bone extending from a light grey to white streak originating from the post-orbital margin down to the posterior edge of the upper lip; vibrance and extent of reddish-orange head color appears to become more vibrant and complete in high-breeding males; a pair of thin medial bands are present on the upper lip; snout with irregular reddish-orange streaks terminating at the upper lip margin; uniform yellow color of pelvic fins and in some cases pectoral fin; Males feature a black spot between 1st and 2nd dorsal spines of males but may also occur in females as a faint black smudge. Females are drabber in color, featuring the same pale grey to flesh tone base color, but with fewer less-defined orange spots and softer and less extensive reddish-orange color on the face and operculum; banding on dorsal, anal, and caudal fin in females (Figures 23 – 25).

H. cf. aequipinnis co-occurs with *H. multifilis* in both sites of collection and in on artificial reefs off Mexico Beach, Florida. but is most morphologically similar to *H. pseudoaequipinnis* and *H. aequipinnis*. The site of specimens collected from Texas contained both species at the same

shallow depth, but specimens of *H. cf. aequipinnis* were collected at a small size (<20 mm SL), indicating recent settlement at the time of collection. The new species differs from *H. pseudoaequipinnis* primarily in the number of cephalic sensory pores, lateral line pore system and coloration of the head. *H. cf. aequipinnis* features a Type A lateral line pore system and a high density of cephalic sensory pores relative to size whereas *H. pseudoaequipinnis* has a Type B lateral line and fewer cephalic pores relative to size (Figure 19). Coloration between *H. cf. aequipinnis* and *H. pseudoaequipinnis* is most evident in the size and shape of spot along the body; *H. pseudoaequipinnis* features numerous small red to orange spots of uniform round shape along the body and across the head on the snout, upper lip, nape, and operculum whereas *H. cf. aequipinnis* features larger irregularly shaped spots along the body and nape but lacks spots on the snout, upper lip, and operculum (Figure 25 & Table 10).

Comparative Material

Hypleurochilus bermudensis: UF 171047, 32.62 mm SL, Fort Lauderdale, Florida; UF 179526, 34.86 mm SL, Florida Keys, Florida; UF 211808, 32.96 mm SL, Florida Keys, Florida; UF 217685, 25.99 mm SL, Florida Keys, Florida; UF 217982, 30.73 mm SL, Florida Keys, Florida; UF 208206 (36.85 mm) Florida Keys, Florida; RIE 4154, 49.40 mm SL, Palm Beach County, Florida; UF 142426, 18.03 mm SL. *Hypleurochilus pseudoaequipinnis*: UF 62242, 31.30 mm SL, Palm Beach County, Florida; UF 62948, 14.73 mm SL, Martin County, Florida; UF 106101, 14.68 mm SL, Miami, Florida; UF 178784, 22.35 mm SL, St. Thomas Virgin Islands; UF 204072, 34.61 mm SL, Miami, Florida; UF 204625, 24.87 mm SL, Destin, Florida; UF 212568, 15.61 mm SL, Trinidad and Tobago, Trinidad; UF 212997, 26.49 mm SL, Los Roques Islands, Venezuela; UF 214160, 31.85 mm SL, Los Roques Islands, Venezuela; RIE 4118, 30.98 mm SL, Palm Beach

County, Florida; RIE 4151, 38.86 mm SL, Blue Heron Bridge, Florida. *Hypleurochilus springeri*: UF 205490 (1of2), 31.44 mm SL, Exuma Cays, Bahamas; UF 205490 (2of2), 23.46 mm SL, Exuma Cays, Bahamas; UF 213243 (1of2), 32.39 mm SL, Portland County, Jamaica; UF 213243 (2of2), 24.23 mm SL, Portland, Jamaica; UF 227347, 28.40 mm SL, Berry Islands, Bahamas, UF 228882 (1of2), 28.26 mm SL, Los Roques Islands, Venezuela; UF 228882 (2of2), 30.03 mm SL, Los Roques Islands, Venezuela; UF 99976 (1of3), 45.32 mm SL, Palm Beach County, Florida; UF 223091, 20.54 mm SL, Cayos de Albuquerque, Columbia. *Hypleurochilus multifilis*: RIE 1069, 67.65 mm SL, Port Aransas, Texas; RIE 1192, 70.88 mm SL, Port Aransas, Texas; RIE 1331, 71.10 mm SL, Pensacola, Florida; RIE 1333, 66.16 mm SL, Pensacola, Florida; RIE 1346, 42.22 mm SL, Pensacola, Florida; RIE 1354, 42.28 mm SL, Pensacola, Florida; RIE 1685, 41.05 mm SL, Galveston, Texas; RIE 2213, 49.79 mm SL, Galveston, Texas; RIE 3405, 64.50 mm SL, Pensacola, Florida; RIE 3420, 55.17 mm SL, Pensacola, Florida; RIE 3423, 61.25 mm SL, Pensacola, Florida; RIE 3424, 50.65 mm SL, Pensacola, Florida; RIE 3426, 47.02 mm SL, Pensacola, Florida; RIE 4268, 77.34 mm SL, Galveston, Texas. *Hypleurochilus geminatus*: RIE 3841, 43.26 mm SL, Oregon Inlet, North Carolina; RIE 3853, 58.25 mm SL, Oregon Inlet, North Carolina, RIE 3856, 45.54 mm SL, Oregon Inlet, North Carolina; RIE 3870, 40.10 mm SL, Oregon Inlet, North Carolina; RIE 3873, 45.75 mm SL, Oregon Inlet, North Carolina; RIE 3874, 46.31 mm SL, Oregon Inlet, North Carolina; RIE 3875, 43.58 mm SL, Oregon Inlet, North Carolina; RIE 3876, 44.54 mm SL, Oregon Inlet, North Carolina; RIE 3906, 68.78 mm SL, Oregon Inlet, North Carolina; RIE 3908, 71.89 mm SL, Oregon Inlet, North Carolina. *Hypleurochilus caudovittatus*: RIE 1135, 33.39 mm SL, Galveston, Texas; RIE 1401, 50.15 mm SL, Destin, Florida; RIE 2118, 37.84 mm SL, Destin, Florida; RIE 2161, 46.02 mm SL, Panama City, Florida; RIE 2181, 32.70 mm SL, Panama City, Florida; RIE 2443, 48.89 mm SL, Destin, Florida; RIE

2444, 57.96 mm SL, Destin, Florida; RIE 2461, 36.30 mm SL, Destin, Florida; RIE 2923, 23.35 mm SL, Destin, Florida; RIE 2924, 27.51 mm SL, Destin, Florida; RIE 2925, 25.21 mm SL, Destin, Florida.

Distribution of *Hypleurochilus cf. aequipinnis* in the Northwest Atlantic and Gulf of Mexico

Northern Gulf of Mexico from rocky jetties and groins along Galveston Island, Texas shoreline and nearshore artificial reef habitat on offshore platforms off the Louisiana coast. Photographs of fish from Mexico Beach, FL and Bonaire suggest an extensive range of this *Hypleurochilus* blenniid, and a possible recent introduction into the western Atlantic and Gulf of Mexico.

DISCUSSION

An integrated molecular-taxonomic approach reveals that specimens of unknown *Hypleurochilus* species collected from Galveston Island, Texas and Ship Shoal reefs off Louisiana represent a lineage unique from western Atlantic congeners occurring in the northern Gulf of Mexico and the northwestern Atlantic. Initial observations indicated a superficial resemblance to the Atlantic oyster blenny (*H. pseudoaequinnis*), but further examination revealed discrepancies both in morphology and phylogenetic placement indicate these to be distinct taxa. Phylogenetic analyses identify all representative specimens of this unknown species as a putative lineage outside those of the two western Atlantic clades included in this study. This species is morphologically similar to the eastern Atlantic *H. aequipinnis* of the tropical eastern Atlantic, sharing diagnostic traits and superficial similarities; however, material of *H. aequipinnis* was unobtainable for this

study. Thus, we designate this species as likely *H. cf. aequipinnis* until comparative study confirms this identity or distinction.

Morphological analyses of museum and specimens collected in this lab reveal a clear morphological distinction between *H. cf. aequipinnis* and the examined species. Pair-wise multiple comparison tests revealed significant variation in morphometric traits with *H. cf. aequipinnis* featuring a higher cephalic sensory pore count relative to size than any other species and a longer snout length and shorter peduncle length either species in clades 1 and 2. Lateral line pore Type A arrangement appears in all *H. cf. aequipinnis* specimens and a portion of *H. multifilis* while all other species feature Type B. A similar condition to Type A was reported in *H. multifilis* by Bath (1994) but not in either *H. pseudoaequipinnis* or *H. aequipinnis*. Principal component analyses (PCAs) of each clade performed reasonably well to explain variance between groups based on the multivariate dataset of 14 morphometric characters. Despite some differences in internal branching, COI and multilocus trees were largely concordant and phylogenetic analyses support *H. cf. aequipinnis* as a unique species. Both discovery and validation species delimitation methods used provide further support this designation and correctly assign all individuals of c.f. *H. aequipinnis* as a valid operational taxonomic unit.

In addition to identifying *H. cf. aequipinnis* as putative lineage designated to, the phylogenetic relationship between *H. multifilis* and *H. caudovittatus* was examined as the molecular evidence for this distinction not previously been established. GMYC models and COI tree reconstructions suggest a collapse of sequences from these two species into a single lineage. However, multilocus species trees and BPP delimitation method support *H. caudovittatus* as a valid lineage. To our knowledge this is the first instance of a multilocus reconstruction and species

delimitation model involving both *H. multifilis* and *H. caudovittatus*, thus, this study supports the current classification of *H. caudovittatus* as a valid species (Figure 26).

Often overlooked in reef communities, new studies are revealing the ecological structural value of CFs despite their diminutive size and relatively low standing biomass (Brandl et al., 2019). Combtooth blennies are among these essential groups of CFs that contribute disproportionately high amounts of energy to reef food webs through a steady larval supply and high mortality by predation (Brandl et al., 2019). Capable of wide larval dispersal, combtooth blennies are in many cases the most abundant fishes associated with artificial structures in shallow, coastal waters making them prime candidates for biological invasion of new areas beyond their native habitats (Sheehy and Vik 2010). Surveys these artificial structures and natural reefs may at times underreport and/or misidentify combtooth blennies and other CFs due to their reclusive nature and cryptic appearance. To our knowledge, no published reports of fish assemblage associated with artificial structures in the GoM have identified *H. cf. aequipinnis*. The Featherduster blenny (*H. multifilis*) is particularly widespread and abundant among nearshore structures across the northern GoM and reported often where present (Topolski and Szedlmayer, 2004). Specimens from the Ship Shoals platforms in Louisiana were originally identified as *H. multifilis*, of which many specimens were, but closer inspection revealed a portion of these unique. Moreover, studies have revealed that artificial structures serve as transport vectors for non-indigenous species (NIS) to regions beyond their normal range (Pajuelo et al., 2016). With this information in mind and the level of divergence from western Atlantic congeners, it may be the case that *H. cf. aequipinnis* is a recent transplant to the northern GoM introduced via artificial vectors; however, further sampling and research is recommended to further support or refute this conjecture.

CHAPTER IV

CONCLUSIONS

This is the first study to examine gape morphology and patterns of allometric growth during ontogeny of early development in a blenniid species. Further study applying similar metrics to additional blenniid species, namely estuarine species as well as fully marine species, can facilitate a broader understanding of blenniid larval growth dynamics and determine if there is a model of shared pattern of development and timing of rate changes. Florida blenny (*C. saburrae*) larvae reach settlement and complete metamorphosis earlier in development than other studied GoM blennies species and express changes in allometric growth rates of body depth, gape morphology, and pectoral fin length during two thresholds of ontogeny, the completion of notochord flexion and prior to settlement and the onset of metamorphosis. Inflection points of allometric rate change during flexion occurred from 5.80 – 6.09 mm SL while lower jaw length, gape width, and anal length rates changes between 8.28 – 8.57 mm SL. Based upon the shifting allometric growth coefficients, character state morphological features, and larviculture observations, the data indicates that settlement occurs between 8.93 and 9.27 mm SL. Size at settlement by both direct observation and assignment to the settler interval of development occurs at a smaller size and earlier in the ontogeny of *C. saburrae* than those observed in the five coastal species examined in Ditty et al. (2003), suggesting that the estuarine-dependent Florida blenny develops and reaches settlement before combtooth blennies living in fully marine environments. This early life history information may help ecologists and researchers better understand the larval dynamics and food web contributions by *C. saburrae* and relatives occupying estuarine ecosystems in the norther GoM.

Capable of wide larval dispersal, combtooth blennies are in many cases the most abundant fishes associated with artificial structures in shallow, coastal waters making them prime candidates for biological invasion of new areas beyond their native habitats (Sheehy and Vik 2010). Surveys of artificial structures and natural reefs may at times underreport and/or misidentify combtooth blennies and other CFs due to their reclusive nature and cryptic appearance. To our knowledge, no published reports of fish assemblage associated with artificial structures in the GoM have identified *H. cf. aequipinnis* or any species other than *H. multifilis*. The Featherduster blenny (*H. multifilis*) is particularly widespread and abundant among nearshore structures across the northern GoM and reported often where present (Topolski and Szedlmayer, 2004).

Studies have revealed that artificial structures serve as transport vectors for non-indigenous species (NIS) to regions beyond their normal range (Pajuelo et al., 2016). With this information in mind and the level of divergence from western Atlantic congeners, it may be the case that *H. cf. aequipinnis* is a recent transplant to the northern GoM introduced via artificial vectors; however, further sampling and research is recommended to further support or refute this conjecture. The western Atlantic has seen the expansion of two confirmed blenniid species beyond their native ranges into the western Atlantic with established populations. The tessellated blenny (*Hypsoblennius invemar*) has become ubiquitous on artificial structures and nearshore reefs throughout the northern GoM and in parts of the northwestern Atlantic (Sheehy and Vik, 2010). Similar to the report of this study, H. invemar was first documented on oil platforms off Cameron, LA, and Galveston, TX in 1979 and not present at Galveston prior to 1979 (Dennis and Bright, 1988). The muzzled blenny (*Omobranchus punctatus*), native to the Indo-Pacific region, has become a common sight among mangrove habitats in coastal environments of the southwestern Atlantic (Gerhardinger et al., 2006). Both species are associated with biofouling community on

hard substrates in their native ranges and both are generally considered to be introduced through shipping or transport of oilrigs occupying the similar fouling communities often associated with artificial structures. It can be reasoned that the *Hypleurochilus* species, here designated *H. cf. aequipinnis,* has been introduced to the northern GoM in a similar manner, occupying similar biofouling communities in its native range in northwest Africa.

Given the geographic proximity to one another and phenotypic similarities, there is a likelihood that *H. cf. aequipinnis* could be misidentified as *H. pseudoaequipinnis* during future reporting. Data from this study reveal these to be unique taxa and should aid in correct distinction between the two species. Previous taxonomic confusion surrounding *H. pseudoaequipinnis* and H. *aequipinnis* and a lack of genetic information from *H. aequipinnis* leaves further uncertainty now that *H. aequipinnis* has likely transplanted to the northern GoM. To our knowledge only one study has included sequence data of *H. aequipinnis* from Equatorial Guinea (Levy et al. 2013). This study also included *H. pseudoaequipinnis* from São Tomé and Príncipe, yet still classify this tissue as belonging to the western Atlantic *H. pseudoaequipinnis*. This is problematic as no taxonomic evidence for the classification of either fish was presented, calling into question the correct species assignment. Both specimens could have been *H. aequipinnis* as both were collected in the eastern Atlantic (Levy et al. 2013). *H. aequipinnis* sequence data was not comparable as the same genetic markers were not utilized in this study and tissue of *H. aequipinnis* was not available for this study. Only three small specimens acquired from the FMNH of *H. aequipinnis* from the Gulf of Guinea were available in the museum material examined for this study but were not used in morphological analyses due to inadequate sample size and small size. More material of *H. cf. aequipinnis* from the northern GoM will be required to provide a more in-depth analysis of its potential as a new invasive species. Fresh material from the native range of *H. aequipinnis* is also required to confirm

the species identity. Our work and that of past studies has shown that despite the scarcity of studies involving *Hypleurochilus* blennies there is much to learn about the evolutionary history of this group, its cryptic diversity, and distribution potential.

Combtooth blennies are among the essential groups of CRFs that contribute disproportionately high amounts of energy to reef food webs through a steady larval supply and high mortality. New studies are revealing the ecological value of CFs despite their diminutive size and relatively low standing biomass and the studies presented here highlight the importance of continued investigation and description of early life history and development in CRFs to incorporate this information in models of ecosystem function. Moreover, the importance of ongoing genetic and biodiversity inventories on coral reefs and artificial structures is crucial as biogeographic landscapes change and species extend distributions into new areas which can lead to competition with native species and alter ecosystem dynamics. This is particularly relevant to artificial habitats as natural reef habitat is increasingly under threat and artificial habitats grow in number and ecological value.

REFERENCES

Ackerman, J. L., & Bellwood, D. R. (2000). Reef fish assemblages: a re-evaluation using enclosed rotenone stations. Marine Ecology Progress Series, 206, 227-237.

Ahmadia, G. N., Pezold, F. L., & Smith, D. J. (2012). Cryptobenthic fish biodiversity and microhabitat use in healthy and degraded coral reefs in SE Sulawesi, Indonesia. Marine Biodiversity, 42(4), 433-442.

Ajemian, M. J., Wetz, J. J., Shipley-Lozano, B., Shively, J. D., & Stunz, G. W. (2015). An analysis of artificial reef fish community structure along the northwestern Gulf of Mexico shelf: potential impacts of "Rigs-to-Reefs" programs. PloS one, 10(5).

Almada, F., Almada, V. C., Guillemaud, T., & Wirtz, P. (2005). Phylogenetic relationships of the north-eastern Atlantic and Mediterranean blenniids. Biological Journal of the Linnean Society, 86(3), 283-295.

Araujo, G., Vilasboa, A., Britto, M., Bernardi, G., von der Heyden, S., Levy, A., & Floeter, S. (2019). Phylogeny of the comb-tooth blenny genus *Scartella* (Blenniiformes: Blenniidae) reveals several cryptic lineages and a trans-Atlantic relationship. Zoological Journal of the Linnean Society.

Atchison, A. D., Sammarco, P. W., & Brazeau, D. A. (2008). Genetic connectivity in corals on the Flower Garden Banks and surrounding oil/gas platforms, Gulf of Mexico. Journal of Experimental Marine Biology and Ecology, 365(1), 1-12.

Bath, H. (1980). Rediscovery of *Hypleurochilus aequipinnis* (Günther 1861) in West Africa (Pisces: Blenniidae).

Bath, H. (1994). Untersuchung der Arten *Hypleurochilus geminatus* (Wood 1825), *H. fissicornis* (Quoy & Gaimard 1824) und H. aequipinnis (Günther 1861). mit Revalidation von *Hypleurochilus multifilis* (Girard 1858) und Beschreibung von zwei neuen Arten. Senckenbergiana Biologica, 74, 59-85.

Biomatters. (2014). Geneious, version 8.1.9.

Bouckaert, R., Heled, J., Kühnert, D., Vaughan, T., Wu, C.-H., Xie, D., . . . Drummond, A. J. (2014). BEAST 2: a software platform for Bayesian evolutionary analysis. PLoS Comput Biol, 10(4), e1003537.

Brandl, S. J., Goatley, C. H., Bellwood, D. R., & Tornabene, L. (2018). The hidden half: ecology and evolution of cryptobenthic fishes on coral reefs. Biological Reviews, 93(4), 1846-1873.

Brandl, S. J., Tornabene, L., Goatley, C. H., Casey, J. M., Morais, R. A., Côté, I. M., . . . Bellwood, D. R. (2019). Demographic dynamics of the smallest marine vertebrates fuel coral reef ecosystem functioning. Science, 364(6446), 1189-1192.

Brandl, S. J., Casey, J. M., & Meyer, C. P. (2020). Dietary and habitat niche partitioning in congeneric cryptobenthic reef fish species. Coral Reefs, 39(2), 305-317.

Burgess, A. I., & Callan, C. K. (2018). Effects of supplemental wild zooplankton on prey preference, mouth gape, osteological development and survival in first feeding cultured larval yellow tang (*Zebrasoma flavescens*). Aquaculture, 495, 738-748.

Dennis, G. D., & Bright, T. J. (1988). New records of fishes in the northwestern Gulf of Mexico, with notes on some rare species. Gulf of Mexico Science, 10(1), 1.

Ditty, J. G. (2002). Ontogeny and intervals of development in five reef-associated species of blenny from the northern Gulf of Mexico (Teleostei: Blenniidae).

Ditty, J. G., Fuiman, L. A., & Shaw, R. F. (2003). Characterizing natural intervals of development in the early life of fishes: an example using blennies (Teleostei: Blennidae). Paper presented at the The Big Fish Bang, Proceedings of the 26th Annual Larval Fish Conference. Institute of Marine Research, Bergen, Norway.

Ditty, J., Shaw, R., & Fuiman, L. (2005). Larval development of five species of blenny (Teleostei: Blenniidae) from the western central North Atlantic, with a synopsis of blennioid family characters. Journal of Fish Biology, 66(5), 1261-1284.

Eytan, R. I., & Hellberg, M. E. (2010). Nuclear and mitochondrial sequence data reveal and conceal different demographic histories and population genetic processes in Caribbean reef fishes. Evolution: International Journal of Organic Evolution, 64(12), 3380-3397.

Flot, J. F. (2010). SeqPHASE: a web tool for interconverting PHASE input/output files and FASTA sequence alignments. Molecular ecology resources, 10(1), 162-166.

Friendly, M., Fox, J., & Friendly, M. M. (2021). Package 'candisc'.

Fuiman, L. (1983). Growth gradients in fish larvae. Journal of Fish Biology, 23(1), 117-123.

Fuiman, L. A., & Higgs, D. M. (1997). Ontogeny, growth and the recruitment process. In Early life history and recruitment in fish populations (pp. 225-249): Springer.

Gerhardinger, L. C., Freitas, M. O., Andrade, Á. B., & Rangel, C. A. (2006). *Omobranchus punctatus* (Teleostei: Blenniidae), an exotic blenny in the Southwestern Atlantic. Biological Invasions, 8(4), 941-946.

Gill, Theodore. "Catalogue of the Fishes of the Eastern Coast of North America, from Greenland to Georgia." *Proceedings of the Academy of Natural Sciences of Philadelphia*, vol. 13, 1861, pp. 1–63.

Grabowski, T. B. (2002). Temporal and spatial variability of blenny (Perciformes: Labrisomidae and Blenniidae) assemblages on Texas jetties. Texas A&M University,

Groover, E. M., Alo, M. M., Ramee, S. W., Lipscomb, T. N., Degidio, J.-M. L., & DiMaggio, M. A. (2021). Development of early larviculture protocols for the melanurus wrasse Halichoeres melanurus. Aquaculture, 530, 735682.

Guma'a, S. (1978). The food and feeding habits of young perch, *Perca fluviatilis*, in Windermere. Freshwater Biology, 8(2), 177-187.

Harding, J. M. (1999). Selective feeding behavior of larval naked gobies, Gobiosoma bosc, and blennies Chasmodes bosquianus and Hypsoblennius hentzi: preferences for bivalve veligers. Marine Ecology Progress Series, 179, 145-153.

Hastings, P. A., & Springer, V. G. (2009). Systematics of the Blenniidae (combtooth blennies). The biology of blennies, 69, 91.

Hastings, P. A., & Springer, V. G. (2009). Systematics of the Blennioidei and the included families Dactyloscopidae, Chaenopsidae, Clinidae and Labrisomidae. The Biology of Blennies, Science Publishers, Enfield, New Hampshire, 3-30.

Hay, D. (1981). Effects of capture and fixation on gut contents and body size of Pacific herring larvae. Rapports et Procès-Verbaux des Réunions, Conseil International pour l'Exploration de la Mer, 178, 395-400.

Hubbs, C., & Lagler, K. (1958). Fishes of the Great Lakes Region. Ann Arbor: University of Michigan Press. xv+ 213 pp.

Hundt, P. J., Iglésias, S. P., Hoey, A. S., & Simons, A. M. (2014). A multilocus molecular phylogeny of combtooth blennies (Percomorpha: Blennioidei: Blenniidae): multiple invasions of intertidal habitats. Molecular phylogenetics and evolution, 70, 47-56.

Kaiser, M. J., & Pulsipher, A. G. (2005). Rigs-to-reef programs in the Gulf of Mexico. Ocean Development & International Law, 36(2), 119-134.

Kassambara, A., & Kassambara, M. A. (2020). Package 'ggpubr'.

Kiørboe, T., Munk, P., & Støttrup, J. G. (1985). First feeding by larval herring *Clupea harengus* L. Dana, 5, 95-107.

Krebs, J. M., & Turingan, R. G. (2003). Intraspecific variation in gape–prey size relationships and feeding success during early ontogeny in red drum, Sciaenops ocellatus. Environmental Biology of Fishes, 66(1), 75-84.

Lanfear, R., Frandsen, P. B., Wright, A. M., Senfeld, T., & Calcott, B. (2017). PartitionFinder 2: new methods for selecting partitioned models of evolution for molecular and morphological phylogenetic analyses. Molecular Biology and Evolution, 34(3), 772-773.

Lê S, Josse J, Husson F (2008). "FactoMineR: A Package for Multivariate Analysis." Journal of Statistical Software, 25(1), 1–18.

Leaché, A. D., & Fujita, M. K. (2010). Bayesian species delimitation in West African forest geckos (*Hemidactylus fasciatus*). Proceedings of the Royal Society B: Biological Sciences, 277(1697), 3071-3077.

Léger, P., Vanhaecke, P., & Sorgeloos, P. (1983). International study on Artemia XXIV. Cold storage of live Artemia nauplii from various geographical sources: Potentials and limits in aquaculture. *Aquacultural engineering*, *2*(1), 69-78.

Lencer, E. S., & McCune, A. R. (2018). An embryonic staging series up to hatching for *Cyprinodon variegatus*: An emerging fish model for developmental, evolutionary, and ecological research. Journal of morphology, 279(11), 1559-1578.

Levy, A., Wirtz, P., Floeter, S. R., & Almada, V. C. (2011). The Lusitania Province as a center of diversification: The phylogeny of the genus *Microlipophrys* (Pisces: Blenniidae). Molecular phylogenetics and evolution, 58(2), 409-413.

López-Herrera, D. L., de la Cruz-Agüero, G., Aguilar-Medrano, R., Navia, A. F., Peterson, M. S., Franco-López, J., & Cruz-Escalona, V. H. (2021). Ichthyofauna as a Regionalization Instrument of the Coastal Lagoons of the Gulf of Mexico. Estuaries and Coasts, 1-16.

Maechler, M. (2019). Finding Groups in Data": Cluster Analysis Extended Rousseeuw et. R package version, 2(0).

Moorhead, J. A., & Zeng, C. (2010). Development of captive breeding techniques for marine ornamental fish: a review. Reviews in Fisheries Science, 18(4), 315-343.

Moorhead, J. A., & Zeng, C. (2017). Establishing larval feeding regimens for the Forktail Blenny *Meiacanthus atrodorsalis* (Günther, 1877): effects of Artemia strain, time of prey switch and co-feeding period. Aquaculture research, 48(8), 4321-4333.

Muggeo, V. M. (2008). Segmented: an R package to fit regression models with broken-line relationships. R news, 8(1), 20-25.

Nowosad, J., Kupren, K., Biegaj, M., & Kucharczyk, D. (2020). Allometric and ontogenetic larval development of common barbel during rearing under optimal conditions. Animal, 100107.

Ogilvie, H. A., Bouckaert, R. R., & Drummond, A. J. (2017). StarBEAST2 brings faster species tree inference and accurate estimates of substitution rates. Molecular Biology and Evolution, 34(8), 2101-2114.

Olivotto, I., Piccinetti, C. C., Avella, M. A., Rubio, C. M., & Carnevali, O. (2010). Feeding strategies for striped blenny *Meiacanthus grammistes* larvae. Aquaculture research, 41(9), e307-e315.

Osse, J., & Van den Boogaart, J. (1995). Fish larvae, development, allometric growth, and the aquatic environment. Paper presented at the ICES Marine Science Symposia.

Osse, J., & van den Boogaart, J. G. (2004). Allometric growth in fish larvae: timing and function. Paper presented at the development of form and function in fishes and the question of larval adaptation.

Pajuelo, J. G., González, J. A., Triay-Portella, R., Martín, J. A., Ruiz-Díaz, R., Lorenzo, J. M., & Luque, Á. (2016). Introduction of non-native marine fish species to the Canary Islands waters through oil platforms as vectors. Journal of Marine Systems, 163, 23-30.

Peters, K. M. (1981). Reproductive biology and developmental osteology of the Florida blenny, *Chasmodes saburrae* (Perciformes: Blenniidae). Gulf of Mexico Science, 4(2), 2.

Penning, M., Reid, G., Koldewey, H., Dick, G., Andrews, B., Arai, K., & Tanner, K. (2009). Turning the tide: a global aquarium strategy for conservation and sustainability. World Association of Zoos and Aquariums, Berna, Suiza.

Pillar, V. D. (1999). How sharp are classifications? Ecology, 80(8), 2508-2516.

Pinheiro, H. T., Gasparini, J. L., & Rangel, C. A. (2013). A new species of the genus *Hypleurochilus* (Teleostei: Blenniidae) from Trindade Island and Martin Vaz archipelago, Brazil. Zootaxa, 3709(1), 095-100.

Pons, J., Barraclough, T. G., Gomez-Zurita, J., Cardoso, A., Duran, D. P., Hazell, S., Vogler, A. P. (2006). Sequence-based species delimitation for the DNA taxonomy of undescribed insects. Systematic biology, 55(4), 595-609.

Putt, R. E. (1982). *A quantitative study of fish populations associated with a platform within Buccaneer oil field, northwestern Gulf of Mexico* (Doctoral dissertation, Texas A&M University).

Rambaut, A. (2014). FigTree 1.4. 2 software. Institute of Evolutionary Biology, Univ. Edinburgh.

Rambaut, A., & Drummond, A. (2014). TreeAnnotator v1. 8.2. In: UK: BEAST.

Randall, J. E. (1966). The West Indian blenniid fishes of the genus *Hypleurochilus*, with the description of a new species.

Rauch, T. J. (2004). Predators and the distribution and abundance of blennies on offshore petroleum platforms. Gulf and Caribbean Research, 16(2), 141-146.

Rhyne, A. L., Tlusty, M. F., Schofield, P. J., Kaufman, L., Morris Jr, J. A., & Bruckner, A. W. (2012). Revealing the appetite of the marine aquarium fish trade: the volume and biodiversity of fish imported into the United States. PloS one, 7(5), e35808.

Rooker, J., Dokken, Q., Pattengill, C., & Holt, G. (1997). Fish assemblages on artificial and natural reefs in the Flower Garden Banks National Marine Sanctuary, USA. Coral Reefs, 16(2), 83-92.

Rowlands, W. L., Dickey-Collas, M., Geffen, A., & Nash, R. (2006). Gape morphology of cod *Gadus morhua* L., haddock *Melanogrammus aeglefinus* (L.) and whiting *Merlangius merlangus* (L.) through metamorphosis from larvae to juveniles in the western Irish Sea. Journal of Fish Biology, 69(5), 1379-1395.

Saruwatari, T. (1997). Cyanine blue: a versatile and harmless stain for specimen observation. *Copeia, 1997*, 840-841.

Schael, D. M., Rudstam, L. G., & Post, J. R. (1991). Gape limitation and prey selection in larval yellow perch (*Perca flavescens*), freshwater drum (*Aplodinotus grunniens*), and black

crappie (*Pomoxis nigromaculatus*). *Canadian Journal of Fisheries and Aquatic Sciences, 48*(10), 1919-1925.

Sheehy, D. J., & Vik, S. F. (2010). The role of constructed reefs in non-indigenous species introductions and range expansions. Ecological Engineering, 36(1), 1-11.

Shirota, A. (1970). Studies on the mouth size of fish larvae. Bull. Jpn. Soc. Sci. Fish., 36, 353-369.

Solomon, F. N., Rodrigues, D., Gonçalves, E. J., Serrão, E. A., & Borges, R. (2017). Larval development and allometric growth of the black-faced blenny *Tripterygion delaisi*. Journal of Fish Biology, 90(6), 2239-2254.

Sorgeloos, P., Dhert, P., & Candreva, P. (2001). Use of the brine shrimp, *Artemia* spp., in marine fish larviculture. Aquaculture, 200(1-2), 147-159.

Springer, V. G., & Gomon, M. F. (1975). Revision of the blenniid fish genus *Omobranchus*, with descriptions of three new species and notes on other species of the tribe Omobranchini. Smithsonian Contributions to Zoology.

Sprugel, D. (1983). Correcting for bias in log-transformed allometric equations. Ecology, 64(1), 209-210.

Stephens, M., Smith, N. J., & Donnelly, P. (2001). A new statistical method for haplotype reconstruction from population data. The American Journal of Human Genetics, 68(4), 978-989.

Stevens, E. G., & Moser, H. G. (1982). Observations on the early life history of the mussel blenny, hypsoblennius jenkinsi, and the bay blenny, hypsoblennius gentilis, from specimens reared in the laboratory.

Strauss, R. E., & Fuiman, L. A. (1985). Quantitative comparisons of body form and allometry in larval and adult Pacific sculpins (Teleostei: Cottidae). Canadian Journal of Zoology, 63(7), 1582-1589.

Suzuki, R., & Shimodaira, H. (2006). Pvclust: an R package for assessing the uncertainty in hierarchical clustering. Bioinformatics, 22(12), 1540-1542.

Tavolga, W. N. (1958). Underwater sounds produced by males of the blenniid fish, *Chasmodes bosquianus*. Ecology, 39(4), 759-760.

Tellock, J., & Alig, F. (1998). Aquaculture potential of the lyretail blenny, *Meiacanthus atrodorsalis*, for the marine ornamental fish trade. Paper presented at the Aquaculture'98 book of abstracts.

Topolski, M. F., & Szedlmayer, S. T. (2004). Vertical distribution, size structure, and habitat associations of four Blenniidae species on gas platforms in the northcentral Gulf of Mexico. Environmental biology of fishes, 70(2), 193-201.

Van Snik, G., Van Den Boogaart, J., & Osse, J. (1997). Larval growth patterns in *Cyprinus carpio* and *Clarias gariepinus* with attention to the finfold. Journal of Fish Biology, 50(6), 1339-1352.

Van Tassell, J., Robertson, D.R.(2019). Shorefishes of the Greater Caribbean: an online system.

Ripley, B., Venables, B., Bates, D. M., Hornik, K., Gebhardt, A., Firth, D., & Ripley, M. B. (2013). Package 'mass'. *Cran r*, *538*, 113-120.

Von Linden, J., DiMaggio, M., Patterson, J., & Ohs, C. (2020). Aquaculture applications of the Family Blenniidae. EDIS, 2020(4).

Watson, W. (1987). Larval development of the endemic Hawaiian blenniid, *Enchelyurus brunneolus* (Pisces: Blenniidae: Omobranchini). Bulletin of marine science, 41(3), 856-888.

Wickham, H. (2011). ggplot2. *Wiley Interdisciplinary Reviews: Computational Statistics*, *3*(2), 180-185.

Wittenrich, M. L., & Turingan, R. G. (2011). Linking functional morphology and feeding performance in larvae of two coral-reef fishes. Environmental Biology of Fishes, 92(3), 295-312.

Yang, Z. (2015). The BPP program for species tree estimation and species delimitation. Current Zoology, 61(5), 854-865.

Yu, G., Smith, D. K., Zhu, H., Guan, Y., & Lam, T. T. Y. (2017). ggtree: an R package for visualization and annotation of phylogenetic trees with their covariates and other associated data. Methods in Ecology and Evolution, 8(1), 28-36.

Yúfera, M., & Darias, M. (2007). The onset of exogenous feeding in marine fish larvae. Aquaculture, 268(1-4), 53-63.

APPENDIX A

TABLES

Table 1. Summary information for ontogenetic index values and character state scores for the Florida blenny (*C. saburrae*). Intervals (Larvae, Metamorphs, Settlers) were determined by cluster analysis of total character scores for 10 discrete morphological characters. Total character score is the sum of scores assigned each of the 10 characters listed in used in Ditty et al., 2003. All sizes are mm SL and statistics provided are mean and (range). Size at juvenile (L_{juv}) used to designate the start of the juvenile period was determined using wild-caught specimens of *C. saburrae* collected from the same region as that of broodstock used in this study.

Category	*Chasmodes saburrae*
Overall summary	
Sample size	115
Size range	3.37 - 14.49
Range of ontogenetic index	41 - 89
Range of total character score	0 - 35[1]
All Larvae	
Cluster Interval	Larvae
Sample size	52
Size	4.87 (3.37 - 6.40)
Ontogenetic index	52.3 (40.6 - 62.0)
Total character score	4.6 (0 - 11)
Preflexion Larvae	
Cluster Interval	Larvae
Sample size	16
Size	3.81 (3.37 - 4.32)
Ontogenetic index	44.5 (40.6 - 48.8)
Total character score	0.4 (0.0 - 2.0)
Flexion Larvae	
Cluster Interval	Larvae
Sample size	19
Size	5.05 (4.12 - 5.75)
Ontogenetic index	53.9 (47.3 - 58.4)
Total character score	4.9 (1.0 - 8.0)
Postflextion Larvae	
Cluster Interval	Larvae
Sample size	17
Size	5.68 (5.17 - 6.40)
Ontogenetic index	57.9 (54.8 - 62.0)
Total character score	8.2 (6.0 - 11.0)
Metamorphs	
Cluster Interval	Metamorph
Sample size	48
Size range	7.63 (6.28 - 9.27)
Ontogenetic index	67.7 (61.3 - 74.3)
Total character score	17.4 (13.0 - 26.0)
Settlers	
Cluster Interval	Settler
Sample size	15
Size range	11.24 (8.67 - 14.49)
Ontogenetic index	80.3 (72.1 - 89.2)
Total character score	32.1 (28.0 - 35.0)
Size at juvenile (L_{juv})	20.0

Table 2. Significance of canonical roots in discriminating intraspecific intervals of development in the Florida blenny (*C. saburrae*) computed in this study and those of five species of blenny from the northern Gulf of Mexico included in Ditty (2002) and Ditty et al., (2005) adapted for this study.

Taxa	Canonical Root	Eigenvalue	Variability Explained (%)	Canonical Correlation	Chi-square	p-value	Author
Intraspecific							
Hypsoblennius invemar	1	83.9	91.7	0.994	253.9	<0.0001	Ditty, 2002
	2	7.6	100	0.943	82.9	<0.0001	
Hypsoblennius ionthas	1	53.9	92.8	0.991	149.7	<0.0001	Ditty, 2002
	2	4.2	100	0.898	43.5	<0.0001	
Hypleurochilus multifilis	1	26.5	91.8	0.982	142.6	<0.0001	Ditty, 2002
	2	2.4	100	0.893	28.3	<0.0001	
Parablennius marmoreus	1	70	95.4	0.993	192.5	<0.0001	Ditty, 2002
	2	3.4	100	0.879	49.7	<0.0001	
Scartella cristata	1	23.5	84.7	0.979	102	<0.0001	Ditty, 2002
	2	4.2	100	0.9	34.8	<0.0001	
Chasmodes saburrae	1	18.5	71.2	0.949	122.062	<0.0001	this study
	2	7.5	100.0	0.88	86.394	<0.0001	

Table 3. Canonical root means computed from discriminate function analysis used to discriminate intervals of development for Florida blenny (*C. saburrae*). Distance between means indicates contribution of the canonical variate to separate intervals. Root means contributing most to separation are in bold.

Interval of Development	*N* specimens	Size range (mm SL)	Root 1	Root 2
Larvae	52	3.37 - 6.40	-3.379	2.0501
Metamorphs	48	6.28 - 9.27	0.57721	**-3.1668**
Settlers	15	8.67 - 14.49	**9.86682**	3.0267

Table 4. Standardized coefficients for each of the 10 characters included in Discriminant Function Analysis of character states from the Florida blenny (*C. saburrae*) computed in this study and five species of blenny from the northern Gulf of Mexico included in Ditty (2002) and Ditty et al., (2005) adapted for this study. Relative contribution of a character to each canonical root is listed and primary discriminating characters are in bold.

	Intraspecific coefficients					
Species	*Chasmodes saburrae*		*Hypsoblennius invemar*		*Hypsoblennius ionthas*	
Author	this study		Ditty, 2002		Ditty, 2002	
Character	**Root 1**	**Root 2**	**Root 1**	**Root 2**	**Root 1**	**Root 2**
Preopercular spine	0.296	**-0.520**	-0.571	0.495	0.144	-0.085
Orbital cirrus	**0.463**	0.319	-0.012	0.698	0.373	-0.318
Nasal cirrus	- -	- -	**-1.006**	**1.104**	0.041	**0.708**
Number of teeth	**0.610**	-0.120	0.341	-0.128	-0.313	-0.293
Dorsal/anal rays	-0.145	0.307	-0.594	-0.678	**0.899**	-0.196
Pectoral fin	0.033	-0.343	0.574	**-1.405**	0.077	**0.822**
Pelvic pigmentation	0.174	0.186	-0.491	-0.500	**-1.148**	0.388
Caudal fin	-0.063	**-0.451**	-0.637	0.454	**1.148**	-0.610
Body pigmentation	**0.451**	**0.718**	-0.145	-0.108	0.078	0.629
Lateral line	-0.014	0.170	0.673	0.380	0.235	-0.666
dorsal spines	-0.043	**0.557**	- -	- -	- -	- -
Species	*Hypleurochilus multifilis*		*Scartella cristata*		*Parablennius marmoreus*	
Author	Ditty, 2002		Ditty, 2002		Ditty, 2002	
Character	**Root 1**	**Root 2**	**Root 1**	**Root 2**	**Root 1**	**Root 2**
Preopercular spine	0.264	**0.981**	**-0.445**	**0.909**	0.476	-0.506
Orbital cirrus	0.350	0.243	- -	- -	**-1.192**	0.151
Nasal cirrus	-0.013	-0.143	0.089	0.190	0.581	-0.109
Number of teeth	-0.128	-0.220	-0.279	**0.745**	0.333	**-0.665**
Dorsal/anal rays	0.296	-0.211	-0.200	-0.455	**-1.077**	**0.755**
Pectoral fin	-0.036	-0.070	-0.130	-0.157	0.120	0.102
Pelvic pigmentation	0.037	0.129	0.117	-0.369	0.455	-0.237
Caudal fin	**0.800**	0.146	0.099	0.070	-0.457	0.096
Body pigmentation	0.115	**-0.921**	**-0.447**	-0.081	**-0.936**	0.134
Lateral line	-0.119	**0.721**	-0.355	-0.672	-0.120	-0.474
dorsal spines	- -	- -	- -	- -	- -	- -

Table 5. Threshold estimates for timing and variation of settlement as indicated by three scaling metrics applied to the Florida blenny (*C. saburrae*) in this study and five species of blenny from the northern Gulf of Mexico included in Ditty (2002) and Ditty et al., (2005) adapted for this study. Thresholds were calculated from means and (coefficients of variation) of the three largest metamorphs and three smallest settlers based on standard length (SL).

Species	Habitat	Development Threshold	SL (mm) Mean (CV)	Total Character State Score Mean (CV)	Ontogenetic Index Mean (CV)	Author
Chasmodes saburrae	Estuarine	Larvae Metamorph	6.32 (1.3%)	11.3 (3.3%)	61.5 (0.7%)	this study
Chasmodes saburrae	Estuarine	Metamorph - Settler	9.2 (2.3%)	23.7 (24.9%)	74.2 (1.0%)	this study
Hypsoblennius invemar	Coastal	Metamorph - Settler	12.5 (6.0%)	25.3 (17.2%)	87.4 (2.4%)	Ditty, 2002
Hypsoblennius ionthas	Coastal/Estuarine	Metamorph - Settler	11.7 (5.1%)	25.0 (32.0%)	86.8 (2.0%)	Ditty, 2002
Hypleurochilus multifilis	Coastal	Metamorph - Settler	12.5 (4.6%)	30.2 (16.6%)	86.6 (1.8%)	Ditty, 2002
Scartella cristata	Coastal	Metamorph - Settler	11.0 (6.2%)	25.7 (14.3%)	82.8 (2.6%)	Ditty, 2002
Parablennius marmoreus	Coastal	Metamorph - Settler	20.1 (7.1%)	29.4 (18.6%)	86.8 (0.5%)	Ditty, 2002

Table 6. Regression analysis of measure morphometric characters from the Florida blenny (*C. saburrae*). Power functions computed from linear and nonlinear regression analysis on $\log_{10}$ transformed data, coefficient of determination (R^2), associated ANOVA with *F*-statistic, AIC scores and back-transformed inflection point in mm SL are provided. All significances were at the $p < 0.01$ level.

Character	Regression Model	R^2	AIC	Segment	n	b	SL: point of inflection (mm)	Power Function
Head length (HL)	single	0.977	-466.6	- -	115	1.39	- -	$y = 0.125x^{1.39}$
	segmented	0.981	-484.5	segment 1	49	1.58	<6.09 mm SL	$y = 0.094x^{1.58}$
		- -	- -	segment 2	66	1.26	>6.09 mm SL	$y = 0.167x^{1.26}$
Pectoral length (PL)	single	0.943	-283.7	- -	100[1]	1.59	- -	$y = 0.068x^{1.59}$
	segmented	0.959	-317.8	segment 1	40	2.14	<5.81 mm SL	$y = 0.029x^{2.14}$
		- -	- -	segment 2	60	1.32	>5.81 mm SL	$y = 0.123x^{1.32}$
Depth at anus (DAN)	single	0.964	-400.1	- -	115	1.48	- -	$y = 0.088x^{1.48}$
	segmented	0.975	-440.7	segment 1	49	1.82	<6.01 mm SL	$y = 0.051x^{1.82}$
		- -	- -	segment 2	66	1.24	>6.01 mm SL	$y = 0.145x^{1.24}$
Depth at pelvic (DAP)	single	0.983	-514.3	- -	115	1.32	- -	$y = 0.129x^{1.32}$
	segmented	0.984	-523.2	segment 1	46	1.45	<5.81 mm SL	$y = 01.06x^{1.45}$
		- -	- -	segment 2	69	1.24	>5.81 mm SL	$y = 0.152x^{1.24}$
Anal length (AL)	single	0.985	-543.9	- -	115	1.23	- -	$y = 0.272x^{1.23}$
	segmented	0.988	-572.4	segment 1	93	1.17	<8.57 mm SL	$y = 0.302x^{1.17}$
		- -	- -	segment 2	22	1.48	>8.57 mm SL	$y = 0.155x^{1.48}$
Gape width (GW)	single	0.961	-393.8	- -	115	1.45	- -	$y = 0.041x^{1.45}$
	segmented	0.964	-401.5	segment 1	89	1.37	<8.33 mm SL	$y = 0.047x^{1.37}$
		- -	- -	segment 2	26	1.73	>8.33 mm SL	$y = 0.022x^{1.73}$
Snout length (SNL)	single	0.902	-283.5	- -	115	1.44	- -	$y = 0.024x^{1.44}$
	segmented	0.954	-364.8	segment 1	46	2.13	<5.81 mm SL	$y = 0.008x^{2.13}$
		- -		segment 2	58	1.18	5.81 mm SL< X <9.55 mm SL	$y = 0.044x^{1.18}$
		- -		segment 3	11	0.54	>9.55 mm SL	$y = 0.187x^{0.54}$
Eye diameter	single	0.966	-482.7	- -	115	1.06	- -	$y = 0.093x^{1.06}$
Upper jaw length	single	0.940	-418.0	- -	115	1.05	- -	$y = 0.090x^{1.05}$
	segmented	0.968	-487.7	segment 1	47	1.46	<5.86 mm SL	$y = 0.048x^{1.46}$
		- -	- -	segment 2	68	0.80	>5.86 mm SL	$y = 0.153x^{0.80}$
Lower jaw length	single	0.923	-337.2	- -	115	1.31	- -	$y = 0.034x^{1.31}$
	segmented	0.929	-343.3	segment 1	88	1.21	<8.28 mm SL	$y = 0.043x^{1.21}$
		- -	- -	segment 2	27	1.63	>8.28 mm SL	$y = 0.018x^{1.63}$
Gape size Guma'a (G_{SG})	single	0.940	-437.3	- -	115	1.15	- -	$y = 22.33x^{1.15}$
	segmented	0.963	-453.6	segment 1	25	1.52	<4.94 mm SL	$y = 52.772x^{1.52}$
		- -	- -	segment 2	90	1.04	>4.94 mm SL	$y = 112.253x^{1.04}$

[1] linear and segmented regressions were performed on a portion (n = 100) of larval specimens based on measurability of pectoral length from captured images.

Table 7. List of recognized *Hypleurochilus* species. Species and counts of specimens used in morphological and molecular analyses during this study including specimens designated *H. cf. aequipinnis* based on similarity to description of recognized *H. aequipinnis* from which no know genetic tissue is available.

Species	Distribution	Morphological Data	Sequence Data
H. bermudensis (Bebbe & Tee-Van, 1933)	Western Atlantic: Bermuda to SW GoM	n = 7	n = 1 [COI]
H. springeri (Randall, 1966)	Western Atlantic: Florida to S Caribbean	n = 9	n = 6 [COI, RAG1, MYH6, PLAG12, SH3PX3]
H. pseudoaequipinnis (Bath, 1994)	Western Atlantic: GoM to Brazil	n = 11	n = 6 [COI, RAG1, MYH6, PLAG12, SH3PX3]
H. multifilis (Girard, 1858)	Western Atlantic: GoM	n = 14	n = 15 [COI, RAG1, MYH6, PLAG12, SH3PX3]
H. caudovittatus (Bath, 1994)	Western Atlantic: W Florida	n = 11	n = 9 [COI, RAG1, MYH6, PLAG12, SH3PX3]
H. geminatus (Wood, 1825)	Western Atlantic: East Coast US	n = 10	n = 10 [COI, RAG1, MYH6, PLAG12, SH3PX3]
H. aequipinnis (Gunther, 1861) *(*GoM specimens in this study designated *H. cf. aequipinnis*)	Eastern Atlantic: Tropical Africa; Western Atlantic: Northern GoM	n = 23*	n = 20 [COI, RAG1, MYH6, PLAG12, SH3PX3]
H. brasil (Pinheiro et al., 2013)+A10:A12	Western Atlantic: Trinidade Island Martine Vas Archipelago Brazil	- -	- -
H. fissicornis (Quoy & Gaimard, 1824)	Western Atlantic: Brazil to Uruguay and Argentina	- -	- -
H. bananensis (Fowler, 1923)	Eastern Atlantic: Tropical Africa and Mediterranean	- -	- -
H. langi (Fowler, 1923)	Eastern Atlantic: Tropical Africa	- -	- -

**H. cf. aequipinnis specimens used for morphological data collection includes 11 individuals for in-hand observation and 12 individuals with photograph only observation.*

Table 8. Loading scores of four principal components computed from Principal Component Analysis (PCA) for clades I and II, both of which included specimens of likely *H. cf. aequipinnis* for comparison.

	Clade 1				Clade 2			
Morphometric Character	**PC1**	**PC2**	**PC3**	**PC4**	**PC1**	**PC2**	**PC3**	**PC4**
Dorsal Notch	0.2435	-0.2102	-0.3158	0.2352	**0.466**	-0.155	0.141	-0.158
Supraorbital Cirri	-0.0965	**0.4859**	0.2846	-0.0218	-0.135	-0.038	-0.391	-0.337
Cephalic Pores	-0.2800	0.2819	0.0090	0.4770	**-0.414**	0.187	-0.111	-0.028
Depth at Pelvic	**0.4162**	-0.2667	-0.2427	-0.1099	**-0.420**	**-0.335**	0.059	-0.114
Depth at Anus	**-0.3210**	**-0.4260**	-0.0875	-0.3206	-0.203	**-0.610**	0.012	0.089
Head Length	0.2551	-0.1941	0.2660	0.1687	0.123	-0.241	-0.288	0.430
Eye Diameter	0.0849	0.2461	-0.4426	0.3334	0.022	**0.499**	-0.175	-0.302
Anal Length	0.0726	**-0.4318**	0.1863	0.5889	0.013	0.095	-0.487	0.157
Peduncle Length	**0.3783**	-0.1546	-0.1464	-0.1066	**0.447**	-0.012	0.226	-0.075
Maxillary Length	**-0.3184**	-0.2246	0.0506	0.2965	-0.098	0.088	0.403	0.102
Upper Lip Thickness	-0.1872	0.0015	-0.3603	0.0034	-0.081	0.225	0.298	0.485
Snout Length	**-0.4009**	0.1267	-0.1610	0.1263	**-0.378**	0.197	0.329	-0.028
Interorbital Distanct	0.2427	0.1124	-0.5212	-0.0104	0.020	0.204	-0.221	0.536
Eigenvalue	1.8870	1.4335	1.3329	1.0460	1.6842	1.4316	1.3506	1.1486
Proportion	**0.2739**	**0.1581**	0.1367	0.0842	**0.2182**	**0.1576**	0.1403	0.1015
Cumulative	0.2739	0.4320	0.5687	0.6528	0.2182	0.3759	0.5162	0.6177

Table 9. Morphometric and meristic character data from specimens designated *H. cf. aequipinnis*. All measurements are measured to the nearest 0.01 mm.

Specimen	RIE 4389	RIE 4366	RIE 2596	RIE 2597	RIE 2598	RIE 4365	RIE 4371	RIE 4367	RIE 2598	RIE 4370	RIE 4369
Sex	Male	Male	Male	Female	Female	Male	Male	Male	Female	Female	Female
Standard length	52.5	44.3	49.0	48.4	38.5	57.5	58.7	54.3	39.8	34.8	39.8
Total length	59.9	51.9	57.2	55.9	44.8	67.3	67.8	60.9	45.1	39.3	46.7
Head length	16.9	14.0	15.2	13.7	10.7	18.4	17.8	15.0	11.8	9.2	11.2
Depth at Pelvic Insertion	16.5	14.7	14.7	13.9	10.7	19.4	17.3	16.9	10.8	8.3	10.2
Depth at Anus	14.0	12.2	12.2	10.9	8.9	16.9	15.2	14.0	9.0	6.4	8.3
Anal length	27.5	25.6	27.1	25.8	21.8	29.7	29.9	29.2	22.9	19.2	21.2
Snout length	5.5	4.8	4.7	4.2	3.1	6.5	5.9	5.0	3.8	2.9	3.7
Peduncle length	1.7	1.7	1.9	1.8	1.0	1.9	1.7	1.6	1.5	1.4	1.4
Orbit diameter	3.5	3.0	3.0	3.3	2.6	3.6	3.7	3.6	3.4	2.9	3.5
Interorbital distance	1.5	1.4	1.1	1.2	1.0	1.7	1.7	1.5	1.0	1.0	1.0
Upper jaw length	6.3	5.6	5.6	5.4	3.8	6.7	6.9	6.4	4.1	3.3	4.2
Upper lip thickness	2.5	1.8	2.1	2.2	1.6	2.9	3.3	2.5	1.8	1.3	1.9
Length of last dorsal spine	2.6	2.2	2.1	1.0	1.4	2.0	2.0	2.9	1.9	1.1	1.5
Length of 1st dorsal soft ray	7.0	4.8	4.8	4.0	3.8	6.6	6.6	6.3	3.2	2.8	4.0
Height of dorsal notch	4.4	2.5	2.7	3.0	2.4	4.6	4.6	3.4	1.3	1.7	2.5
Meristics											
Dorsal soft rays	13	13	13	13	13	13	14	13	13	13	13
Dorsal spines	XII	XI	XI	XI	XII	XII	XII	XII	XII	XII	XII
Anal soft rays	II, 16	II, 15	II, 15	II, 16	II, 15	II, 15	II, 16	II, 15	II, 16	II, 16	16
Pectoral rays	14	14	14	14	14	14	14	14	14	14	14
Pelvic-fin rays	I,4	I,4	I,4	I,4	I,4	I,4	I,4	I,4	I,4	I,4	I,4
Total dorsal elements	25	24	24	24	25	25	26	25	25	25	25
Supraorbital cirri	11	12	16	12	12	19	10	10	10	8	9
Nasal cirri	2	5	2	6	2	4	3	2	2	2	2
cephalic pores (left side)	241	106	149	155	191	152	199	173	123	121	131

Table 10. Counts and measurements of seven western Atlantic and Gulf of Mexico species of *Hypleurochilus* blennies. Specimens are designated *H. cf. aequipinnis* based on description of *H. aequipinnis* material from the eastern Atlantic and direct comparison to material from the other six species included in this study.

Species		SL (mm)	Lateral Line	Cephalic Pore Count	Cephalic Pore Ratio	Dorsal Indentation Ratio
	Count				*pore count : SL* (pores/mm)	*last dorsal spine : 1st segmented dorsay ray*
H. bermudensis	7	18.0 - 49.4	Type B (n = 7)	41 - 72 (59)	1.70	0.47
H. pseudoaequipinnis	11	14.7 - 38.9	Type B (n = 11)	36 - 81 (53)	2.13	0.44
H. springeri	9	20.5 - 45.3	Type B (n = 9)	57 - 86 (71)	2.38	0.42
H. cf. aequipinnis (TX)	11	34.8 - 58.7	Type A (n = 11)	106 - 241 (158)	3.39	0.39
H. cf. aequipinnis (LA) [*photographs]*	*12*	*26.1 - 48.0*	- -	- -	- -	- -
H. geminatus	10	40.2 - 64.4	Type B (n = 10)	46 - 72 (55)	1.01	0.73
H. multifilis	14	41.1 - 77.3	Type A (n = 8)/Type B (n = 5)*	70 - 187 (127)	2.45	0.66
H. caudovittatus	11	23.4 - 58.0	Type B (n = 11)	37 - 93 (57)	1.51	0.62

Species		Anal fin elements			Segmented dorsal rays		
	Count	*II, 15*	*II, 16*	*II, 17*	*12*	*13*	*14*	*15*
H. bermudensis	7	7			2	4	1	
H. pseudoaequipinnis	11	11				7	4	
H. springeri	9	9				9		
H. cf. aequipinnis (TX)	11	5	6			10	1	
H. cf. aequipinnis (LA) [*photographs]*	*12*	*1*	*8*	*3*		*4*	*7*	*1*
H. geminatus	10		2	8				10
H. multifilis	14	1	7	6				14
H. caudovittatus	11	11				7	4	

Species		Dorsal spines			Total Dorsal Elements		
	Count	*11*	*12*	24	25	26	27
H. bermudensis	7	7		3	3	1	
H. pseudoaequipinnis	11		11		7	4	
H. springeri	9		10	1	7	1	
H. cf. aequipinnis (TX)	11	4	7	3	6	1	
H. cf. aequipinnis (LA) [*photographs]*	*12*	*1*	*11*		*5*	*6*	*1*
H. geminatus	10		10				10
H. multifilis	14		14		1		13
H. caudovittatus	11		11		7	4	

APPENDIX B

FIGURES

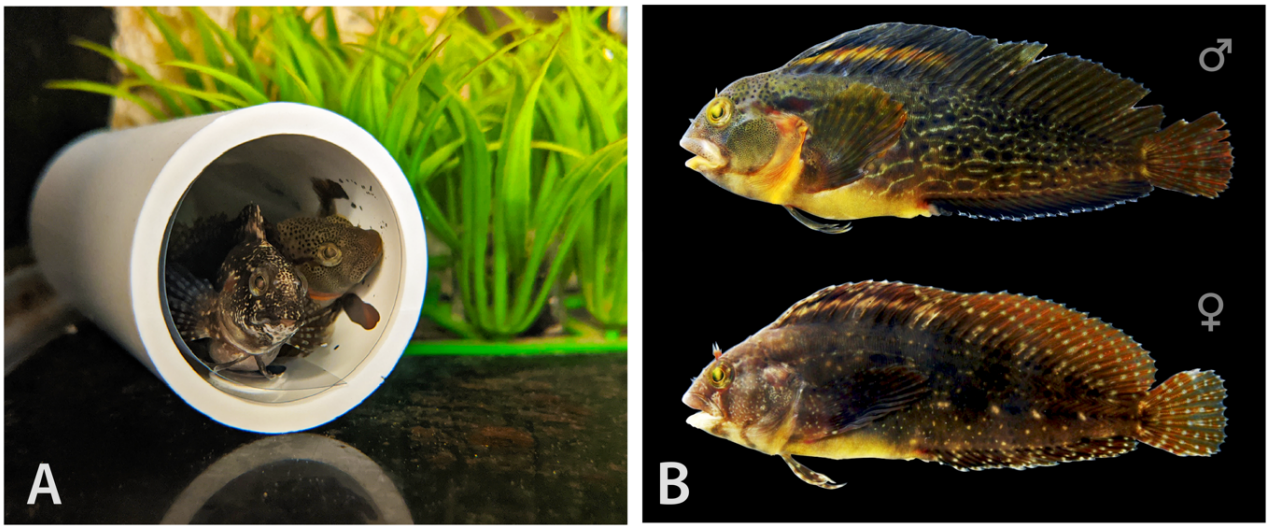

Figure 1. A) Florida blenny (*C. saburrae*) breeding pair [female (right) and male (left)] inside spawning tube prepared with transparency film as the egg-laying substrate. B) Lateral view of male and female representatives of broodstock species used in this study.

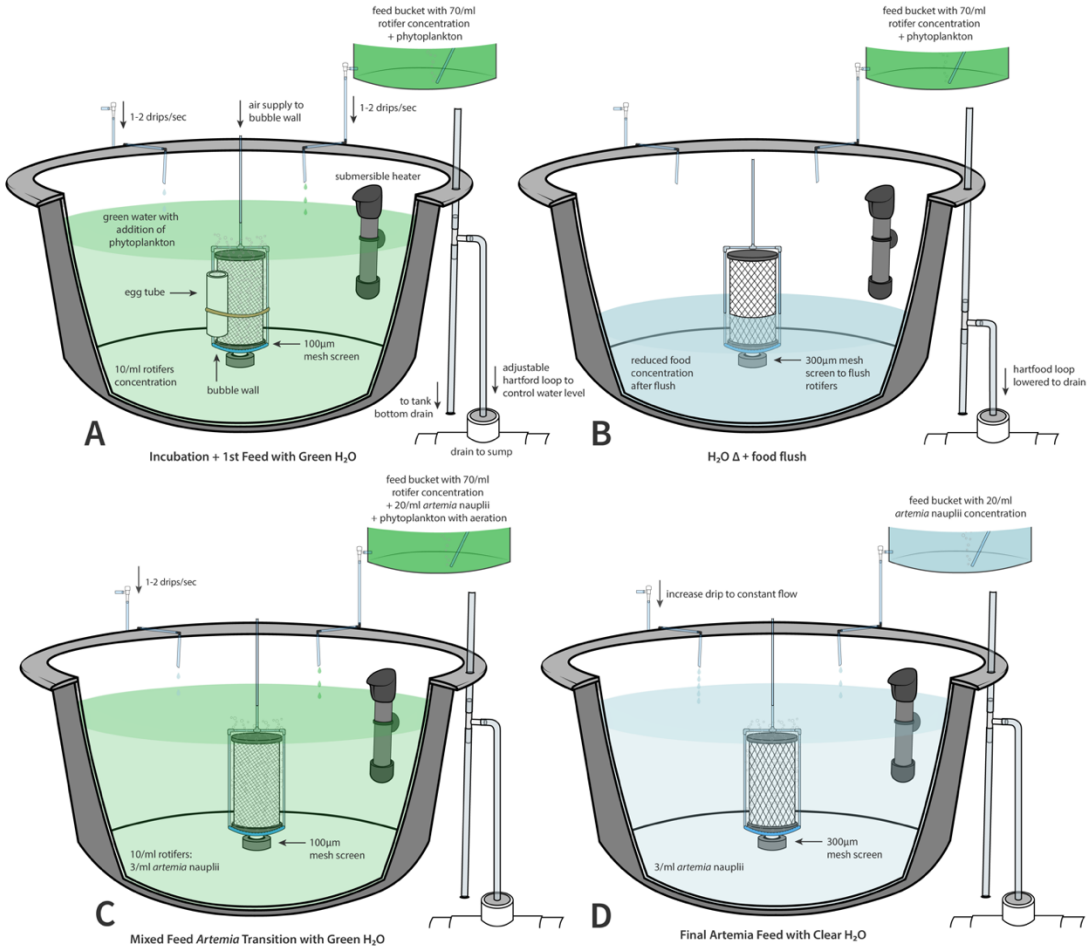

Figure 2. Diagram of larval culture tank construction and culture protocol used during this study. A) Initial egg incubation and hatching step with spawning tube secured vertically to 100 µm drain screen. First feed of S-type *B. rotundiformis* rotifers at a concentration of 5 ind. mL^{-1}. Addition of phytoplankton during feed as designated by the green-water technique of culture. B) Water volume exchange and flush of uneaten live foods by lowering hartford loop and changing drain screen to a 300 µm mesh size to clear tank of food items too large for consumption and maintain appropriate food densities. Water and air flow are turned off during this phase to allow adequate suction of live foods through drain screen. C) Mixed live food transition period and introduction of first *A. salina* nauplii live food at concentration of 3 ind. mL^{-1} with continued use of phytoplankton in green-water technique. D) 48-h *A. salina* only feeds with increased water flow and discontinued used of green-water technique.

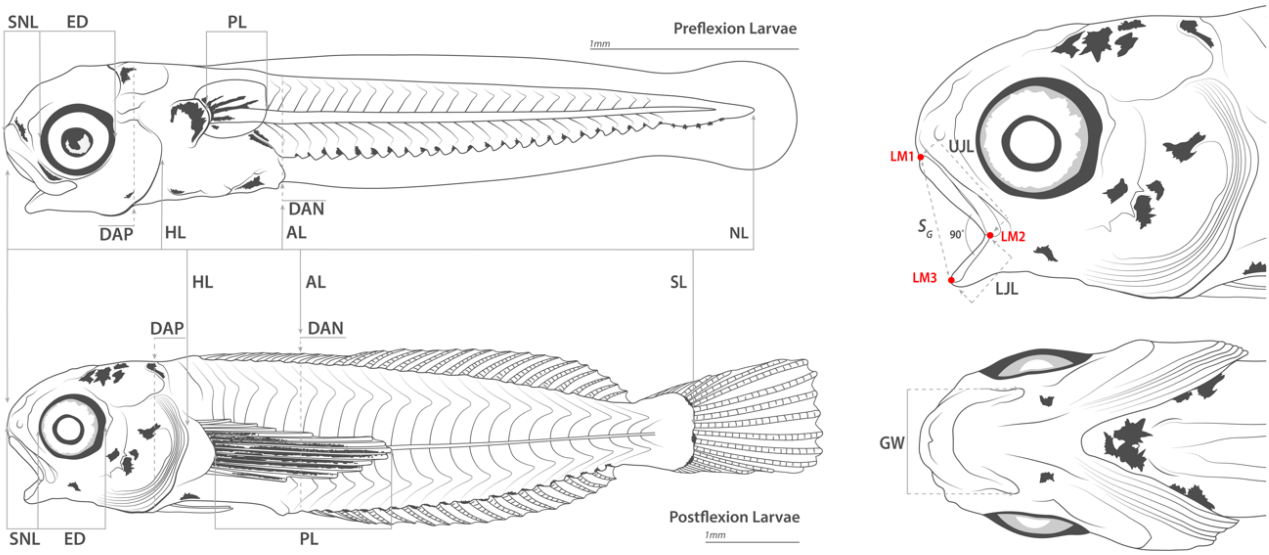

Figure 3. Morphometric characters measured from Florida blenny (*C. saburrae*) larvae. Standard length (SL) and notochord length (NL) measured for body size; snout length (SNL), eye diameter (ED), pectoral length (PL) depth at pelvic (DAP), head length (HL), anal length (AL), depth at anus (DAN) measurement for single character assessment; upper jaw length (UJL), lower jaw length (LJL), and gape width (GW) used for gape morphology character assessment and calculation of maximum gape size (S_G); landmarks (LM1, LM2, and LM3) used as secondary measure of max gape size.

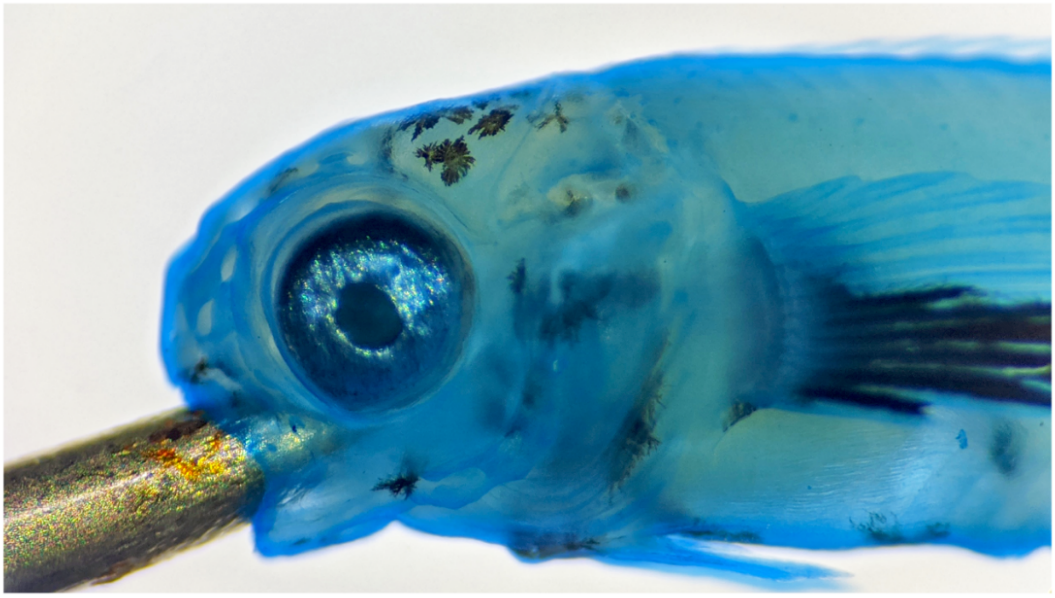

Figure 4. Florida blenny (*C. saburrae*) larval specimen with taxidermy pin inserted in mouth to obtain gape angle of 90˚ and stained with Acid Blue 113 to improve contrast of anatomical structures examined for character state scores and assignment of intervals of development.


A1
250 µm
0-8 hpf
B1
250 µm
1 dpf
C1
250 µm
2 dpf
D1
250 µm
3 dpf
E1
250 µm
4 dpf
F1
250 µm
5 dpf
G1
250 µm
6 dpf
A2
1 mm
1 dph
2 dph
3 dph
B2
1 mm
4 dph
5 dph
C2
1 mm
6 dph
7 dph
8 dph
1 mm
9 dph
D2
1 mm
10 dph
E2
1 mm
11 dph
12 dph
F2
1 mm
13 dph
G2
1 mm
14 dph
H
1 mm
15 dph
I
1 mm
16 dph
J
1 mm
17 dph
18 dph
19 dph
K
1 mm
20 dph
L
1 mm
21 dph
M
1 mm
Settler
1 mm
Settler
N
1 mm
Juvenile

Figure 5. Embryonic of eggs and larval development series of the Florida blenny Florida blenny (*C. saburrae*). Shown are multiple individuals sampled from two larval batches, Group A and B. Scale bars = 1.0 mm. (A1 – G1) embryonic incubation period from 8 hours post fertilization (hpf) to 6 days post hatch (dph) just prior to hatching. (A2): 1-dph preflexion larva with functional mouth, absent yolk reserve, medium fin fold, and ventral stellate melanophore pigmentation. Pigmentation present on pectoral fin bud (B2): 4-dph flexion larva with initial upward flexion of notochord with initial formation of caudal fin ray elements. Stellate melanophores visible atop cranium (C2): 6-dph flexion larva with anteroposterior elongation of the head and melanophore present at jaw hinge intersection of maxillary and dentary bones (D2): 10-dph flexion larva with complete resorption of caudal fin fold and median fin folds along the trunk. Dorsal ray formation appears to proceed those of anal fin. (E2): 11-dph postflexion larva with hyplural plate and caudal fin rays. Increased cephalic pigmentation. (F2): 13-dph postflexion larva with emergence of pelvic fin bud. (G2-I): 14-16-dph postflexion larvae with continued formation of dorsal, anal, pelvic, and caudal fin elements. Larvae begin to stay close to vertical structure of culture tank wall indicating soon to occur bottom settlement and metamorphosis (J): 17-dph postflexion larva with all dorsal and anal spines and rays visible with dorsal indentation. Settlement begins to occur with fish settling on bottom of larval culture tank. (K): 20-dph settler with metamorphosis complete, increased cephalic pigmentation and emergence of pelvic soft rays. Snout and maxillary elongation resulting in slight downward turn of mouth. (L): 21-dph settler with complete formation of all fin elements, deepening of body depth, beginnings of juvenile/adult coloration with gradient of cryptic pigmentation fading towards the posterior. (M): 21+dph settler with complete coverage of body coloration and loss/absence of pectoral fin pigmentation. Continue elongation of snout and maxillary bones. (N): juvenile fully pigmented with juvenile coloration appearing on both sexes

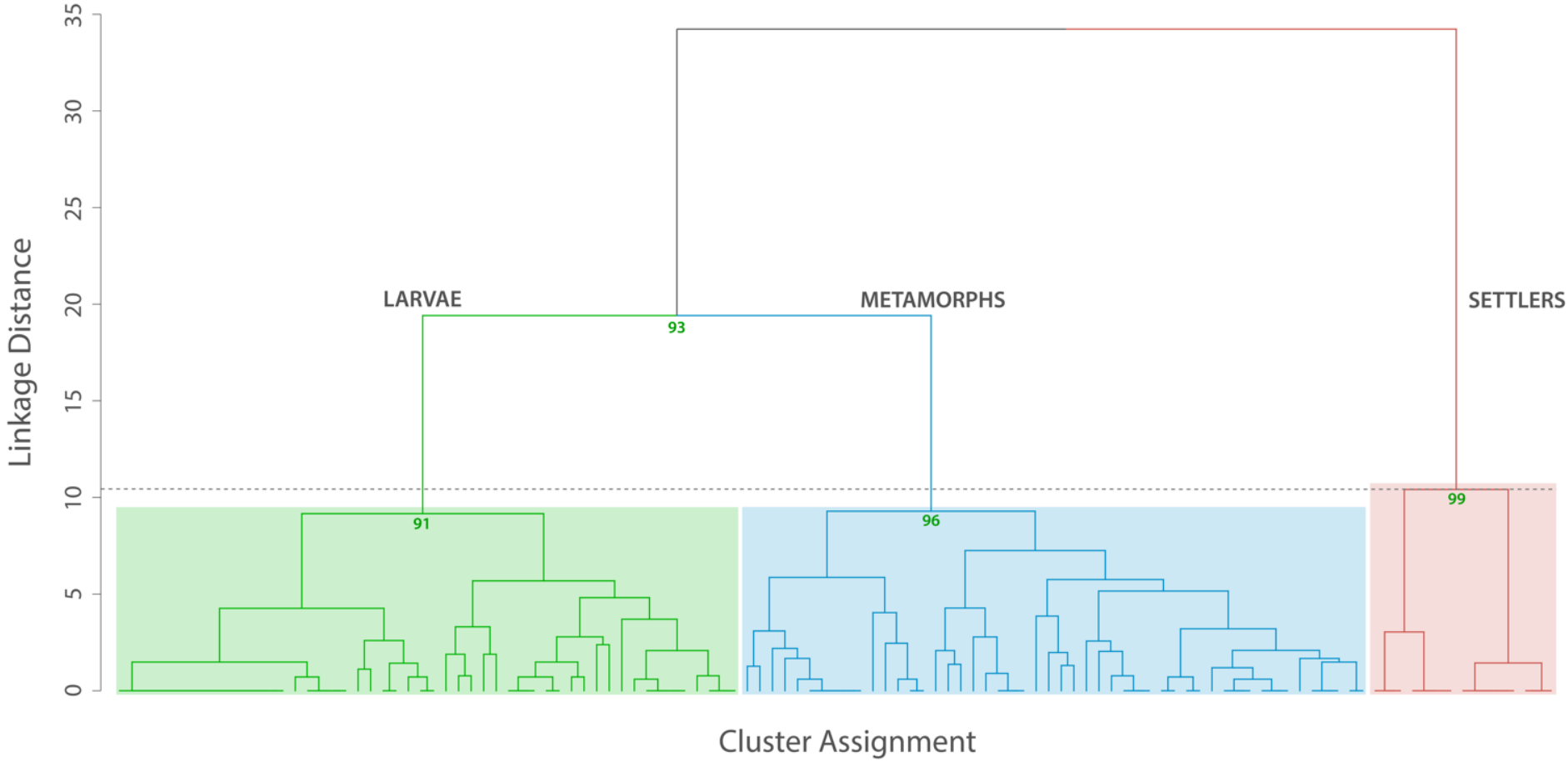

Figure 6. Dendrogram from hierarchical cluster analysis of character state scores from Florida blenny (*C. saburrae*) larval development. Approximately unbiased (AU) *p*-values indicate support of cluster stability ($\alpha = 0.90$); results from cluster analysis indicate three well-supported stable clusters designated as intervals of development (larvae, metamorph, and settler).

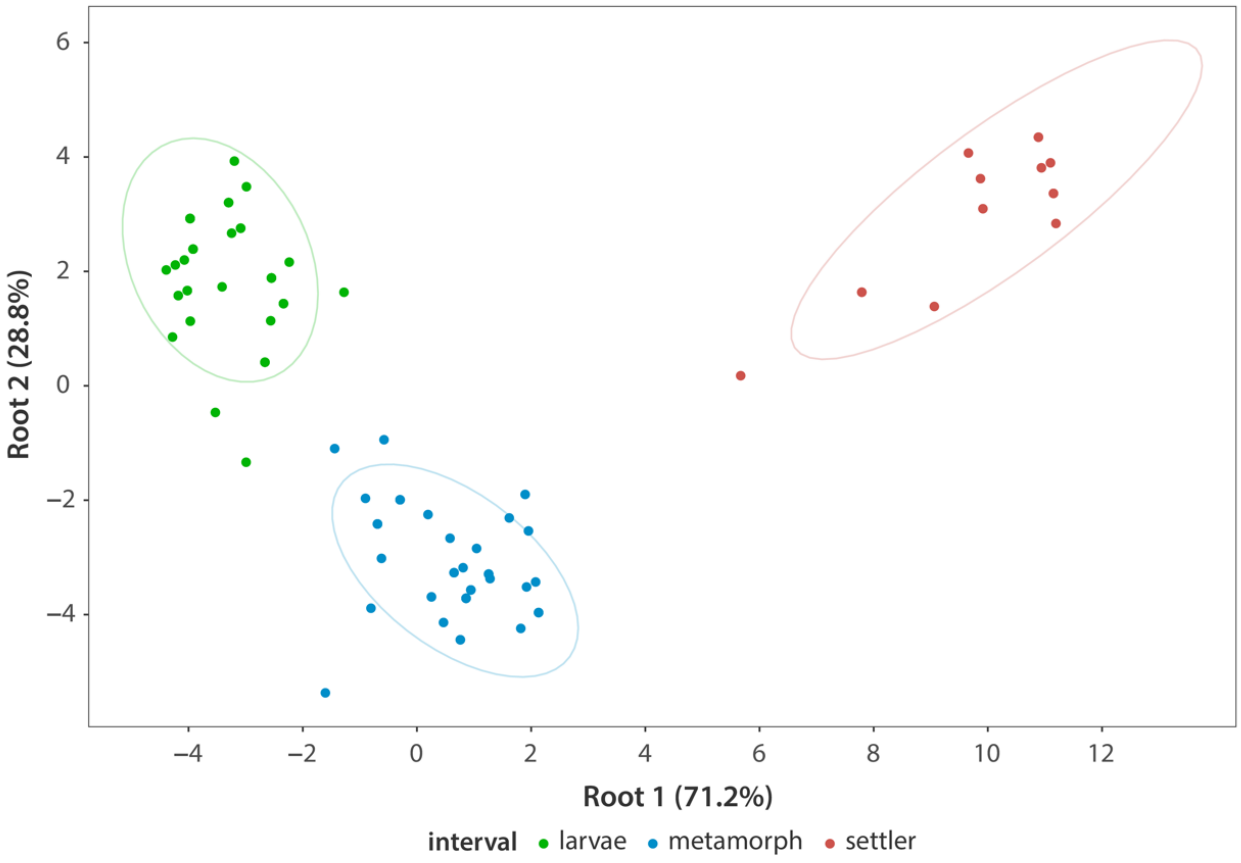

Figure 7. Plot of canonical variates (roots 1 and 2) computed from discriminant function analysis and their relative contribution (% variability) to discriminating intervals of development assigned to Florida blenny (*C. saburrae*) specimens following cluster analysis.

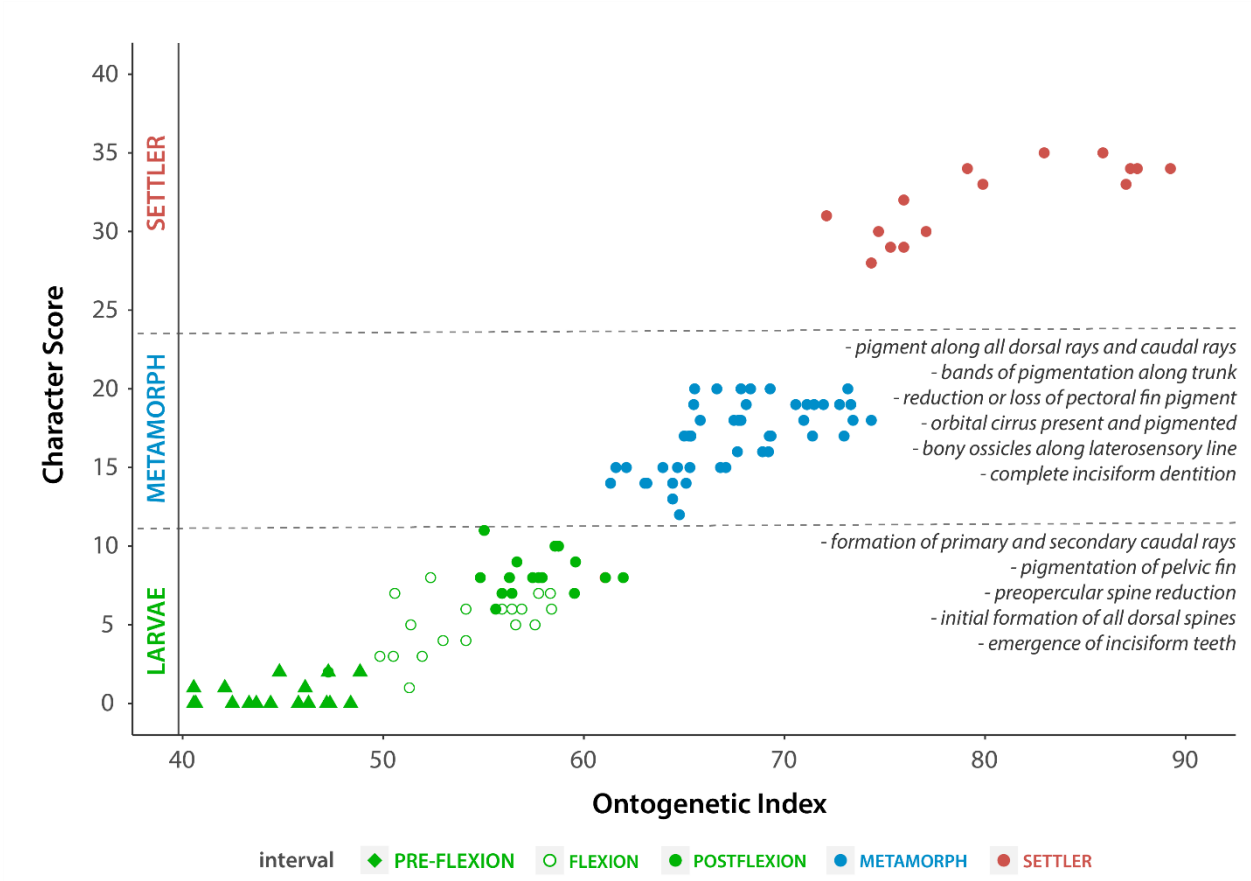

Figure 8. Change in total character state score during ontogeny for the Florida blenny (*C. saburrae*); intervals of development are demarcated with dashed lines and thresholds of traits and character states that characterize transition between intervals are listed.

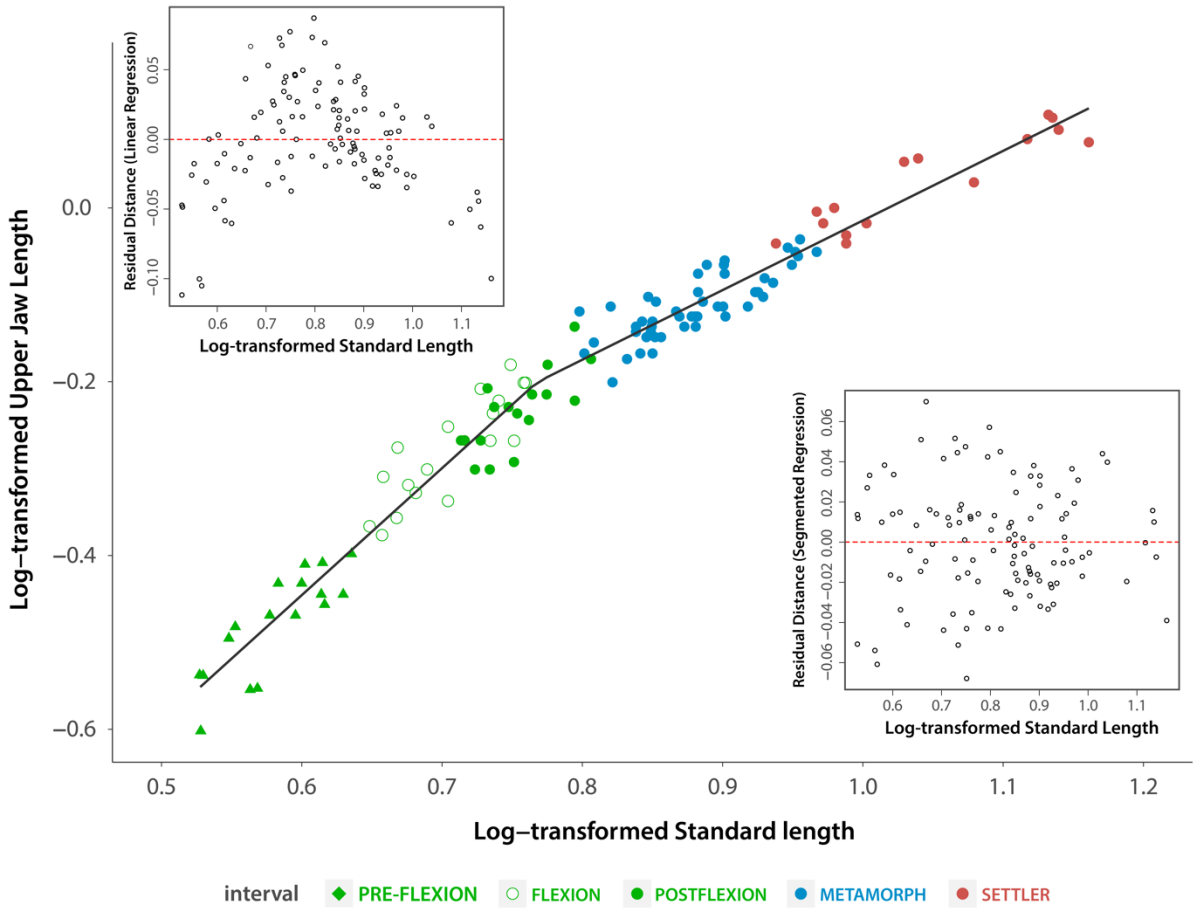

Figure 9. Plot of $\log_{10}$-transformed upper jaw length (UJL) and standard length (SL) for the Florida blenny (*C. saburrae*). Residuals plots from (A) single linear regression and (B) piecewise linear regression.

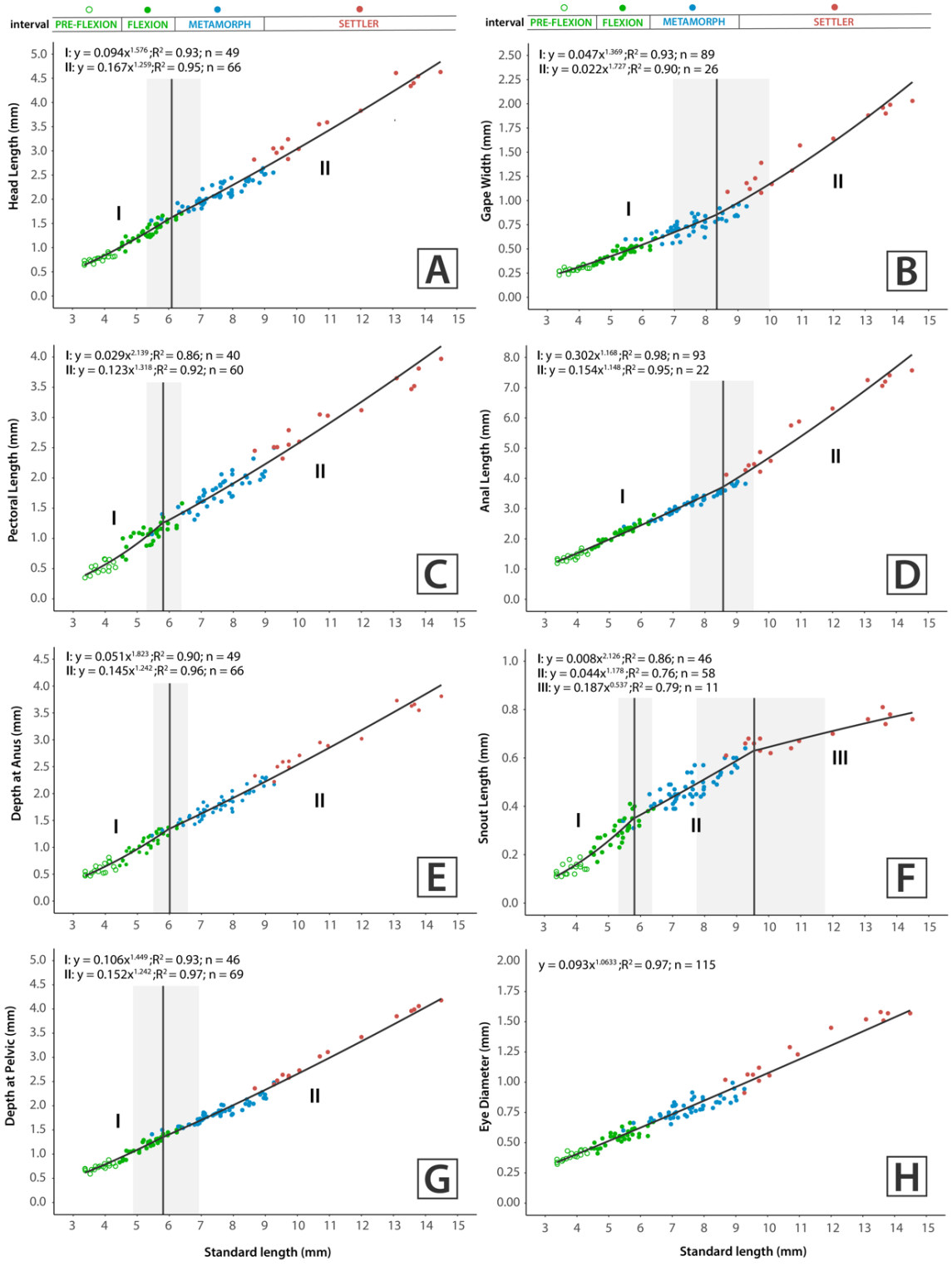
interval
PRE-FLEXION
FLEXION
METAMORPH
SETTLER
Head Length (mm)
I: y = 0.094x^1.576;R² = 0.93; n = 49
II: y = 0.167x^1.259;R² = 0.95; n = 66
A
Gape Width (mm)
I: y = 0.047x^1.369;R² = 0.93; n = 89
II: y = 0.022x^1.727;R² = 0.90; n = 26
B
Pectoral Length (mm)
I: y = 0.029x^2.139;R² = 0.86; n = 40
II: y = 0.123x^1.318;R² = 0.92; n = 60
C
Anal Length (mm)
I: y = 0.302x^1.168;R² = 0.98; n = 93
II: y = 0.154x^1.148;R² = 0.95; n = 22
D
Depth at Anus (mm)
I: y = 0.051x^1.823;R² = 0.90; n = 49
II: y = 0.145x^1.242;R² = 0.96; n = 66
E
Snout Length (mm)
I: y = 0.008x^2.126;R² = 0.86; n = 46
II: y = 0.044x^1.178;R² = 0.76; n = 58
III: y = 0.187x^0.537;R² = 0.79; n = 11
F
Depth at Pelvic (mm)
I: y = 0.106x^1.449;R² = 0.93; n = 46
II: y = 0.152x^1.242;R² = 0.97; n = 69
G
Eye Diameter (mm)
y = 0.093x^1.0633;R² = 0.97; n = 115
H
Standard length (mm)
Standard length (mm)

Figure 10. Allometric growth equations for morphometric characters and relationship to standard length scaling metric of Florida blenny (*C. saburrae*) larvae during early stages of development. Each point represents measurements from a single specimen. Interval colors indicate interval of development assigned to each specimen. Power functions feature growth coefficients for allometric growth rates and vertical lines indicate the inflection point of change in growth rate between segments. (A) head length, (B) gape width, (C) pectoral length, (D) anal length, (E) depth at anus, (F) snout length, (G) depth at pelvic, and (H) eye diameter.

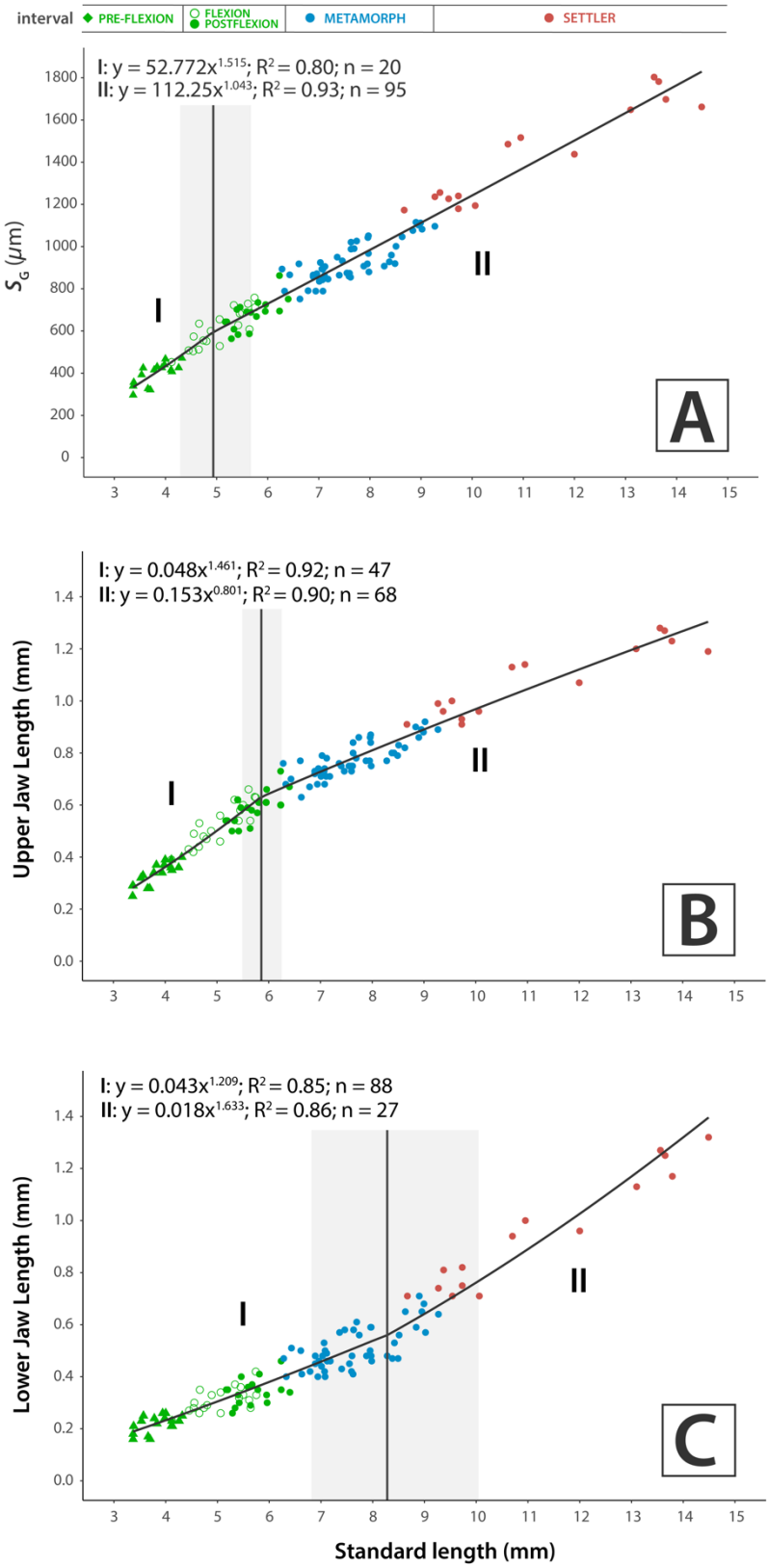
interval
PRE-FLEXION
FLEXION
POSTFLEXION
METAMORPH
SETTLER
I: y = 52.772x^1.515; R² = 0.80; n = 20
II: y = 112.25x^1.043; R² = 0.93; n = 95
S_G (μm)
I
II
A
I: y = 0.048x^1.461; R² = 0.92; n = 47
II: y = 0.153x^0.801; R² = 0.90; n = 68
Upper Jaw Length (mm)
B
I: y = 0.043x^1.209; R² = 0.85; n = 88
II: y = 0.018x^1.633; R² = 0.86; n = 27
Lower Jaw Length (mm)
C
Standard length (mm)

Figure 11. Allometric growth equations of morphometric characters used to calculate maximum gape size and relationship to standard length scaling metric of Florida blenny (*C. saburrae*) larvae during early stages of development. (A) gape size (S_G), (B) upper jaw length, and (C) lower jaw length.

Figure 12. Plot of maximum gape size (max-S_G) and estimated feeding gape size (feeding-S_G) and relationship to age (dph) scaling metric both batches of larvae sampled, Groups A and B.

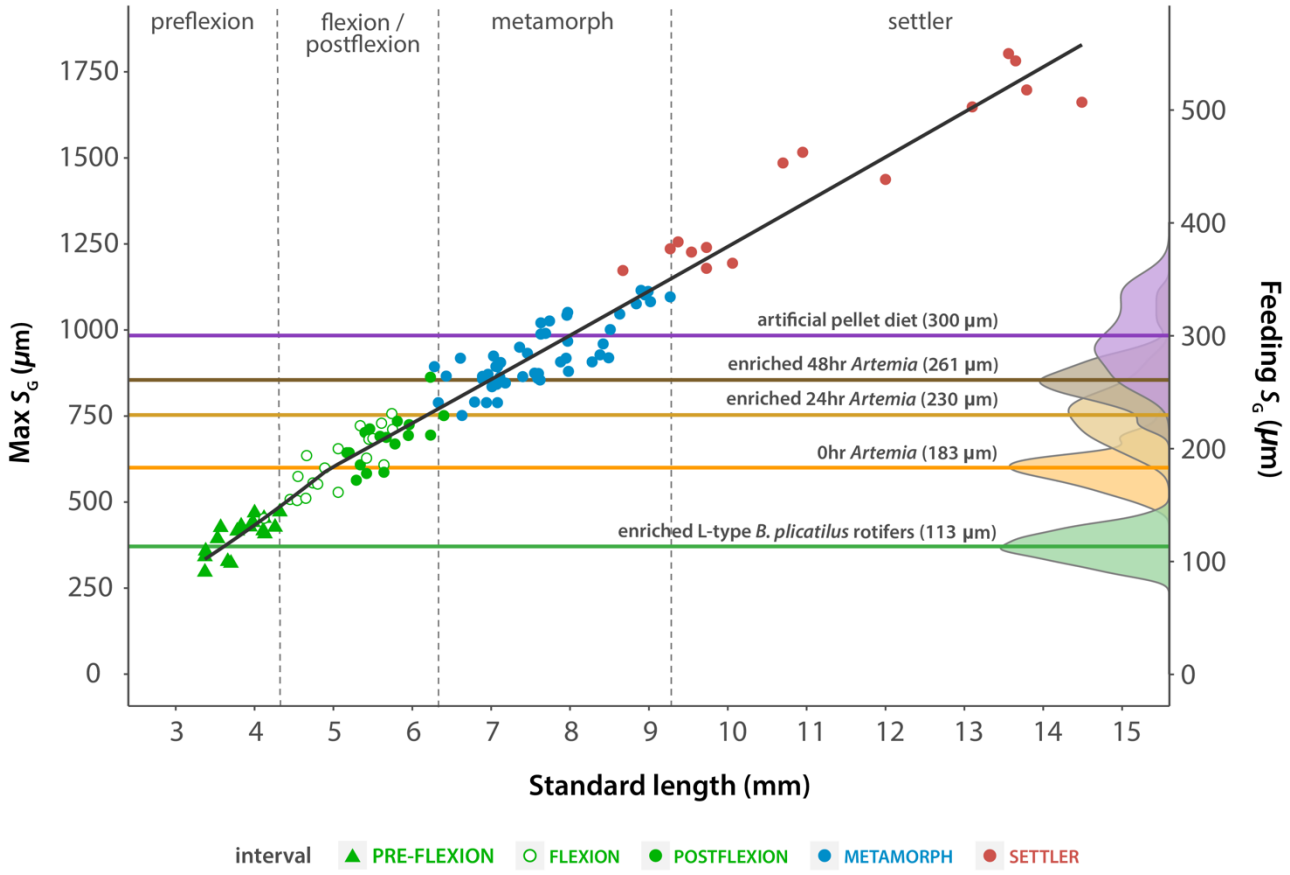

Figure 13. Plot of maximum gape size (max-S_G) and estimated feeding gape size (feeding-S_G) and relationship to standard length (SL) scaling metric for all specimens. Inflection point indicates change in allometric growth rate; dashed lines demarcate intervals of development. Mean width of live food items fed to Florida blenny (*C. saburrae*) larvae during culture are applied to the feeding gape size (feeding-S_G) scale on the secondary y-axis.

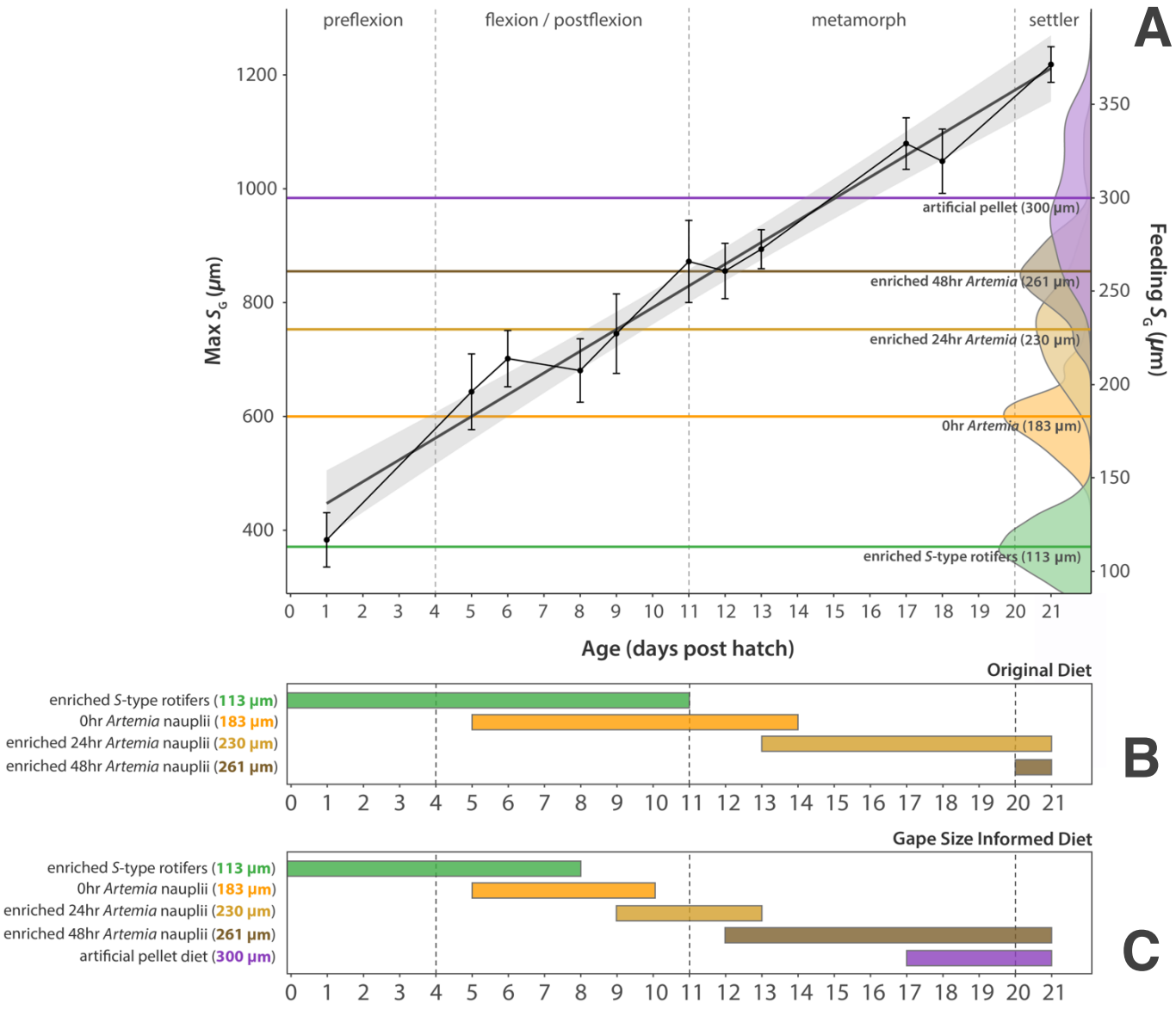

Figure 14. (A) plot of maximum gape size (max-S_G) and estimated feeding gape size (feeding-S_G) and relationship to age (dph) scaling metric for Group A specimens. Dotted lines demarcate intervals of development. Mean width of live food items fed to Florida blenny (*C. saburrae*) during larviculture are applied to the feeding gape size (feeding-S_G) scale on the secondary y-axis. (B) original feeding protocol applied during larviculture of Florida blenny (*C. saburrae*) during this study and estimated optimal feeding protocol based on live food item size and feeding gape size (feeding-S_G).

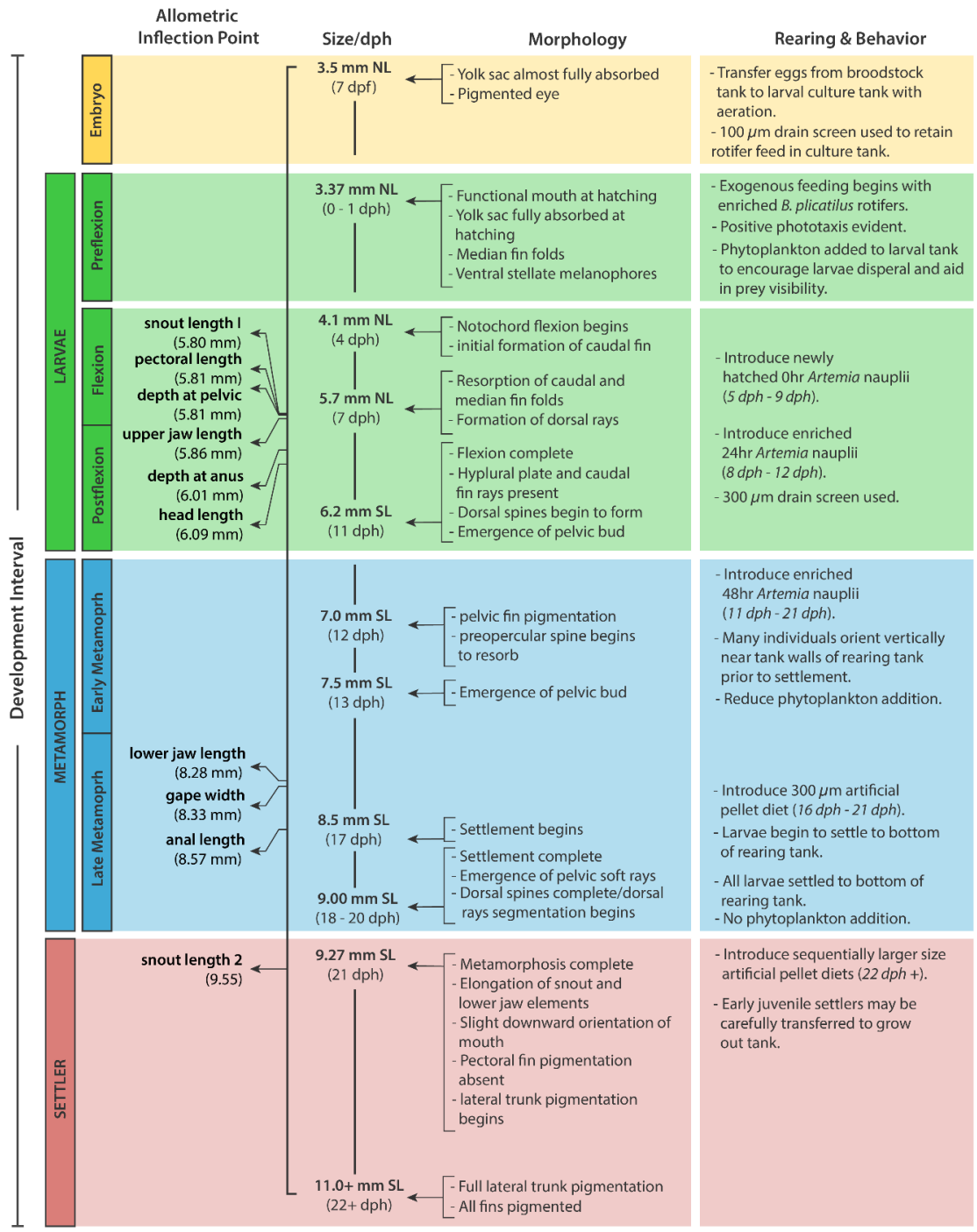

Figure 15. Chart of morphological change and allometric growth patterns summarizing general ontogeny of the Florida blenny (*C. saburrae*).

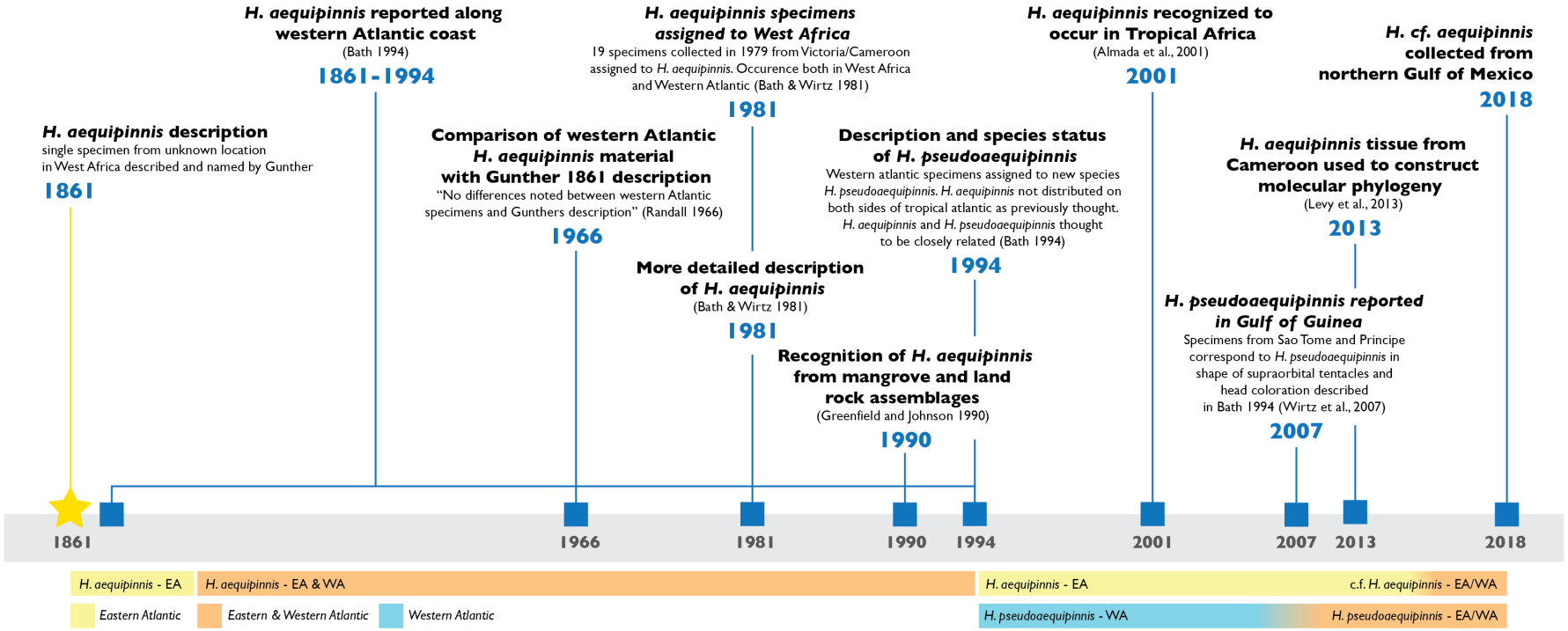

Figure 16. Timeline of published content containing information about Oyster blenny (*H. aequipinnis*) and/or Atlantic oyster blenny (*H. pseudoaequipinnis*) and the taxonomic uncertainty associated with this species pair. Current consensus on geographic range of these two species designates *H. pseudoaequipinnis* and *H. aequipinnis* to the western tropical Atlantic and eastern tropical Atlantic, respectively.

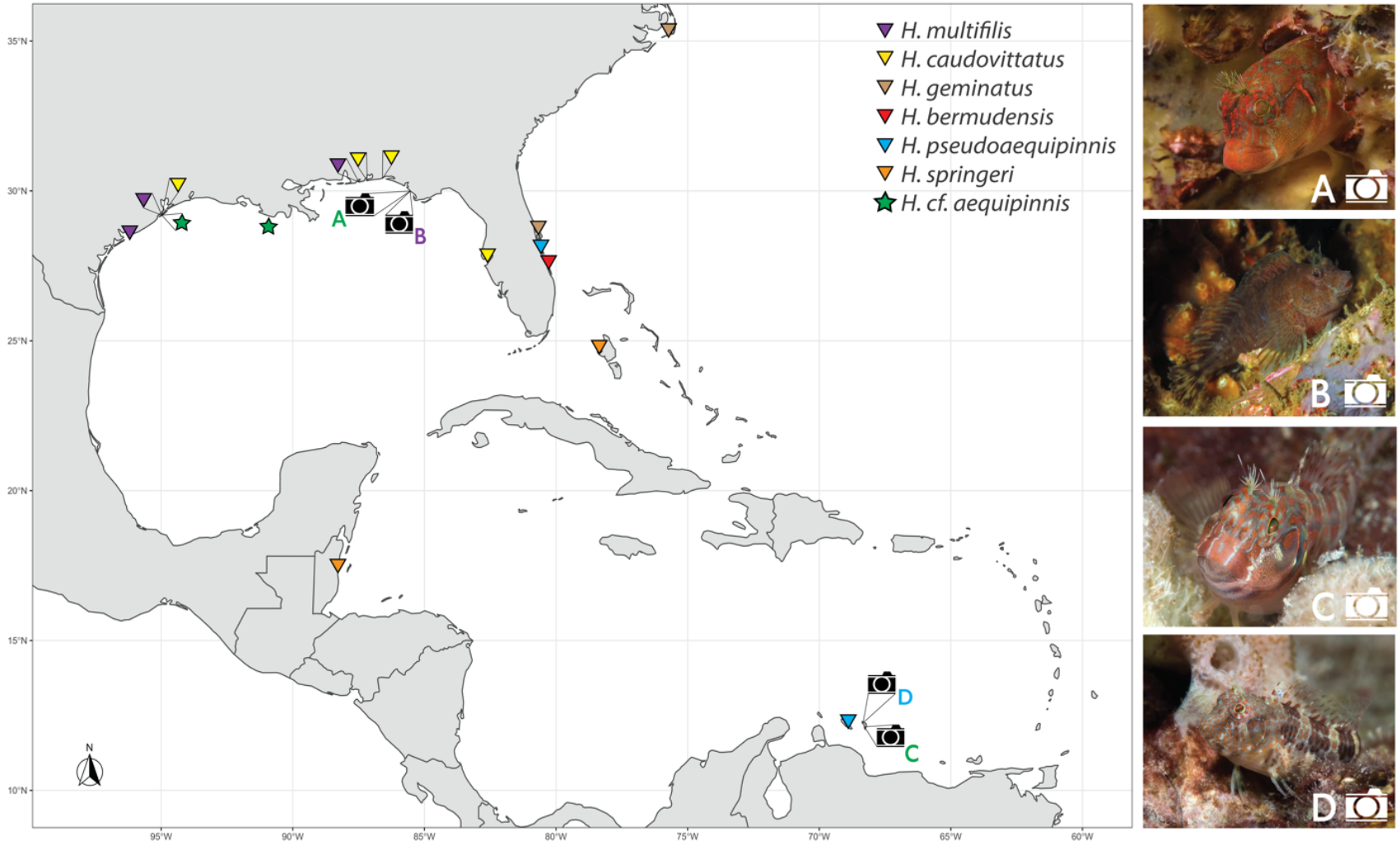
H. multifilis
H. caudovittatus
H. geminatus
H. bermudensis
H. pseudoaequipinnis
H. springeri
H. cf. aequipinnis
A
B
C
D
35°N
30°N
25°N
20°N
15°N
10°N
95°W
90°W
85°W
80°W
75°W
70°W
65°W
60°W
N

Figure 17. Map of collection sites for *Hypleurochilus* used in morphological and/or molecular analyses. Circle/Star indicates sites of specimens collected in this lab. Letters refer to images on the right that do not have associated specimen material. (A) Likely *H. cf. aequipinnis* photographed off Mexico Beach, FL [photo with permission of Carol Cox]. (B) Likely *H. multifilis* photographed co-occurring on the same artificial structure as fish in image A [photo with permission of Carol Cox]. (C) Likely *H. cf. aequipinnis* photographed in Bonaire [photo with permission of John Roach]. (D) Likely *H. pseudoaequipinnis* photographed in Bonaire [photo with permission of John Roach].

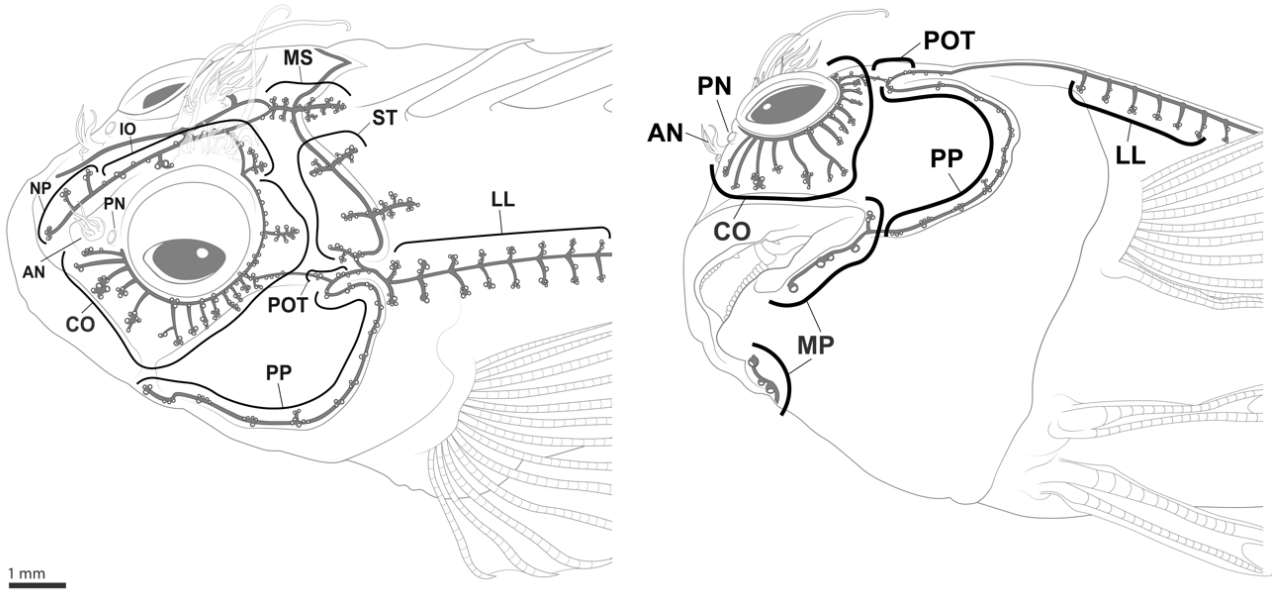

Figure 18. Cephalic sensory pore system of likely *H. cf. aequipinnis* specimen [RIE 4368], male, 58.7 mm SL, Galveston Island, TX, US. AN: anterior nostril; PN: posterior nostril; NP: nasal pores; IO: interorbital pores; MS: median supratemporal commissural pores; ST: supratemporal pores; POT: post-otic pores; PP: pre-opercular pores; CO: circumorbital pores; ST: supratemporal pores; MP: mandibular pores; LL: lateral line.

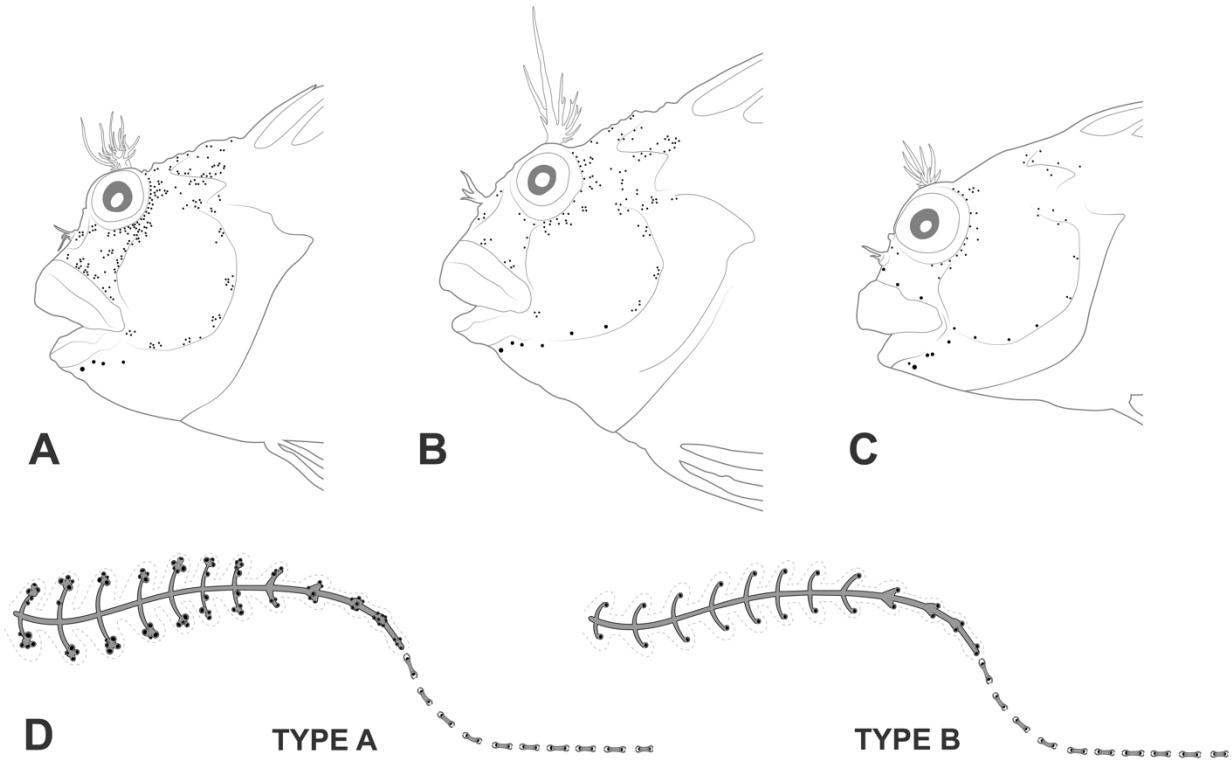

Figure 19. Arrangement of cephalic sensory pores for three species of *Hypleurochilus* – A) Likely *H. cf. aequipinnis*, RIE 4368, 52.5mm SL; B) *H. multifilis*, RIE 3420, 55.2 mm SL; and C) *H. pseudoaequipinnis*, RIE 4151, 38.9 mm SL. D) Two laterosensory conditions observed in the seven *Hypleurochilus* species included in this study.

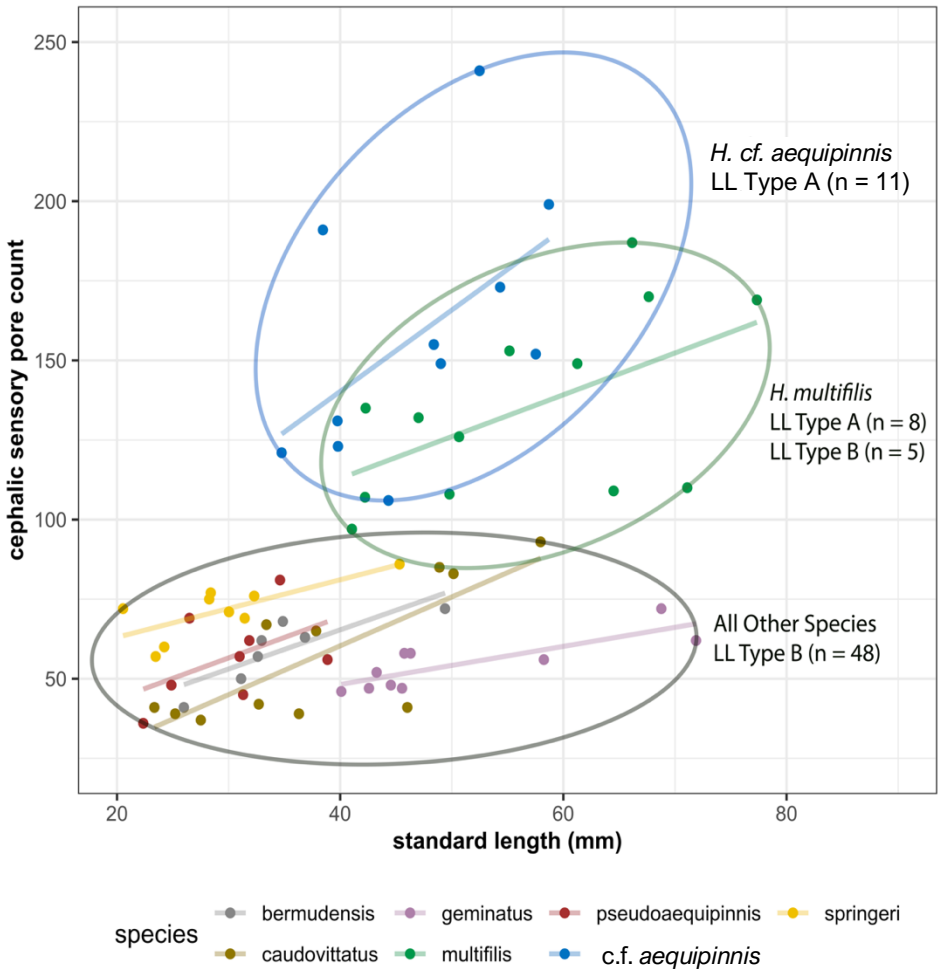

Figure 20. Cephalic sensory pore counts along SL scaling metric in seven *Hypleurochilus* species included in this study. Pore counts were taken from left size perspective only, thus some cephalic pores not visible from this perspective were not counted. Points represent individual specimens color coded by species.

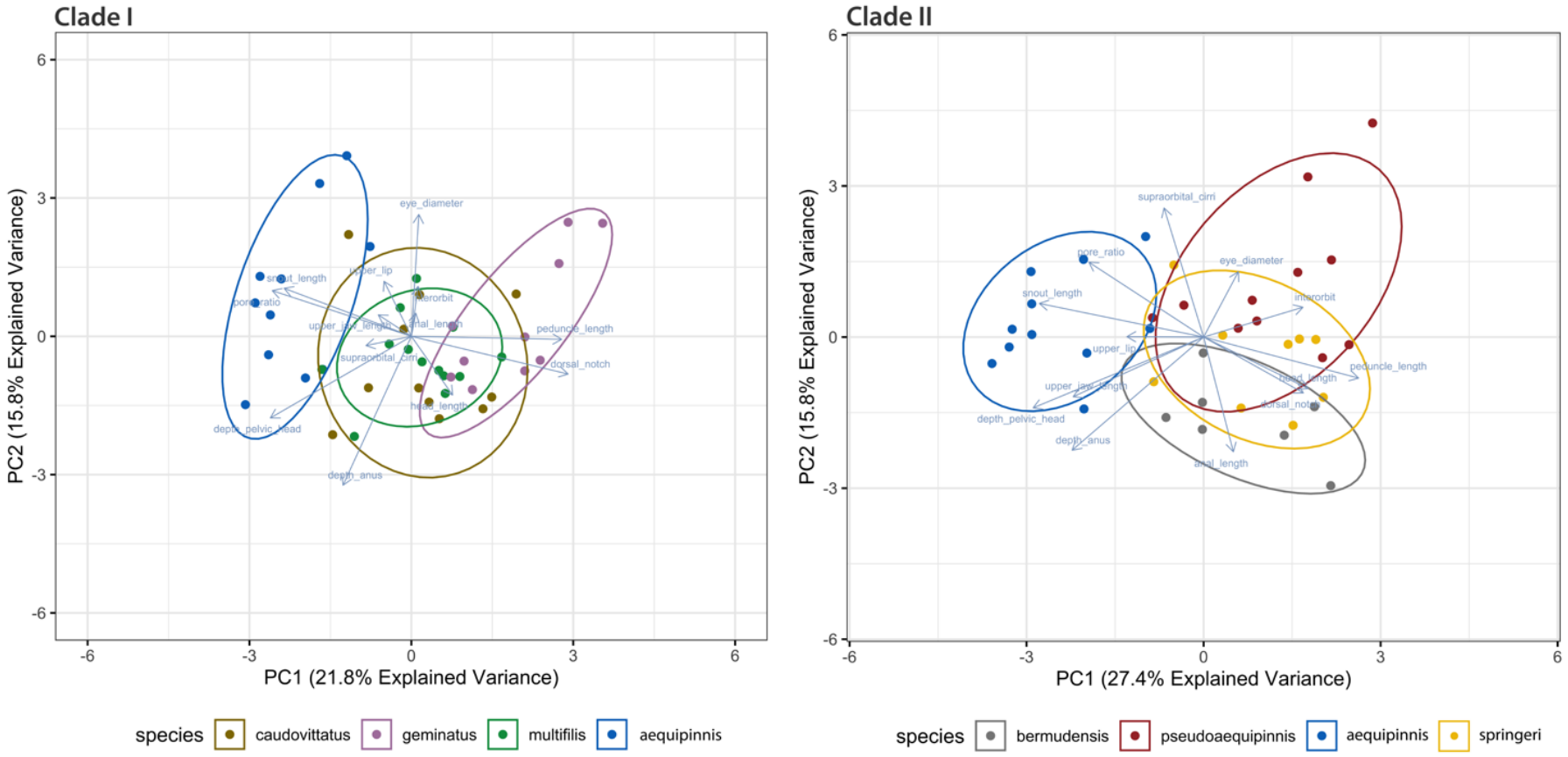
Clade I
PC2 (15.8% Explained Variance)
PC1 (21.8% Explained Variance)
eye_diameter
upper_lip
snout_length
pore_ratio
interorbit
upper_jaw_length
anal_length
peduncle_length
supraorbital_cirri
dorsal_notch
head_length
depth_pelvic_head
depth_anus
species
caudovittatus
geminatus
multifilis
aequipinnis
Clade II
PC2 (15.8% Explained Variance)
PC1 (27.4% Explained Variance)
supraorbital_cirri
pore_ratio
eye_diameter
snout_length
interorbit
upper_lip
peduncle_length
upper_jaw_length
anal_length
dorsal_notch
depth_pelvic_head
depth_anus
species
bermudensis
pseudoaequipinnis
aequipinnis
springeri

Figure 21. Biplots of principal components (PC1 and PC2) of 13 morphometric characters between *H. cf. aequipinnis* specimens and species assigned to clades I and II. Blue axes indicate loading amplitudes and directions of morphometric variables. Points represent individual specimens color coded by species.

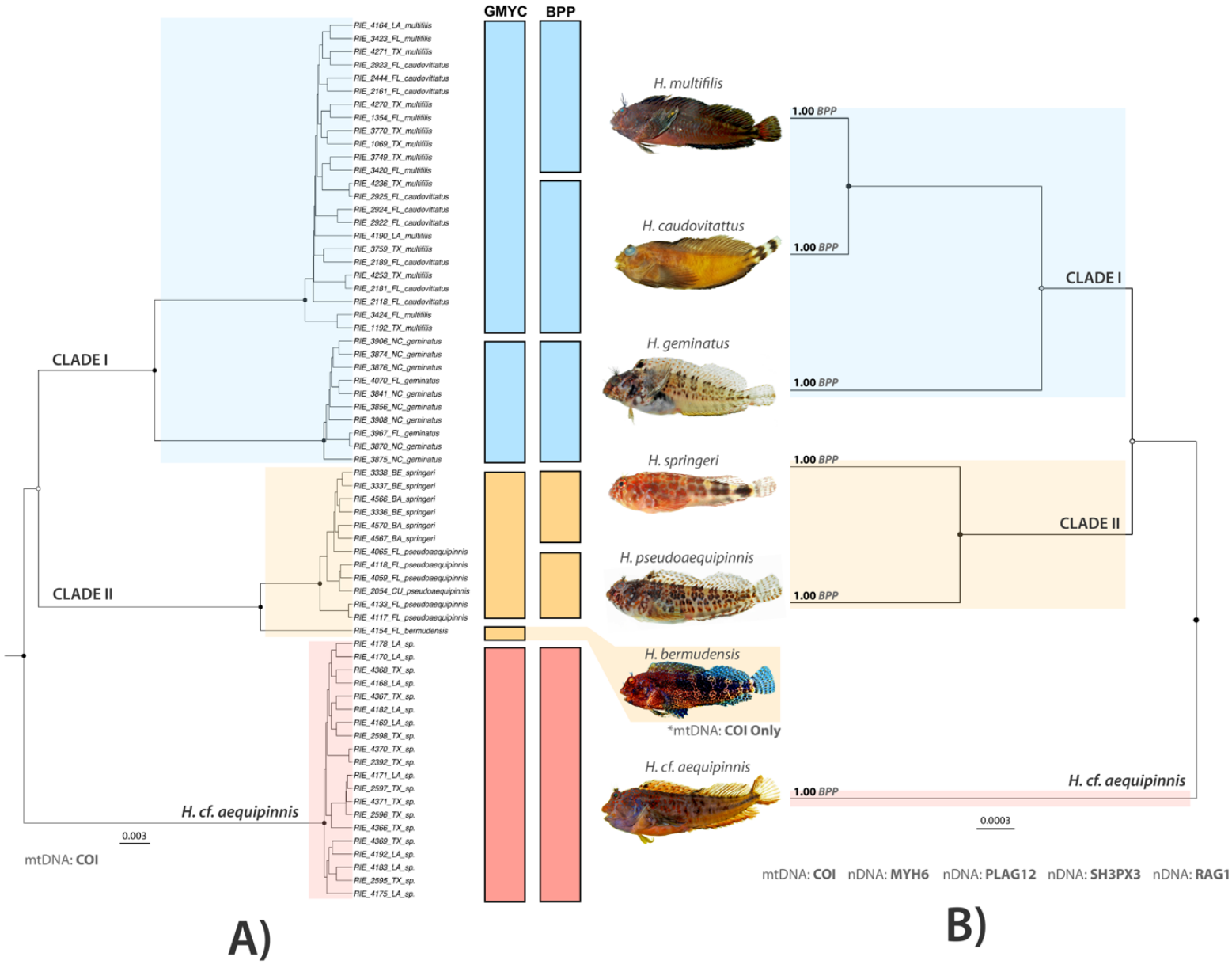
GMYC
BPP
RIE_4164_LA_multifilis
RIE_3423_FL_multifilis
RIE_4271_TX_multifilis
RIE_2923_FL_caudovittatus
RIE_2444_FL_caudovittatus
RIE_2161_FL_caudovittatus
RIE_4270_TX_multifilis
RIE_1354_FL_multifilis
RIE_3770_TX_multifilis
RIE_1069_TX_multifilis
RIE_3749_TX_multifilis
RIE_3420_FL_multifilis
RIE_4236_TX_multifilis
RIE_2925_FL_caudovittatus
RIE_2924_FL_caudovittatus
RIE_2922_FL_caudovittatus
RIE_4190_LA_multifilis
RIE_3759_TX_multifilis
RIE_2189_FL_caudovittatus
RIE_4253_TX_multifilis
RIE_2181_FL_caudovittatus
RIE_2118_FL_caudovittatus
RIE_3424_FL_multifilis
RIE_1192_TX_multifilis
RIE_3906_NC_geminatus
RIE_3874_NC_geminatus
RIE_3876_NC_geminatus
RIE_4070_FL_geminatus
RIE_3841_NC_geminatus
RIE_3856_NC_geminatus
RIE_3908_NC_geminatus
RIE_3967_FL_geminatus
RIE_3870_NC_geminatus
RIE_3875_NC_geminatus
RIE_3338_BE_springeri
RIE_3337_BE_springeri
RIE_4566_BA_springeri
RIE_3336_BE_springeri
RIE_4570_BA_springeri
RIE_4567_BA_springeri
RIE_4065_FL_pseudoaequipinnis
RIE_4118_FL_pseudoaequipinnis
RIE_4059_FL_pseudoaequipinnis
RIE_2054_CU_pseudoaequipinnis
RIE_4133_FL_pseudoaequipinnis
RIE_4117_FL_pseudoaequipinnis
RIE_4154_FL_bermudensis
RIE_4178_LA_sp.
RIE_4170_LA_sp.
RIE_4368_TX_sp.
RIE_4168_LA_sp.
RIE_4367_TX_sp.
RIE_4182_LA_sp.
RIE_4169_LA_sp.
RIE_2598_TX_sp.
RIE_4370_TX_sp.
RIE_2392_TX_sp.
RIE_4171_LA_sp.
RIE_2597_TX_sp.
RIE_4371_TX_sp.
RIE_2596_TX_sp.
RIE_4366_TX_sp.
RIE_4369_TX_sp.
RIE_4192_LA_sp.
RIE_4183_LA_sp.
RIE_2595_TX_sp.
RIE_4175_LA_sp.
CLADE I
CLADE II
H. cf. aequipinnis
0.003
mtDNA: COI
H. multifilis
H. caudovitattus
H. geminatus
H. springeri
H. pseudoaequipinnis
H. bermudensis
*mtDNA: COI Only
H. cf. aequipinnis
1.00 BPP
1.00 BPP
1.00 BPP
CLADE I
1.00 BPP
1.00 BPP
CLADE II
H. cf. aequipinnis
1.00 BPP
0.0003
mtDNA: COI
nDNA: MYH6
nDNA: PLAG12
nDNA: SH3PX3
nDNA: RAG1
A)
B)

Figure 22. A) Bayesian phylogenetic reconstruction based on cytochrome oxidase subunit I (COI). Node symbols are color coded by posterior probability: white <60%n light grey: 60-75%, dark grey: 75-95%, black: >95%. B) Delimited species resulting from BPP and GMYC species delimitation methods depicted with bars colored according to clade assignment. Mitochondrial COI was used to delimit lineages with the discovery method GMYC program. Mitochondrial COI and four nuclear loci were used to delimit lineages with the validation method Bayesian Phylogenetics and Phylogeography (BPP) program. Only one genetic sample was obtained for *H. bermudensis*, thus, it was excluded from BPP analyses. All photos taken by JE Carter except for images of *H. springeri* and H. *pseudoaequipinnis* (photos with permission of Simon Brandl & Jordan Casey).

Figure 23. Specimens of *H. cf. aequipinnis*, captive-raised or captive-bred in the Texas A&M University at Galveston Sea Life Facility; A) RIE 4365 57.5 mm SL, male, live; B) RIE 4369, female, live; C) RIE 4365 57.5 mm SL; D) captive-bred *H. cf. aequipinnis* F1 offspring tending eggs, male, live. Photos by JE Carter.

Figure 24 A) *H. cf. aequipinnis*, RIE 4368, 52.5mm SL, fresh prior to preservation; B) *H. cf. aequipinnis*, RIE 4368, 52.5mm SL, preserved. Photos by JE Carter.

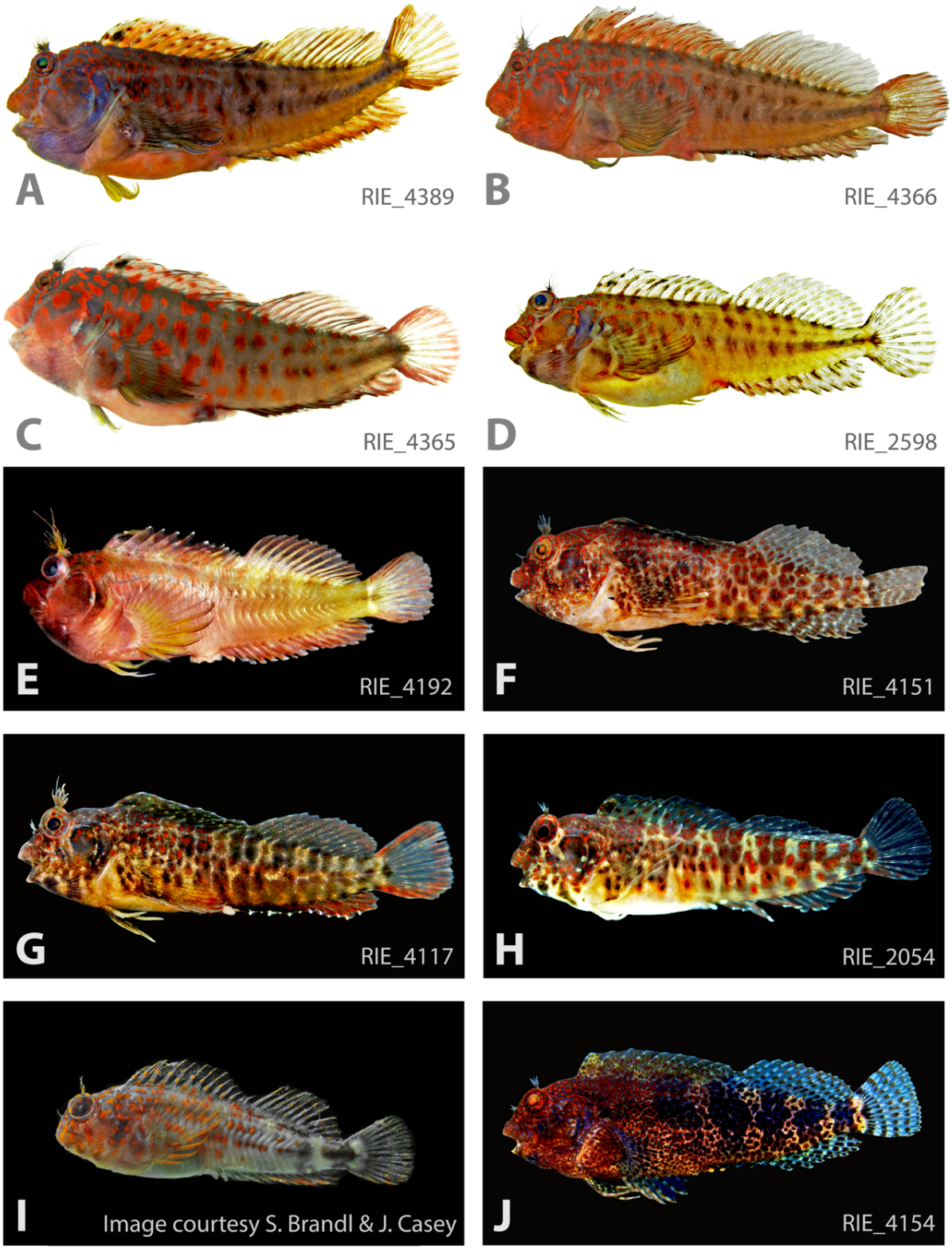
A
RIE_4389
B
RIE_4366
C
RIE_4365
D
RIE_2598
E
RIE_4192
F
RIE_4151
G
RIE_4117
H
RIE_2054
I
Image courtesy S. Brandl & J. Casey
J
RIE_4154

Figure 25. Representatives of Clade II *Hypleurochilus* species and *H. cf. aequipinnis* included in this study. A – D: *H. cf. aequipinnis* specimens collected from Galveston, Texas (RIE 4368 [male], RIE 4366 [male], RIE 4365 [male], and RIE 4369 [female]); E: *H. cf. aequipinnis* collected from offshore platform in Louisiana (RIE 4192 [male]); F and G: *H. pseudoaequipinnis* collected from southeastern Florida (RIE 4151 [female] and RIE 4117 [male]); H: *H. pseudoaequipinnis* collected from Curacao (RIE 2054 [male]); I: *H. springeri* (location unknown [male]); J: *H. bermudensis* collected from southeastern Florida (RIE 4154 [male]). All photos taken by JE Carter except for image I (photos with permission of Simon Brandl & Jordan Casey).

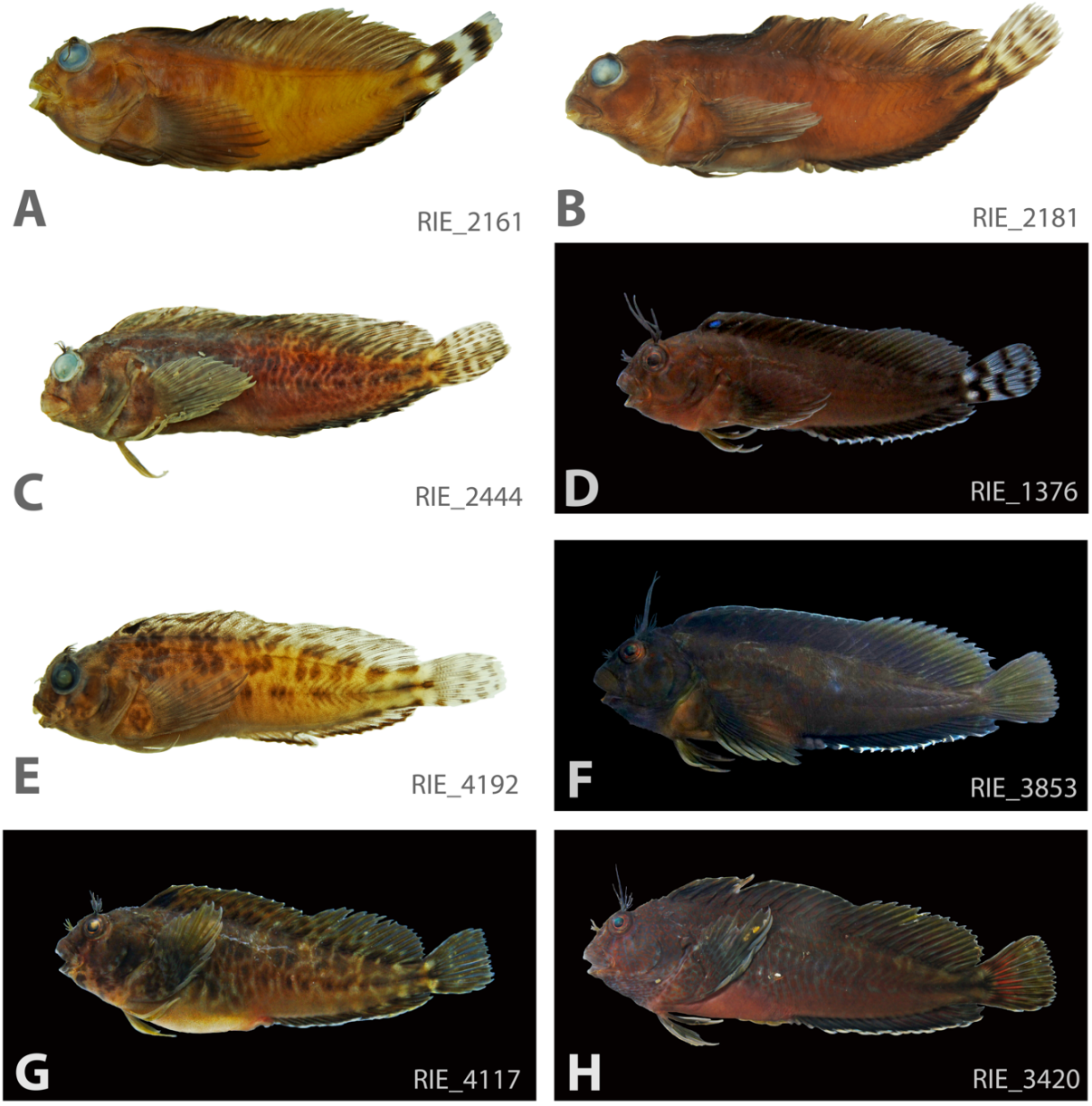
A
RIE_2161
B
RIE_2181
C
RIE_2444
D
RIE_1376
E
RIE_4192
F
RIE_3853
G
RIE_4117
H
RIE_3420

Figure 26. A) Representatives of Clade I *Hypleurochilus* species included in this study. A and B: *H. caudovittatus* collected from Panama City, Florida (RIE 2161 [female] and RIE 2181 [male]); C and D: *H. caudovittatus* collected from Destin, Florida (RIE 2444 [female] and specimen not included in this study [male]); E: *H. caudovittatus* collected from Galveston Bay, Texas (RIE 1135 [female]); F: *H. geminatus* collected from Oregon Inlet, North Carolina (RIE 3853 [male]); G) *H. multifilis* collected from Galveston Island, Texas (RIE 4117 [female]); *H. multifilis* collected from Pensacola, Florida (RIE 3420 [male]). All photos taken by JE Carter.

APPENDIX C

DNA COI BARCODE FOR *HYPLEUROCHILUS CF. AEQUIPINNIS* FROM NORTHERN GULF OF MEXICO

GGCACCCTCTATCTTGTATTTGGTGCTTGAGCTGGAATAGTAGGCACAGCCTTGAGC
CTACTAATCCGAGCCGAACTGAGTCAGCCAGGAGCTCTTCTTGGAGATGACCAGATT
TATAATGTAATCGTTACCGCCCACGCCTTCGTAATGATTTTCTTTATAGTAATACCAA
TTATGATCGGCGGCTTTGGAAACTGACTGATCCCTCTTATGATCGGAGCACCAGACA
TGGCATTCCCCCGAATGAACAACATGAGCTTCTGGCTTCTTCCTCCCTCTTTCCTCCT
CCTTTTAGCCTCTTCCGGAGTTGAAGCAGGTGCTGGAACAGGTTGAACCGTTTACCC
TCCTCTATCTGGAAATCTAGCACATGCGGGGGCATCTGTTGACCTAACTATCTTCTCA
CTTCATCTAGCAGGGATTTCATCAATTCTTGGGGCTATTAACTTCATCACAACGATTA
TTAATATGAAACCCCCAGCTATTTCTCAGTACCAAACCCCTCTGTTTGTATGAGCCGT
ATTAATTACAGCCGTTCTTCTGCTTCTTTCCCTCCCAGTGCTTGCAGCAGGCATTACA
ATGCTCTTAACGGATCGAAACCTAAATACAACATTTTTCGACCCCGCTGGAGGAGGA
GACCCAATTCTATACCAGCATCTCTTTTGA